

DISSERTATION

HEMOCOMPATIBILITY OF HYALURONAN ENHANCED LINEAR LOW-DENSITY
POLYETHYLENE FOR HEART VALVE LEAFLET APPLICATIONS

Submitted by

Rachael Simon-Walker

Graduate Degree Program in Bioengineering

In partial fulfillment of the requirements

For the Degree of Doctor of Philosophy

Colorado State University

Fort Collins, Colorado

Fall 2018

Doctoral Committee:

Advisor: Ketul C. Popat

Melissa Reynolds
Christopher Orton
Adam Chicco

Copyright by Rachael Simon-Walker 2018

All Rights Reserved

ABSTRACT

HEMOCOMPATIBILITY OF HYALURONAN ENHANCED LINEAR-LOW DENSITY POLYETHYLENE FOR HEART VALVE LEAFLET APPLICATIONS

Heart valve disease is a major concern in both developed countries with advanced ageing populations and undeveloped countries which experience a high incidence of rheumatism leading to valvular disease. To reduce mortality and improve quality of life, heart valve implantations have been widely used to assist in improving function of the native cardiovascular system. While mechanical heart valves and tissue-based heart valves have been successfully used to improve quality of life compared to untreated valvular disease, draw-backs are inherent. Mechanical heart valves are prone to thrombosis and require life-long supplemental anti-coagulation therapy. Tissue-based valves are more hemocompatible, but lack the durability required for long-term implantation. To address these issues, polymeric heart valves have been highly sought after due to polymers' abilities to enhance durability and be manufactured to be similar to the native heart valve leaflet. In addition, their surfaces can be modified to increase hemocompatibility. In this work we explore the hemocompatibility and immune response to a novel polymer for use in heart valve leaflet applications; hyaluronan enhanced linear low-density polyethylene. It is proposed that the combination of linear low-density polyethylene with hyaluronan will create a highly durable material that will reduce thrombosis and inflammation due to the anionic and hydrophilic nature of the glycosaminoglycan.

ACKNOWLEDGEMENTS

Research reported in this dissertation was supported by the National Heart, Lung, and Blood Institute of the National Institutes of Health under Award Number R01HL119824. The content is solely the responsibility of the authors and does not necessarily represent the official views of the National Institutes of Health. The author would like to offer her sincerest gratitude to Dr. Ketul Popat, Dr. Lakshmi Prasad Dasi, Dr. Adam Chicco, Dr. Christopher Orton, and Dr. Melissa Reynolds for their support and mentorship. The author would also like to thank the staff at Hartshorn Health Center, especially Nicole Dixon, PBT (ASCP), for providing phlebotomy.

DEDICATION

This work is dedicated to my brothers and sisters who supported me in assisting my inner rose to bloom. Your years of tireless dedication to the greatest of works inspired me even in the darkest of nights.

To my sisters and brothers who held my wings up all these years. Your unconditional love will never be forgotten.

I would especially like to thank Alexander Walker for being my keystone in all that I have accomplished.

To my mother Barbara Simon-Hotalen, who paved the way for me in her life and showed me what it meant to be a strong, determined, and self-reliant woman.

To my beautiful son, I couldn't be prouder of you. Your endless smiles, laughter, and snuggles make every effort worthwhile. You have grown into a young man of integrity and honesty who displays compassion in any circumstance. I hope you continue to grow in light and love.

To Kato, your sweetness has nourished me and keeps me looking forward to the future.

TABLE OF CONTENTS

Abstract.....	ii
Acknowledgements.....	iii
Dedication.....	iv
List of Keywords.....	vi
Introduction.....	1
Hypothesis and Specific Aims.....	2-4
Chapter 1.....	5-80
Literature Review.....	5-80
Chapter 2.....	81-118
Chapter 3.....	119-141
Chapter 4.....	142-172
Chapter 5.....	173-177
Appendix.....	178-196

LIST OF KEYWORDS

Heart Valves

Heart Valve Leaflets

Polymeric Heart Valves

Transcatheter Aortic Valve Replacement

Transcatheter Aortic Valve Implantation

Cardiovascular Medical Implants

Biomaterials

Hemocompatibility

Whole Blood Clotting

Thrombogenicity

Immune Response

Endothelial Cells

Platelets

Leukocytes

INTRODUCTION

Heart valve replacement therapy has become a crucial method of treatment to enhance survival and improve the quality of life of patients with valvular diseases. Heart valves are broadly placed into two categories: mechanical heart valves and tissue-based valves. Despite their overall success they are still plagued with durability and hemocompatibility issues which often result in the need for subsequent replacement and/or life-long anticoagulation therapy. Thus, there is a significant interest in creating heart valve that can address these issues. Polymeric based materials have been proposed for use as heart valve leaflet materials due to their ability to be finely tuned through manufacturing and surface modification to enhance durability, and hemocompatibility. One popular method for enhancing polymeric surfaces is to use biological inspired modifications to mimic the micro-environment of the implant region. Hyaluronan enhancements in particular have gained popularity in the last decade for this purpose. HA is a highly lubricious, anionic polysaccharide ubiquitously found in the human body. It is currently being investigated for a vast array of cardiovascular biomedical applications such as hydrogel based regenerative cell therapies for myocardial infarction, HA-coated stents, and surface modifications of polymers and metals for use in blood-contacting implants. This dissertation addresses the hypothesis that a novel heart valve leaflet material comprised of a sequential interpenetrating polymer network (IPN) of hyaluronan (HA) and the polymer linear low-density polyethylene (LLDPE) will mitigate coagulation and non-specific immune responses.

HYPOTHESIS AND SPECIFIC AIMS

Hypothesis (1): Enhancement of linear low-density polyethylene (LLDPE) with a 2% silyl-high molecular weight hyaluronan (HA) solution will produce a non-toxic surface that will reduce blood protein and cellular adhesion thereby reducing hemostasis and immune response as compared to virgin LLDPE, and pro-coagulant PS.

Specific Aim 1: Determine the effect of 2 % solution enhanced HA-LLDPE surfaces on cytotoxicity, the behavior of protein adhesion, platelet adhesion, activation, and aggregation, coagulation cascade contact activation, and whole blood clotting kinetics. This research is discussed in **Chapter 2**.

- (a) Use a lactate dehydrogenase assay (LDH) to determine if HA-LLDPE is cytotoxic to plasma cell components.
- (b) Investigate the effect of HA-LLDPE on whole blood clotting kinetics quantified via free hemoglobin concentration.
- (c) Investigate clotting on surfaces using thrombin generation assaying.
- (d) Investigate clotting on surfaces using thrombin-anti-thrombin assaying.
- (e) Investigate contact activated thrombosis on HA-LLDPE surfaces via contact activation assay.
- (f) Investigate the effects of HA-LLDPE on platelet adhesion on surfaces visualized through Calcein-AM staining.

- (g) Qualitatively investigate platelet morphology and aggregation on HA-LLDPE surfaces using scanning electron microscopy to determine amount of platelet activation/adhesion.
- (h) Quantitatively investigate platelet activation via platelet factor 4 assaying.

Hypothesis (2): Enhancement of linear low-density polyethylene (LLDPE) with a 2% silyl-high molecular weight hyaluronan (HA) solution will produce a non-toxic surface that will reduce blood protein and cellular adhesion thereby reducing immune response as compared to virgin LLDPE, and pro-coagulant PS.

Specific Aim 2: Determine the effect of HA-LLDPE on the behavior of the immune system. This research is discussed in **Chapter 3**.

- (a) Investigate the effect of HA-LLDPE on fibrinogen adsorption as compared to LLDPE and PS.
- (b) Investigate the effect of HA-LLDPE on the adherence of leukocytes, visualized with actin/DAPI co-stain.
- (c) Investigate the effect of HA-LLDPE on complement system activation by quantifying Scb-59 through assaying.

Hypothesis (3): Enhancement of linear low-density polyethylene (LLDPE) with a 2% silyl-high molecular weight hyaluronan (HA) solution will produce a non-toxic surface that will placate endothelial attachment and proliferation.

Specific Aim (3): Determine the effects of HA surfaces on endothelial cell growth, proliferation, and maintenance. This research will be discussed in **Chapter 4**.

- (a) Investigate the effect of HA-LLDPE surfaces on the functionality (adhesion, proliferation, viability, and morphology) of endothelial cells through assaying and cell staining.
- (b) Investigate the effect of HA-LLDPE surfaces on the endogenous protein expression of endothelial cells.

CHAPTER 1

LITERATURE REVIEW

1.1. Impact of Cardiovascular Disease in the U. S.

In 2017, the National Health and Nutrition Examination Survey (NHANES) reported that approximately 92.1 million American adults suffer from at least one form of cardiovascular disease (CVD) ¹. 2014 mortality data notes CVD accounts for 30.8% of all deaths with approximately 2,200 Americans passing from CVD complications daily (See **Table 1.1**) ^{1,2}. CVD renders an exceptional financial burden upon the United States. Direct medical costs by 2030 are projected to reach \$818 billion with indirect costs ballooning to \$276 billion ¹. Comparatively, the total direct and indirect costs of CVD from 2012-2013 were estimated to be approximately \$316 billion ¹.

While CVD remains the number one cause of death in the United States, it has witnessed a decline in recent years. Between 2004 and 2014, deaths attributed to cardiovascular disease (CVD) in the U.S. declined by 25.3% ¹. However, the actual number of deaths in which CVD was the primary cause of death only decreased by 6.7% ¹. *Increases in the use of evidence based medical therapies for secondary prevention combined with bulk changes in population lifestyle, and environmental factors have led to the decrease in mortality* ¹⁻³. These include but are not limited to implantable cardiovascular medical devices, ⁴⁻⁷ pharmacological based therapies, ⁸⁻¹² and complementary and alternative medicine ^{13,14}. Due to their success in reducing mortality, it is apparent that continued investigations into innovative and affordable medical based therapies are essential to helping reduce the number of CVD attributed deaths.

Table 1.1: Prevalence of Heart Disease and Mortality 2014 ¹

Population	Prevalence of Heart Disease(%) 2011-2014	Mortality 2014
Both Sexes	36.6	807,775
Males	37.4	408,747
Females	35.9	399,028
Caucasian Males	37.7	320,859
Caucasian Females	35.1	316,843
African American Males	46.0	49,210
African American Females	47.4	48,573
Hispanic Males	31.3	24,875
Hispanic Females	33.3	21,571
Asian Males	31.0	9,784
Asian Females	27.0	9,147

1.2 Cardiovascular Medical Devices

1.2.1 Types of Cardiovascular Medical Devices

Of these key interventions, cardiovascular medical devices have been widely used to assist in improving function of the native cardiovascular system, increase life expectancy, and enhance quality of life ¹⁵⁻¹⁸. 2015 estimates concluded that over 400,000 cardiovascular medical devices are implanted into patients annually in the United States ¹⁹. These include but are not limited to: coronary stents ²⁰⁻²³, heart valve replacements ²⁴⁻²⁷, cardiovascular patches ^{28,29}, cardioverter-defibrillators ³⁰⁻³², pace makers ¹⁹, ventricular assist devices ^{33,34}

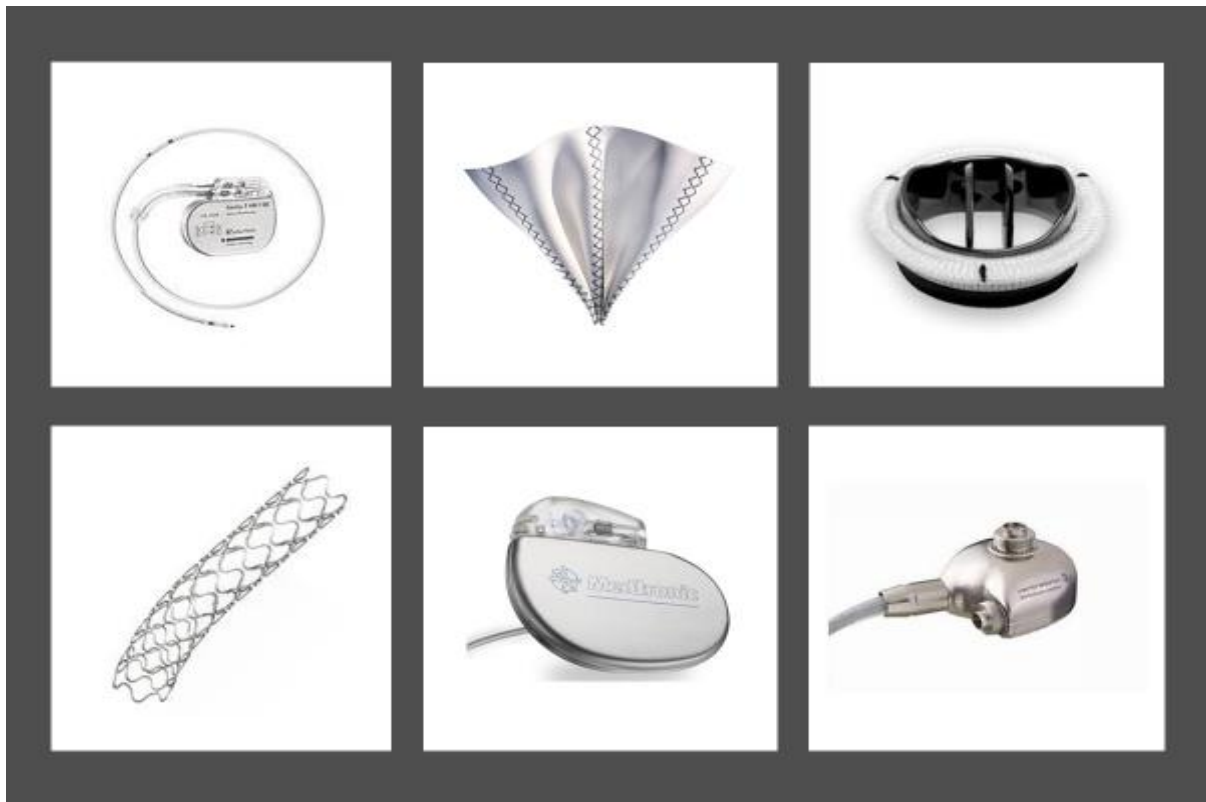


Figure 1.2.1: Examples of widely used implantable cardiac devices to increase mortality and improve quality of life. **Upper (Left):** Biotronik Inc.™ implantable cardiac defibrillator ³⁵ **(Center):** Vascutek® Gelsoft™ vascular patch ³⁶ **Right):** Cryo-Life On-X™ aortic heart valve with conform-x sewing ring ³⁷ **Lower (Left):** Abbot group XIENCE PRIME™ coronary stent ³⁸ **(Center):** Medtronic™ pace-maker ³⁹ **(Right):** Cirtec © left-ventricular assist device ⁴⁰.
Reproduced with permission.

1.2.2 Critical Issues of Cardiovascular Medical Devices

By virtue of their applied therapy, all cardiac medical devices come into some contact with the blood. It is critical that any implantable device be designed to limit adverse blood-contacting related events. **Table 1.2.2** lists the standard length of time for blood interaction with common medical devices. While a myriad of hemocompatible surfaces are consistently being developed, to date, no blood-contacting device or material has attained the optimal hemocompatibility exhibited by the native cardiovascular system⁴¹⁻⁴³. Even with the successes attributed to cardiovascular medical devices, they are still prone to adverse thrombosis, inflammatory responses, infections, and malfunctions. Geometry, regional placement, positioning of the implant, coating enhancements, and bulk material and surface properties, are some of the features that can elicit imbalanced healing responses. Examples include⁴⁴⁻⁴⁸.

- 1) stiffness of materials such as pyrolytic carbon used for mechanical heart valve leaflets which can lead to blood cell lysing as shear stress is heightened during parallel flow across surfaces
- 2) metals used to increase mechanical strength of struts or stents can be particularly thrombogenic due to their surface roughness, chemistry, and topography
- 3) improper choice of surface coatings which can lead to microbial adhesion and proliferation resulting in infections and chronic inflammation

Because medical implants are prone to thrombosis, inflammation, and infection they often require supplemental therapies or treatments to ensure tolerance with the native physiology.

While these treatments may mollify adverse device related complications, supplemental therapies present their own risks. For example, prolonged use of requisite antibiotics can lead to antibiotic resistance, while anticoagulants and anti-platelet therapies leave patients at risk for

bleeding and other complications ⁴⁹⁻⁵¹. Even with the assistance of drug-related therapies, thrombosis due to biomaterial-blood related interactions remains a key issue. Thromboembolism is the most common adverse event stemming from blood-contacting materials and devices ⁵²⁻⁵⁴. Thrombosis and related events are still seen as major complications in vascular grafts, left-ventricular assist devices, bioresorbable scaffolds, pacemakers, defibrillators, stents, and heart-valve replacements ⁵⁵⁻⁶⁰. Thus, it is essential to develop biomaterials and implants that can reduce or negate the need for supplemental therapies and inhibit unfavorable blood related consequences to ensure the least risk to patient health.

Table 1.2.2: Common Time Lengths of Blood Contact on Cardiovascular Devices ⁶¹

(Reproduced with permission)

Device	Time
Catheters	Mins to Days
Guidance Wire	Mins to Hours
Extracorporeal Device	Hours
Pacemakers	10 Years
Vascular Graft	Lifetime
Heart Valve	Lifetime
Stent	Lifetime

1.3 Heart Valve Technology

1.3.1 Heart Valve Replacement Therapy

Heart valve replacement therapy (HVRT) has become the most effective treatment to enhance survival and improve the quality of life of those suffering from severe valvular degeneracies. Valve substitutes are one of the most frequently used implants world-wide ²⁷. Surgical procedures for aortic valve disease alone are the second most common cardio-thoracic surgery in the U.S., and approximately 300,000 procedures are performed per annum world-wide ⁶². Despite the overall success of these implants, even the most advanced heart valves (HV) on the market are plagued with issues such as durability, hemolysis, pannus tissue growth, thrombosis, and calcification often resulting in the need for subsequent replacement and/or life-long anticoagulation therapy ¹⁻³.

1.3.2 Mechanical Heart Valves

Current HVs on the market are broadly placed into two categories: mechanical heart valves (MHV; **Fig. 1.3.2a**) and tissue-based heart valves (TBV; **Fig. 1.3.2b**). MHVs made with synthetic leaflets have been on the markets since the 1970's. They have proven to be highly durable, usually lasting the life of the patient, but can also be exceedingly thrombogenic ⁶³. While the leaflets in MHVs are now made of materials such as pyrolytic carbon that are resistant to thrombosis, the rigid leaflet and hinge design can result in hematocyte lysis, as well as localized regions of turbulent flow, and stasis facilitating thrombus formation ^{6,46,64}. Consequently, obstructive thrombosis in MHV patients occurs at a rate of 0.3-1.3% patient years with thromboembolic events and complications being reported at a rate of 0.7-6 % patient years, even with the use of blood-thinners ⁶⁵.



Figure 1.3.2a: Examples of mechanical heart valves **Left)** Star-Edwards caged ball valve ⁶⁶ **Center)** Medtronic open pivot bileaflet valve ⁶⁷ **Right)** Björk–Shiley tilting disk valve ⁶⁸. **Reproduced with permission.**

While MHV replacement therapy leads to a general increase in life-span and quality of life compared to the natural progression of untreated conditions, the requisite use of chronic anticoagulation therapy potentiates many complications including but not limited to, hemorrhagic events, skin necrosis, hair loss, jaundice, rash, bloating, and diarrhea ^{64,65,69}. Thus, while MHVs offer the longevity that should be expected of an ideal heart valve, other alternatives are often sought out.

1.3.3 Tissue Based Heart Valves

Alternatively, TBVs are composed of animal derived tissue based components offering a thin, flexible, leaflet design similar to the native valve which is vastly more hemocompatible than MHVs ⁶⁴. As a result, patients may be able to reduce or eliminate the need for anticoagulation therapy after the first few months post-surgery. However, thrombosis is still a concern (See **Fig.1.3.3b**). A recent retrospective analysis of 642 patients found an incidence rate of aortic valve clinical thrombosis to be around 2.8% ⁷⁰. Percutaneous valve replacements such as transcatheter heart valve implantation/replacement (TAVI/TAVR) take advantage of the

flexible leaflet design of TBV (See **Fig. 1.3.2.b**). These have been successfully used to decrease the risks associated with open-heart surgery while increasing the ease of serial replacement.

TAVI/TAVR have enjoyed great success in clinical treatment and have progressed from being used only in high risk patients who were unable undergo open heart surgery to low and intermediate risk patients ⁷¹.



Figure 1.3.2b: Examples of tissue-based heart valves **Left)** Bicor™ porcine aortic heart valve ⁷² **Center)** Edwards Sapien 3™ bovine tissue heart valve ⁷³ **Right)** Sorin Mitroflow™ aortic heart valve with Phospholipid Reduction Treatment ⁷².

Unfortunately, TBVs are prone to tissue degradation and calcification (as seen in the native valve; **Fig. 1.3.3.a**) making them inappropriate for use in younger patients. ⁶⁴. The latter process has commonly been associated with the cross-linking of tissue with glutaraldehyde to chemically and biomechanically stabilize the tissue and reduce antigenicity ⁷⁴. It is thought the process of stabilization results in calcium ion influx making the leaflets susceptible to mineralization. However, recent studies suggest the fixing process may not completely render the tissue immunologically inert leaving behind residual antigens that elicit immune responses leading to mineral deposition ⁷⁴. Calcification leads to leaflet thickening and stiffness, reduction

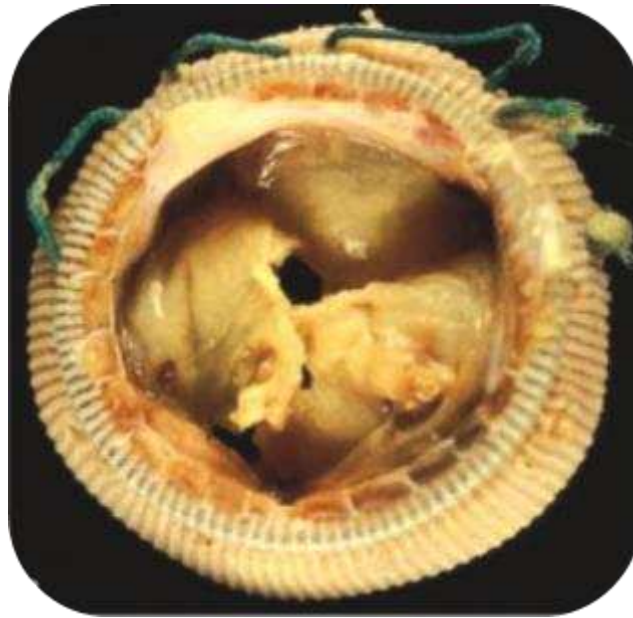


Figure 1.3.3a: Calcified porcine aortic valve

in effective orifice area, increased pressure gradients, leaflet tearing, and in some cases hemolysis^{75,76}. Due to tissue degradation through normal wear and tear, and calcification, TBVs need to be replaced on average every 10-15 years, although the Edwards pericardial valve, determined to be the most durable TBV, has been known to last up to 20 years^{6,77,78}. Any repeated need for any HVRT increases perioperative risks including thromboembolism, stroke, transient ischemic attack, atrial fibrillation, bleeding complications, acute kidney injury, and even death^{13,17,19}. It is apparent that the continued risks to morbidity and mortality associated with both MHVs and TBVs point to a critical need to develop a heart valve which is both hemocompatible and highly durable to mitigate the need for complimentary drug therapies (e.g. anticoagulants) and/or subsequent replacements.

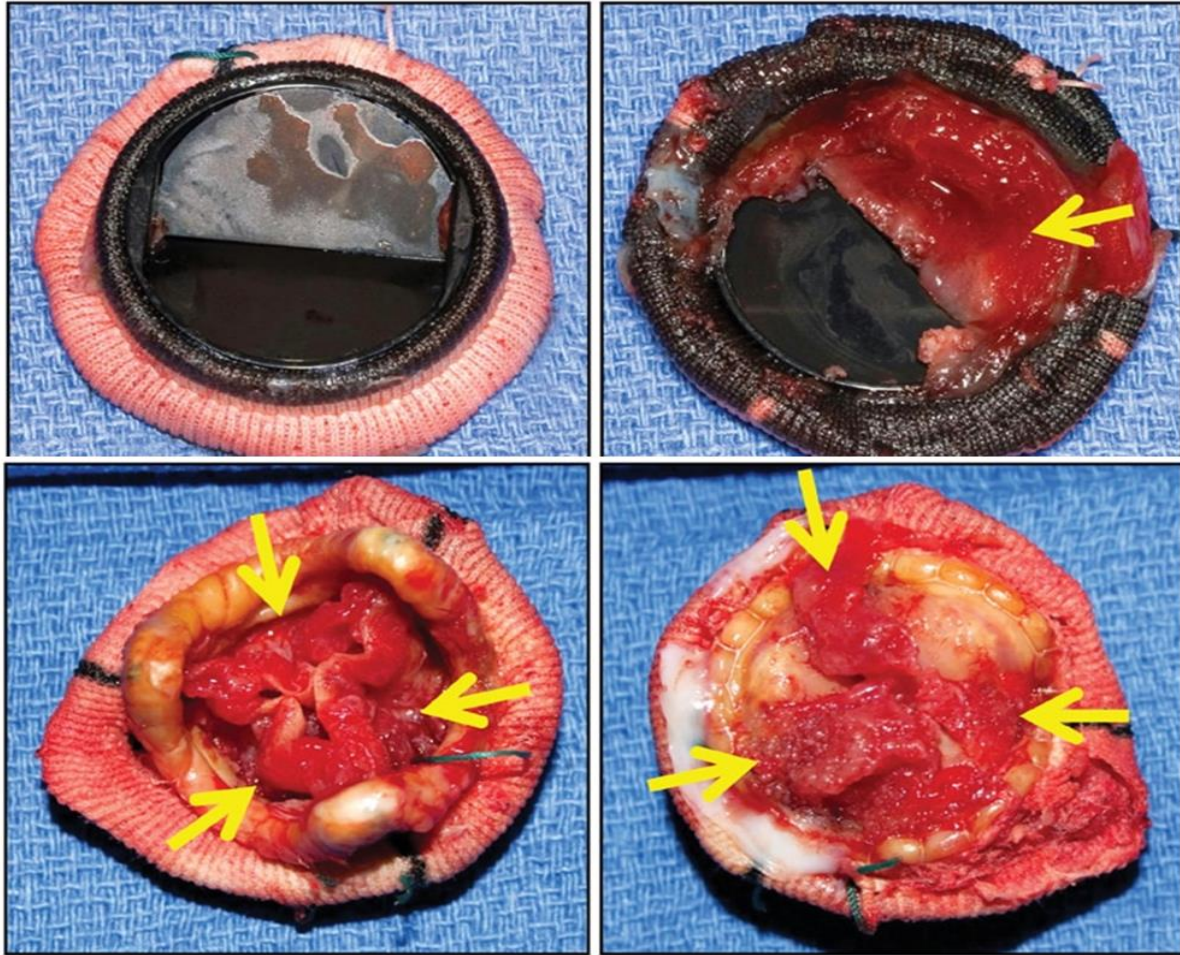


Figure 1.3.3b: (Top): Carbomedics mitral valve prosthesis exhibiting immobilizing thrombus coverage and (Bottom) St Jude trileaflet aortic valve prosthesis presenting with obstructive thrombosis. Arrows indicate thrombus regions ⁷⁹. **Reprinted with permission.**

1.3.4 Polymeric Heart Valves

To address the complications associated with current heart valve designs, polymer-based biomaterials have been widely investigated in hopes of producing leaflets which offer the durability of MHVs and the hemocompatibility of TBVs (**Fig.1.3.4**). Silicone, polyurethane, polyether urethane, polyhexamethylene, polytetrafluoroethylene, and linear low-density polyethylene, are some examples of synthetic polymers which have been utilized for the development of heart valve leaflets ^{27,41}. Polymeric materials have been widely used to generate

superior surfaces which exhibit passivating properties at the blood-biomaterial interface in various cardiovascular applications^{27,41,43,80-83}. The durability of polymers and their ability to be modified through manufacturing and surface engineering allows them to be employed in low or high flow/pressure environments, space filling, wound healing, and cell delivery procedures, among others^{54,84}. The potential benefits of PHVs include^{6, 18,19,63}:

- Enhanced longevity and durability similar or better than MHV
- A thin, flexible, leaflet design which mitigates rigid leaflet lysis
- Percutaneous deployment
- The ability to be finely tuned through proprietary blending and surface modification to reduce or promote cellular adhesion
- Improved hemodynamics due to a high profile and large effective orifice area
- Greater biostability and resistance to calcification and oxidation
- Low cost

Advantages of PHVs are ultimately determined through the combination of the base material, method of fabrication, and modifications⁶³. Early PHV technology suffered from a vast number of issues due to the available polymers at the time which led to issues such as stiffness, tearing,



Figure 1.3.4: Polymeric heart valve developed by Dasi group at Colorado State University

and calcification⁶³. Advances in polymer sciences leading to improved durability of materials and enhanced surface properties has inspired a renewed interest in PHV development²⁷. Yet, while current PHVs have all the physical properties present to lend themselves to the fabrication of an ideal valve, like other biomaterials they tend towards thrombogenicity^{6, 18}. Unlike MHVs whose proclivity for thrombosis is dependent upon valve and flow profiles combined with a rigid leaflet, the affinity for thrombosis in PHVs is contingent upon the inherent surface properties of polymers such as hydrophobicity and charge⁵³. However, the nature of polymers makes them highly amenable to surface alterations which can decrease these proclivities.

1.3.5 Surface Modifications Strategies for Heart Valve Leaflets

To address the thrombogenicity of materials, one of the many methods that cardiovascular biomaterial research has sought to utilize is the modification of surfaces. Surface modifications alter key characteristics of the material exterior such as roughness, topography, charge, wettability, and free energy which affect biological interactions at the interface and determine hemocompatibility (See **Fig. 1.3.5a**)⁸⁵. Mechanical etching, diamond-like carbon thin films, plasma-enhanced chemical vapor deposition, and alkyl-siloxane monolayers on silicone rubber are just a few of the techniques being explored as passivating agents for hemostatic and inflammatory responses^{82,86-88}. One specialized area of research is to modify surfaces with biological components. The hope is to achieve material interfaces which mimic the microenvironments experienced by blood components or inhibit specific portions of the healing cascades to reduce hemostatic end-points. Examples of these include heparin eluting stents, phosphorylcholine coatings on extracorporeal circuits, albumin coated surfaces, glycocalyx inspired nitric oxide releasing surfaces, and hyaluronan enhanced surfaces^{89,90,91}.

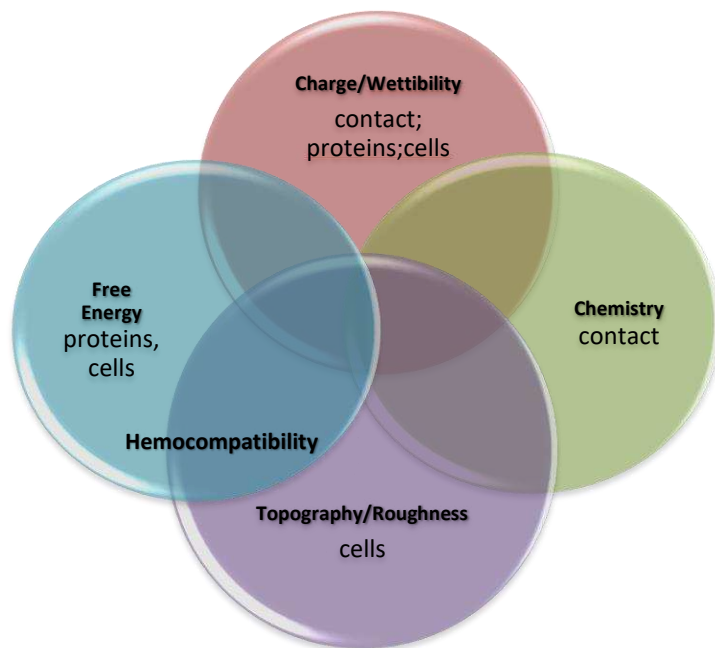


Figure 1.3.5a: Surface properties of biomaterial affect protein adsorption, cell adhesion, and contact activation which intimately work together to determine hemocompatibility.

Heart valve leaflet technology has taken advantage of surface modification technology to improve leaflet materials. Phospholipid-modified polystyrene–polyisobutylene–polystyrene (SIBS) triblock polymer for use in artificial heart valves reduce platelet adhesion ⁹². Diamond-like carbon films and derivative modifications have been found to be chemically inert, hard, wear resistant, and biocompatible ^{86,93,94}. Covalently bonded hirudin protein to PET and Dacron has been shown to reduce platelet adhesion and activation, reduce adverse fibrinogen conformation, and thrombus (See Fig. **1.3.5b**) ⁹⁵. Polyurethane valves with immobilized fibrinolytic enzyme, lumbrokinase was shown to reduce thrombus formation ⁹⁶. These are just a few examples of the many approaches being taken in contemporary science to modify surfaces for superior performance in heart valve technology. In particular, hyaluronan (HA) enhanced surfaces are gaining interest for their thrombo-passivating properties. In this manuscript we investigate the hemocompatibility of a novel polymer for use in heart valve leaflet technology; linear low-

density polyethylene enhanced with hyaluronan (HA) to increase hemocompatibility. This is discussed in further detail below.

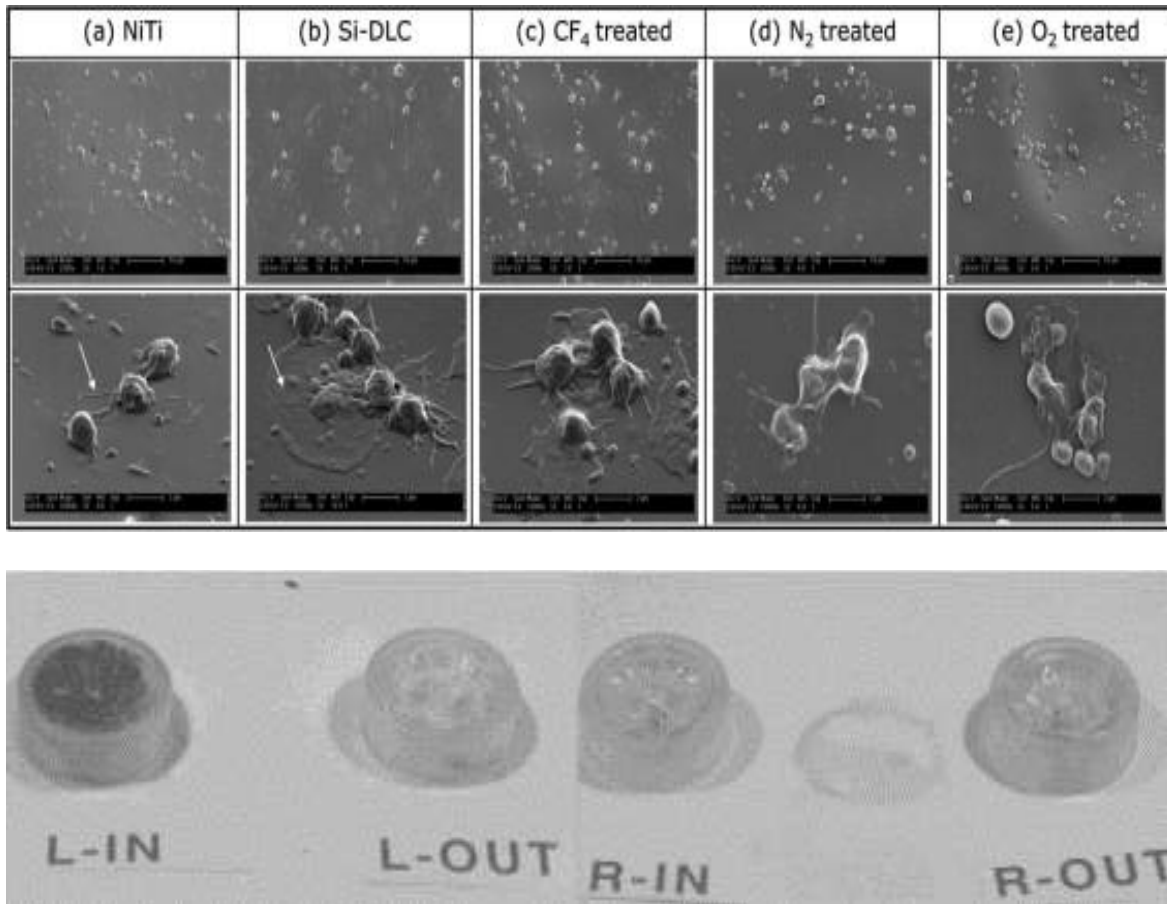


Figure 1.3.5b: Hemocompatibility results of surface treated biomaterials for cardiovascular applications. **Top)** N₂ and O₂ Silicone incorporated diamond thin films exhibit less platelet adhesion and activation than nitinol and untreated silicone enhanced diamond thin films ⁹⁴ **Bottom)** Polymer valves treated with lumrokinase for total artificial hearts exhibit minimal thrombosis ⁹⁶.

1.4 Linear Low-Density Polyethylene

Linear low-density polyethylene (LLDPE), is a polymer containing many straight, short branched chains with densities ranging from 0.915 to 0.935 g/cm^3 ⁹⁷ (See **Fig. 1.4**). It is considered a medical grade plastic and is biologically stable ^{97,98}. LLDPE is commonly made by copolymerizing ethylenes with long chain olefins. The length of the polyolefin chains impart

density with higher degrees of branching corresponding to lower densities ⁹⁸. LLDPE is part of the same family as ultra-low-density polyethylene, very low weight polyethylene, medium chain polyethylene, and high chain polyethylene ⁹⁷. It is well known for its high tensile and tear strength, puncture resistance, low bending stiffness, and low-shear stress sensitivity making it suitable for a wide range of cardiovascular applications including patches, grafts, and heart valve leaflets ^{41,99}. Currently it is being explored as an alternative to mechanical and bioprosthetic heart valve leaflets ⁴¹. Investigations for use in heart valve leaflets reveal that it exhibits hemodynamic properties on par with current industry grade bioprosthetic heart valves ⁴¹. Because of its properties it is a good candidate for a heart valve leaflet material that will offer a flexible leaflet design to limit rigid leaflet lysis, be usable in percutaneous deployment, and be amenable to surface modifications to enhance its hemocompatibility.

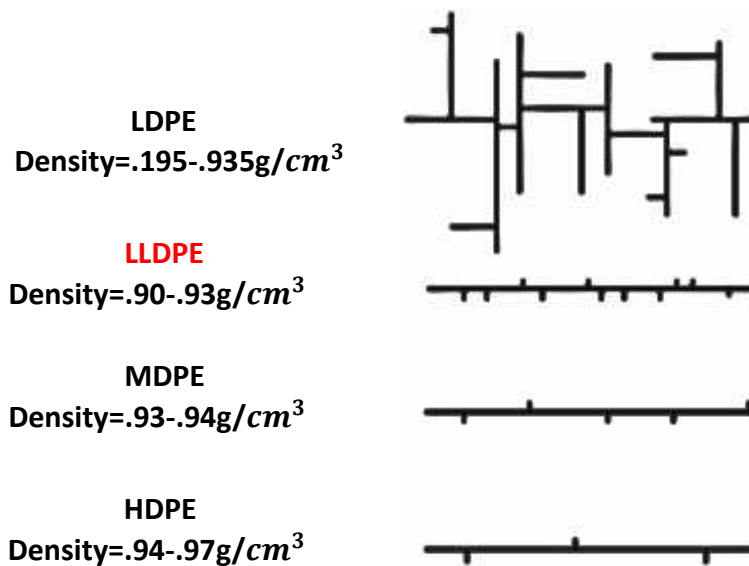


Figure 1.4: The length of polymer chains imparts specific material properties. Higher degrees of branching result in lower densities ⁹⁷.

1.5 Hyaluronan

1.5.1 The Structure and Function of Hyaluronan

Hyaluronan (HA) is a high molecular weight (HMW), hydrophilic, glycosaminoglycan found ubiquitously in higher order animals, especially in the extracellular matrix, viscera, synovial fluids, and apical surface of endothelial cells¹⁰⁰⁻¹⁰³. Intracellular HA has been found to also exist in the cytoplasm, nucleus, and nucleolus^{100,102,104,105}. It is composed of repeating polymeric glucuronic acid and N-acetyl-glucosamine disaccharides conjugated by a glucuronicidic $\beta(1\rightarrow3)$ bond and hexosaminidic $\beta(1\rightarrow4)$ bridges (See **Fig 1.5.1**)¹⁰³. The polymer is secured through parallel hydrogen bonds running the length of the chain axis rendering an inflexible, helical

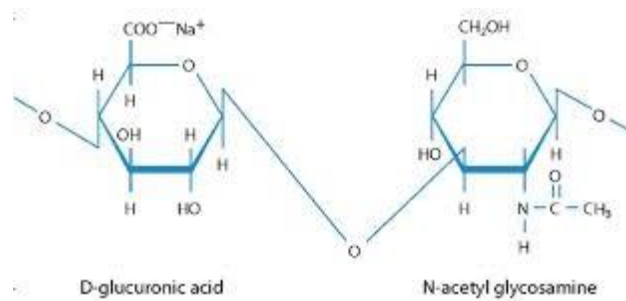


Figure: 1.5.1: Structure of hyaluronan

architecture¹⁰⁶. Its tightly coiled structure allows it to mechanically trap up to one-hundred times its weight in water i.e. the majority of the water is not trapped through hydrogen bonding but is immobilized through the tight helical configuration^{104,106}. Because of its highly anionic nature, HA attracts positive ions that generate an osmotic imbalance causing water to be drawn in towards the molecule¹⁰².

\

1.5.2 Hemocompatibility and Hyaluronan

HA is nontoxic, biodegradable, and non-immunogenic^{100,104}. It is an essential component of the cardiovascular system beginning from its use in embryonic cardiac development, to assisting in wound healing cascades, tissue regeneration, repair, and angiogenesis, and is a key component of heart valve leaflets^{101,102,106}. HA chain length is pertinent to its interaction with biochemical and cellular components of the cardiovascular system (See **Table 1.5.2**). High molecular weight HA (HMW-HA) can reach up to 10^7 kDa in somatic tissues and range between 10^5 and 10^7 Da in the extracellular matrix¹⁰⁷. After injury hyaluronidases cleave HMW-HA (~4000 kDa) into low molecular weight HA (LMW-HA) fragments (~ 100-500 kDa) thus exposing binding sites which have an affinity for proteins such as fibrinogen and allows for migration and proliferation of endothelial cells through the stimulation of Toll-like receptors^{102,103}. LMW-HA has been shown to better support endothelial growth, proliferation, migration, and normal morphology than HMW-HA, and to stimulate angiogenesis, however it is also implicated in exacerbation of immune response by producing pro-inflammatory mediators¹⁰⁸⁻¹¹⁰. In contrast, HMW-HA inhibits platelet, macrophage, and smooth muscle cell adhesion, imparting anti-coagulant, anti-hyperplasia, and anti-immune effects. However, very high molecular weight HA also mitigates endothelial adhesion and migration, both crucial to supporting endothelialization of implanted biomaterial surfaces. Both HMW-HA and LMW-HA mitigate plasma protein adsorption as well as platelet adhesion and activation in hemocompatibility studies^{99,108,111-113}. The manipulation of chain length thus potentiates a wide range of cardiovascular biomaterial applications dependent upon the desired outcome.

Table 1.5.2: Effect of HA MW on Hemocompatibility.; Abbreviations are as follows: (1) branched polyethylenimine (PEI) incorporated into the PU backbone (2) polyurethane (3) titanium (4) co-polymerized polydopamine and hexamethyldiamine; **References:** Rammamurti et al. ¹¹⁴, Amarnath (platelets) ¹¹⁵, Chuang et al. ¹¹⁶, Ruiz et al. ¹¹¹, Li et al. ¹¹⁷, and Li et al. ¹⁰⁹.

<i>Reference</i>	<i>Base Material</i>	<i>Enhancement</i>	<i>MW (kDa)</i>	<i>Outcome on HA Surfaces</i>
114	Hylans	UV scission *	1500	+ Irradiated HA gels showed significantly higher levels of cell attachment +Cells attached to unmodified hylan gels were rounded and non-proliferative +Cells attached to UV modified were either highly extended or irregular in shape.
115	Hylans	UV scission	1500	+HMW-HA and UV-HA showed significantly less platelet attachment/activation, PF-4, and coagulation as compared to control group
				+HA 4.7 and HA 64 supported the best cell adhesion

116	PU-PEI films (1)	Tethered HA	4.7 64 104	<p>+HA 4.7 supported the best proliferation and morphology</p> <p>+HA 104 supported adhesion and spreading, but not proliferation</p>
111	PU (2)	PU-HA	4.7 9.7	<p>+LMW- HA, supported better EC growth than HMW-HA.</p> <p>+Protein adsorption (FBS) was 50-70% less on HMW-HA.</p> <p>+Platelet adhesion was less on HMW surfaces</p>
117	Ti (3)	Co-immobilized collagen IV-HA	1000	<p>+Ti treated only with HMW-HA exhibited the least amount of cell adhesion</p> <p>+500 Collagen +Ti supported best cell adhesion, and morphology</p> <p>+HMW-HA exposed cells exhibited shrunken morphology</p>

109	PDA/HD (4)	Immobilized HA coating	4 100 500	+Platelet attachment decreased as HA MW increased +100kDa HA supported best HUVEC attachment, proliferation +100kDa and 500kDa supported the least amount of macrophage
-----	-----------------------	-----------------------------------	--------------------------	--

1.5.3 Uses of Hyaluronan in Cardiovascular Applications

Native HA presents with poor mechanical properties and must be modified for use in biomaterial applications ¹⁰³. The two most common methods for modification include 1) auto-crosslinking in acidic, neutral, or alkaline conditions producing non-covalent interactions which easily dissociate and can be used for example, in hydrogels needing to disintegrate in vivo ^{103,118} and 2) photopolymerization, and chemical cross-linking through use of such methods as benzoyl cystein derivatives, glutaraldehyde, and xylenes to generate stronger bonds to base materials ^{119,99,103,120,121}. HA conjugates allow biomaterials to be combined with other constituents to further fine-tune effects. Some examples include HA-collagen, HA-chitosan, Collagen II-HA-chondroitin 6 sulfate tri-copolymers, and superoxide-dismutase HA-conjugates ^{113,122,123,84}. The amount and method by which the surface is modified with HA has been found to be critical in developing an optimal biocompatible surface. Excess free HMW-HA attracts the enzyme hyaluronidase which cleaves HA to its low molecular weight state allowing it to interact with blood cells and biomolecules that stimulate thrombosis and inflammation ¹²⁴. Current HA

enhanced surfaces for cardiovascular applications are still in their developmental phase and the data for long-term durability of current HA enhanced surfaces are limited. Previous research has found significant losses of HA under enzymatic digestion and exposure to shear stress during in vitro and in vivo experimentation, concluding current applications may be ineffective for cardiovascular applications such as heart valve leaflets, stents, vascular patches, and vascular prosthesis^{111,124}. Thus, while current HA-enhanced blood contacting materials have shown promise for use in cardiovascular applications, it is essential to consider HA enhancements which are permanent and stable.

1.6 Overview of Dissertation

The relationship between hemocompatibility and surface properties on various implant surfaces is well documented^{54,80,87,89,90,125-127}. Upon initial contact of an implant with the blood, proteins readily attach to the surface forming a bioactive interface that mediates between the implant and the hemostatic response. Surface properties of biomaterials govern the adsorption of proteins and subsequent attachment of cells that can lead to implant rejection and thrombosis¹²⁸⁻¹³². Controlling the interfacial adsorption of proteins and cells through manipulation of surface chemistry, surface charge, and/or wettability can attenuate the provocation of the immune response and coagulation cascades. One method that has gained popularity has been the addition of hyaluronan to various materials for the purpose of reducing thrombosis, inflammation, and to modulate endothelialization on implant surfaces^{99,107,124,133-135}.

This dissertation focuses on the primary hypothesis that *high molecular weight hyaluronan enhanced linear low-density polyethylene will present a hemocompatible surface to cardiovascular tissue components that will mitigate coagulation and inflammatory responses,*

and limit endothelialization making it suitable for heart valve leaflet applications. To achieve the desired surface properties, a “sequential-interpenetrating network” of HMW-HA in linear low-density polyethylene (LLDPE) was fabricated by the James Lab at Colorado State University. Surface enhancement was achieved by cross-linking HMW-HA (~ 750 kDA) to itself within the molecular structure of LLDPE, creating a permanently integrated surface that is anionic, hydrophilic, and proposed to be hemocompatible. This dissertation will explore the underlying mechanisms by which the HA-LLDPE surface interacts with cardiovascular tissue components including blood constituents and endothelial cells. To understand the interaction blood components and cells experience at the biomaterial surface a review of the mechanisms involved in the healing process as modulated by biomaterial surfaces is necessary.

1.6.1 Hemocompatibility Assessments

Hemocompatibility of a biomaterial can be defined as the ability of a foreign material to modulate blood and immune reactions in a manner that facilitates advantageous healing responses and mitigates/negates adverse effects such as exacerbated inflammation, thrombosis and implant rejection. When determining the hemocompatibility of a material it is essential to take into the account the intended use of the material. For example, material compatibility with blood and its constituents can be vastly different depending on flow characteristics in the local environment, the state of the endothelium, and blood composition of the patient⁵³. In addition, testing methods need to be cost-effective, reliable, and give some understanding of what can be expected once the material is implanted.

Blood provides several functions including shuttling nutrients, removing waste, and initiating healing responses in the body. The latter consists of the coagulation and immune

cascades comprised of many proteins, enzymes, cell components, and signaling molecules that work intimately together. When determining the hemocompatibility of a material it is vital to ascertain these cascading events with respect to each other, the environment, and the material characteristics. Thus, there is much to be considered when assessing these complex and inter-related events. However, there have been a number of evaluations developed that provide proven methods for ascertaining a general understanding of a material's hemocompatibility. These vary based on the aim of the studies. Industry standards require a demonstration of a biomaterials conformity to ISO standards to assess thrombosis, hematology, and immunology¹³⁶. While basic science focuses primarily on the interaction of a material with the blood components and molecular modulation to determine why the observed reactions occur⁵³. As the aim of these hemocompatibility evaluations were to ascertain the feasibility of HA-LLDPE to be used in industry heart-valves a mix of basic science evaluations at the blood component and molecular level as well as ISO compatible evaluations were chosen. The following is a list of the test methods utilized in these assessments:

Hemocompatibility

- Lactate Dehydrogenase Assay: establishes if materials are inherently toxic to plasma cells
- Whole Blood Clotting: imparts an understanding of how materials may affect whole blood clotting when all blood constituents are present
- Platelet Adhesion/Activation: determines how platelets interact with material surfaces
- Platelet-Factor 4 Expression: indicates the amount of platelet activation due to material surface exposure
- Contact activation: ascertains the magnitude of contact activation due to materials

- Thrombin Anti-thrombin (TAT) Complex Formation: indicates the amount of thrombin formation due to platelet interactions and contact activation
- Thrombin Generation: determines the speed of thrombin generation on surfaces
- Hemolysis: determines the amount of erythrocyte cell lysis due to material properties and characteristics such as surface properties and leachables.

Adaptive Immune Response Evaluations

- Fibrinogen Binding: determines the amount of fibrinogen bound to the surface which affects non-specific immune response cascades
- Leukocyte Adhesion: determines leukocytes interaction with the material surface
- Complement Activation: evaluate the expression of terminal complex, SC5b-9.

The following sections will review the fundamentals of the coagulation and immune response cascades and offer a detailed understanding of the importance and applicability of the above-mentioned investigations.

1.6.2 Coagulation and Immune Responses at the Blood-Biomaterial Interface

Key to a blood-contacting implants' success are the interactions which occur at the blood-biomaterial interface. Hemostasis, inflammation, and endothelialization resulting from blood contact with biomaterials involve a sophisticated interplay of vascular tissue components and enzymatic reactions which must ultimately reach homeostasis for proper implant tolerance^{128,130,137-140}. The enlistment of vascular bulk phase constituents including plasma protein binding, platelet/leukocyte recruitment, and initiation of the contact and complement systems all determine the degree to which these reactions are propagated¹⁴¹. Under normal physiological

conditions, blood remains in contact with the endothelial layer of the cardiovascular system which contains anticoagulant tissue factors, inhibitors, and receptors that suppress the protective functions of blood until an injury occurs^{41,141}. In addition, blood factors essential to the coagulation cascade circulate as inactive zymogens until stimulated by injury (See **Table 1.6.2a**). Upon tissue injury or implantation of a medical device, platelet-mediated responses and plasma-phase pathways initiate the clotting cascade (Fig. **1.6.2b**). Both are dependent upon the surface

Table 1.6.2a: Hemostatic Factors of the Coagulation Schema¹⁴²

Coagulation Factors	Common Names
FI	Fibrinogen
FII	Prothrombin
FIII	Tissue Thromboplastin
FIV	Divalent Calcium Ion
FV	Proaccelerin (Labile Factor)
FVI	Not assigned
Factor VII	Proconvertin (Stable Factor)
Factor VIII	Antihemophilic Factor
Factor IX	Christmas Factor
Factor X	Stuart Prower Factor
Factor XI	Plasma Thromboplastin Antecedent
Factor XII	Hageman Factor
Factor XIII	Fibrin Stabilizing Factor
Plasma Prekallikrein	Fletcher factor
High Molecular Weight Kininogen	Fitzgerald, Williams, or Flaujeac factor
Plasminogen	-

characteristics of the biomaterial, and the regional flow characteristics at the site of implantation

^{130,131,143}. Plasma related thrombosis is facilitated by two branches, the extrinsic and intrinsic

(contact) pathways. These are a series of zymogen to enzyme conversions producing enzymes that catalyze subsequent events in the cascade eventually leading to the production of thrombin⁵³. Vascular tissue damage initiated by acute injury at the site of implantation primarily activates the extrinsic pathway, while blood contact with biomaterial surfaces is generally responsible for the commencement of intrinsic related thrombosis. These two pathways merge into the common pathway which generates thrombin and fibrin¹⁴⁴. Fibrin oligomerizes resulting in a fibrin matrix that traps and activates platelets. Thrombin is a potent activator of platelets⁵³. In order for blood coagulation on biomaterials to occur both contact activation and platelet adhesion and activation must be present^{129,145}. In addition, blood exposure to biomaterial surfaces distributes proteins across surfaces which can activate platelets. Platelet activation then serves to interact with plasma phase while recruiting inflammatory modulators. Leukocytes and platelets reinforce each other driving inflammation, removing pathogens, and forming hemostatic clots. In the following sections, a brief review of the major events in the coagulation and immune response cascades pertinent in biomaterial evaluations will be offered to lay the foundation for the hemocompatibility assessments of investigative substrates to follow.

1.6.3 Biomaterials Activate the Intrinsic Pathway

Contact between blood and biomaterial surfaces initiates the intrinsic pathway of the coagulation system (aptly referred to as the contact activation pathway). FXII (Hageman Factor), the main constituent in contact activation, is a glycoprotein which circulates in the blood as an inactivate zymogen until stimulated¹³⁰. For biomaterial interactions, standard clinical paradigm asserts that intrinsic pathway activation can be initiated by the binding of at least one

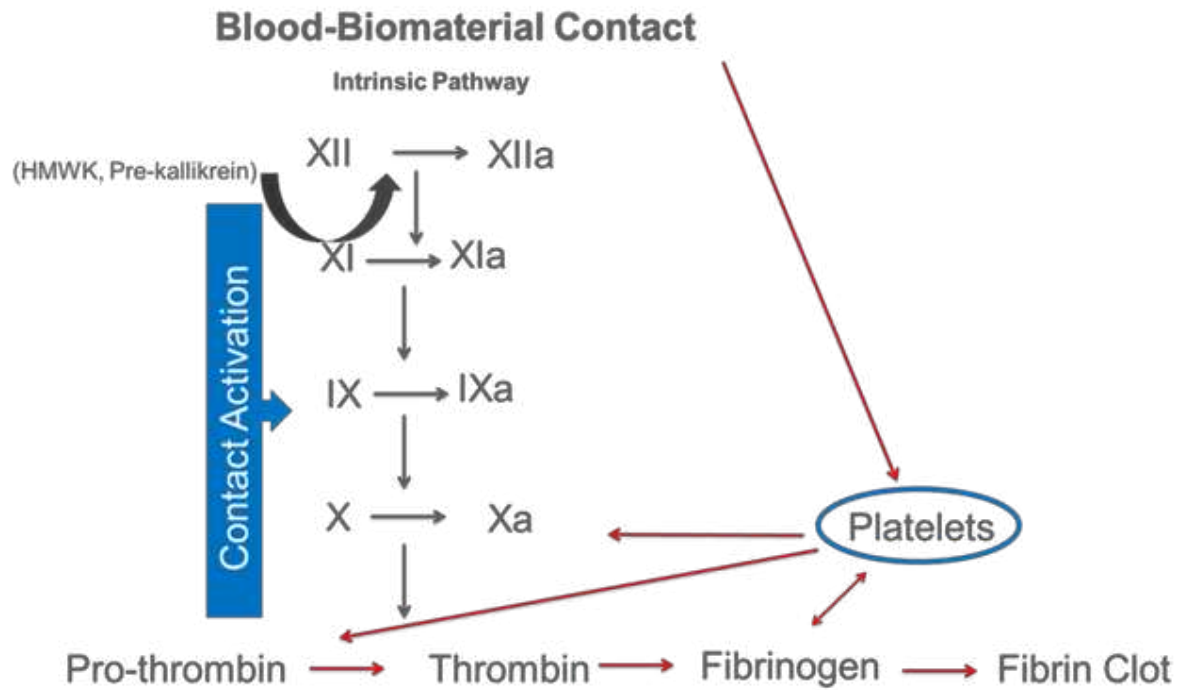


Figure 1.6.2b: Platelet and intrinsic pathway activation of the coagulation cascade

of three zymogens to the material surface which may or may not be converted to active enzymes; Factor XII, which undergoes auto-activation (FXII → FXIIa) upon contact with the surface triggering the cascade; *prekallikrein*, which interacts with FXIIa, initiating a cascade amplifying positive feedback loop; and *high molecular weight kininogen*, which operates as a cofactor for the activation of both prekallikrein and Factor XII^{130,146–148}. The result is the production of the serine protease FIIa (thrombin) which hydrolyzes fibrin. Subsequent fibrin oligomerization renders a matrix which causes plasma to gel thus forming the hemostatic clot. Thus, a pathological thrombus due to blood-biomaterial contact is formed. Contact activation is usually measured by two methods 1) procoagulant activity using plasma clotting assays comparing clotting time against a standard curve of known activators or 2) amidolytic assays which measure the proteolytic cleavage of chromogen by contact activation enzymes⁵³. Pre-kallikrein is the

only one released into the plasma and can be most accurately quantified to determine the magnitude of thrombosis dependent on contact activation for purposes of evaluating hemocompatibility¹⁴⁹.

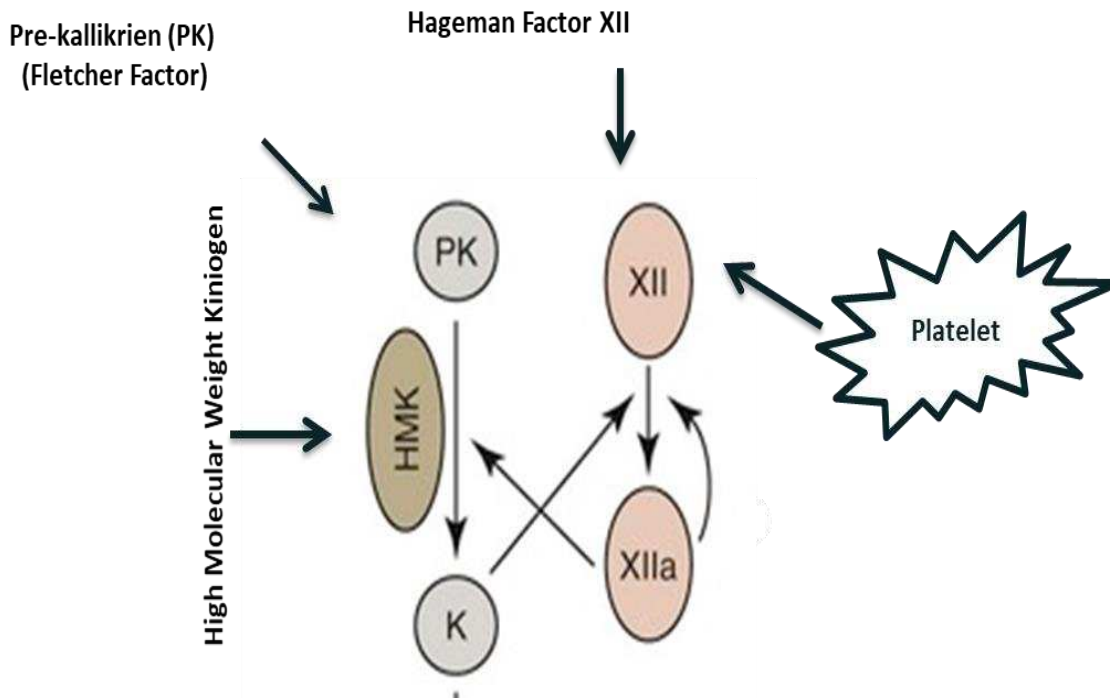


Figure 1.6.3: The intrinsic pathway is activated by the binding of contact proteins that can reinforce each other to progress the clotting cascade.

It has been traditionally accepted that contact activation is specific to negatively charged surfaces⁵³. Multiple domains on the FXII protein chain are implicated in the binding of FXII to negatively charged surfaces; most specifically fibronectin type I, fibronectin type II, and kringle domains¹⁵⁰. It is thought that anionic surfaces induce conformational changes on FXII domains facilitating proteolytic activation¹⁵¹. Studies utilizing platelet poor plasma to mollify cellular effects in coagulation demonstrate that contact activated coagulation increases exponentially with increasing surface energy¹⁵². In addition, natural activating substances which present with

negatively charged characteristics such as activated platelets, microparticles shed from platelets and erythrocytes, collagen, and misfolded proteins have been identified as activators of the contact system^{53,153}. However, recent investigations have revealed that contact activation may not be specific to anionic surfaces as previously assumed^{130,131,148}. Findings suggest, pro-coagulant surfaces may modulate activation of the contact schema through protein competition rather than the formulation of the protein complexes described above. This supports previous investigations which identified that FXII is not preferentially adsorbed onto activating surfaces, but instead become active through protein competition dependent upon the surface features present¹³⁰. Thus, surfaces which promote plasma protein adhesion, especially contact stimulating proteins, may be more likely to enhance intrinsic pathway activation. These contradictory sets of findings illustrate that the exact mechanisms by which biomaterials can activate the contact pathway are still unknown.

1.6.4 Protein Adsorption Determines Future Events of Healing Responses

Initial events after implantation of a blood-contacting device begin with competitive adsorption of proteins at the material surface known as the Vroman effect^{154,155,156}. The architecture of this bio-layer helps determine the long-term success of the implant and is governed by the surface properties exposed to the native physiology. The interplay between surface charge, wettability, free energy, roughness, topography, and chemistry determine the amount and type of proteins adsorbed to the surface, as well as their conformation, density, and orientation¹⁵⁷. Over three-hundred distinct proteins exist in plasma¹⁵⁸. Of these, three proteins dominate and regulate the healing response; albumin, immunoglobulin-G (IgG), and fibrinogen. In addition, proteins implicated in the contact and complement pathways assist in plasma

coagulation at the surface ^{130,159}. Surface competition changes the architecture of the bio-film overtime determining future protein and cell fates at the interface ¹⁵⁵. Initial protein adsorption is dominated by albumin and IgG. Neither play major roles in the activation of the coagulation or immune response cascades, but rather act as carriers of anticoagulant factors and subdue acute inflammation after initial contact with the surface of the implant ¹⁶⁰. Overtime, albumin and IgG tend to be replaced by other proteins such as fibrinogen and von Willebrand factor which encourage platelet mediated responses ¹⁶¹.

1.6.5 Fibrinogen Adsorption Facilitates Coagulation Responses

Fibrinogen (FI) adsorption plays a major role in the healing response. FI promotes the adhesion and aggregation of platelets, binds to the integrins of immune cells, facilitates the formation of hemostatic clots, and plays intimate roles in the contact and complement coagulation cascades ^{108,162}. After adsorption on an implant surface, denaturation and dehydration of fibrinogen promotes strong adherence to the surface thereby increasing the surface area to which platelets and leukocytes can bind (See **Fig.1.6.5**) Previous studies have shown a strong correlation between the rate and amount of fibrinogen denaturation and the severity of inflammation and platelet adhesion ^{139,140,163,164}.

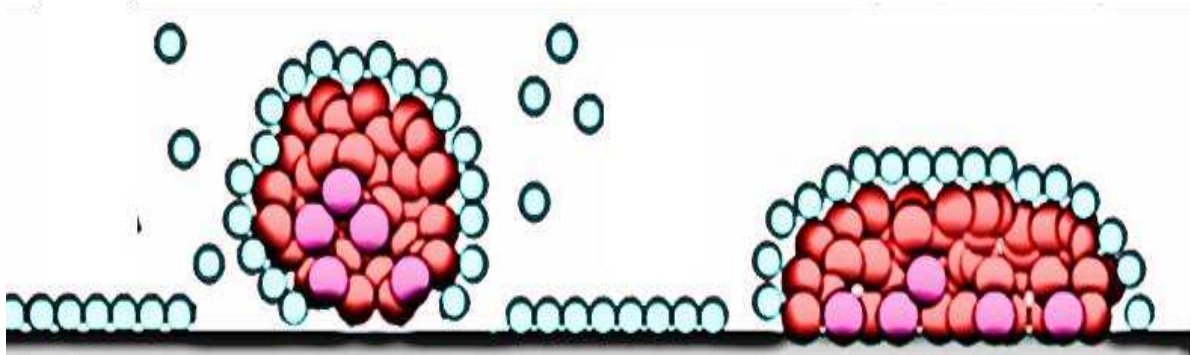


Figure 1.6.5: Dehydration and denaturation of the protein fibrinogen generates a larger surface area on biomaterials for protein and blood cells to adhere to.

Previous studies have noted that conformation changes in fibrinogen may be more important to the subsequent adhesion of plasma cells than total amount of bound fibrinogen^{139,140}. Platelet aggregation triggers conformational transmutation of their glycoprotein GIIb/IIa surface receptors, encouraging platelet adhesion and coupling to fibrinogen adsorbed surfaces. Fibrinogen subsequently cross-links platelets forming bridges between the GIIb/GIIa of adjacent platelets¹⁶⁴. As fibrinogen-platelet aggregates stabilize, platelets secrete their internal storage contents consisting of effector molecules in a process known as degranulation. These exocytotic factors determine future events in subsequent healing cascades including magnitude of coagulation and inflammatory responses. Once platelets bind to a surface they are more likely to be activated through intrinsic and extrinsic pathways of the coagulation cascade. Fibrinogen is then cleaved by the protease thrombin (FII) promoting polymerization followed by the formation of an insoluble fibrin matrix integral to the development of the hemostatic clot. Long strands of fibrin formulate an adhesive net which radiates from the platelets further entrapping those in the immediate surrounding environment. In addition, these insoluble fibrin netting controls the delivery of growth factors essential in the wound healing process¹⁶⁵.

While this process is designed to promote healing, incompatible interface interactions at biomaterial surfaces can exacerbate fibrinogen adsorption, thereby recruiting excessive amounts of platelets leading to increased inflammation and a risk of thrombosis^{139,140}. Assays which determine the amount of fibrinogen bound to the material surface can indicate the proclivity of a surface's thrombogenicity.

1.6.6 Platelet and Leukocyte Adhesion/Activation Play Reinforcing Roles

The bioactive protein layer on a material surface provides the foundation for coagulation/immune responses to take place however, it is the binding and activation of cells to this film that are the key events in their stimulation. Platelet-mediated regimes are essential to the hemostatic process, assisting in the formation of the fibrin clot. Adsorbed proteins are recognized by platelet and leukocyte receptors allowing them to interact and spread across the biomaterial surface. Upon activation, platelets manifest a series of routine modifications that include morphological transmutation, membrane budding, adhesion, aggregation, and degranulation¹⁶⁶⁻¹⁶⁸. To accomplish this, platelets must first be activated either through the binding of plasma proteins or by the molecular production and self-release of activating factors. Various effector molecules which modulate the coagulation cascade are emancipated by platelet bodies containing special secretory organelles known as alpha and dense granules¹⁶⁹. Alpha granules contain polypeptides that bind to thrombin stimulated platelets⁸⁵, hemostatic factors¹⁷⁰, growth factors which promote wound healing and angiogenesis^{171,172}, heparin binding molecules¹⁷³, adhesion molecules which are transferred to the membrane after synthesis assisting in leukocyte and platelet recruitment^{174,175}, and protease inhibitors that augment thrombin

production¹⁷⁶. Dense granules contain platelet recruitment factors such as adenosine diphosphate (ADP), adenosine triphosphate (ATP), serotonin and calcium¹⁶⁹.

Exocytotic movement of storage granules constituents during platelet body transmutation is dependent upon the level of platelet activation. During activation, platelets undergo cytoskeletal dependent membranous shape changes. This commences with the disassembly of the microtubule ring followed by actin polymerization to form dendritic extensions that release chemo-attractants and summon additional platelets to form aggregates and commence production of the platelet plug¹⁶⁶. Five morphological groups of dendritic expressions on implant surfaces have been identified and correspond with increasing levels of activation: *round* (un-activated): disc shaped with no pseudopodia present; *dendritic* (partially activated): early pseudopodia i.e. short reversible dendritic extensions; *spread-dendritic* (moderately activated): irreversible long-dendritic extensions with some spreading, some pseudopodial flattening; *spreading* (fully activated): pseudopodia almost fully flattened, some hyaloplasmic spreading; and *fully spread* (fully activated): no pseudopodia present, full hyaloplasmic spreading (See **Fig. 1.6.6**)^{166,168}.

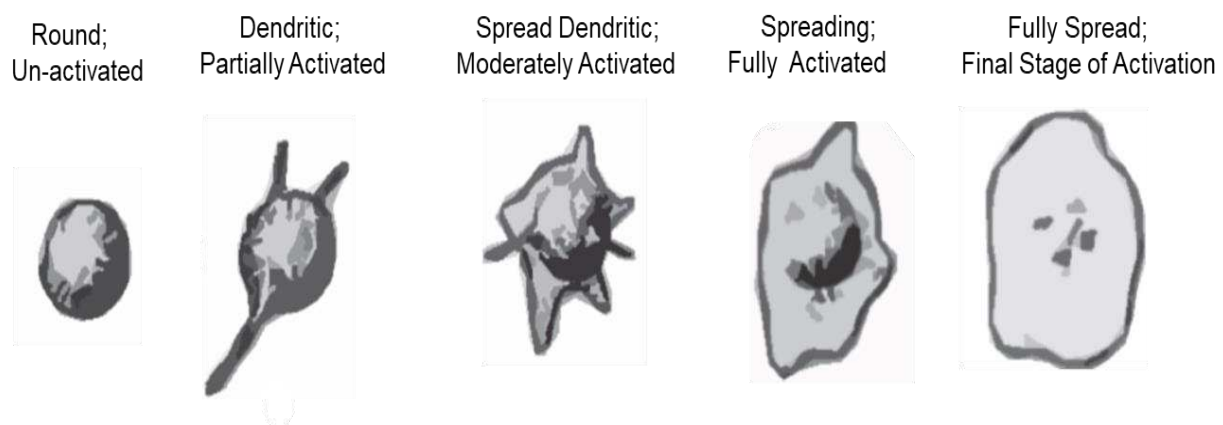


Figure 1.6.6: Stages of morphological change correspond to increasing levels of platelet activation¹⁶⁶.

1.6.7 Resultant Thrombin from the Coagulation Cascade Must Be Measured Indirectly

Once platelets and leukocytes trigger the coagulation system, the protease thrombin (fibrinogenase) cleaves the protein fibrin causing it to polymerize and produce the fibrin clot. During this process, a sequence of biochemical markers is produced which can be measured to determine the extent to which these clotting factors are generated. These include pro-thrombin, which determines the amount of thrombin being generated; and the thrombin-antithrombin-complex (TAT), which determines the amount of thrombin that was inhibited^{177,178}. Although thrombin bound to fibrin is preserved from the inhibition of antithrombin III, and thus omitted from TAT complex integration, it still provides a highly sensitive marker for the activation of coagulation schema. Ideally, testing specifically for the protease would lead to the most accuracy in determining thrombin formation. However, thrombin is rapidly bound and inactivated by antithrombin during the regulatory process. Thus, thrombin can only be measured indirectly through quantification of the cleavage products produced by prothrombin or through the measurements of the TAT complex¹⁷⁹.

1.7 Immune Response on Blood-Contacting Surfaces

1.7.1 The Immune Response is Intimately Connected to the Coagulation Cascade

The capacity to mitigate adverse immune responses to biomaterial surfaces is essential for determining favorable outcomes of implantable biomedical devices. All biomaterials initiate an immune response immediately following activation of the coagulation cascades when implanted into native tissue, marking the first steps in tissue repair¹²⁹. Contemporary implant design is currently seeking to achieve biomaterial surfaces which use the immune response to improve implant patency while mitigating any aggravating effects^{129,180}. Adverse perpetuation of

the immune response can lead to implant rejection, and/or fibrosis of the implant, chronic inflammatory responses, and foreign body giant cells^{137,167,181,182}. Biomaterial surfaces play key roles in the modulation of the immune response in the first two to six weeks after implantation, although risk of foreign body reaction is present for the life of the implant while it remains present in the host¹⁸³. Thus, it is essential to develop biomaterials which modulate the immune response in an appropriate way to support proper functioning of medical implants.

The coagulation and immune responses are intimately connected and co-trigger complementary responses in the healing cascades. Upon platelet activation, conformational changes in the membrane lead to the exposure of high affinity binding sites for fibrinogen which further assists in platelet aggregation and the formation of platelet-leukocyte complexes^{137,184}. In addition, conformational changes in fibrinogen expose integrin sites capable of activating phagocytes. Some evidence has suggested that phagocytes sense fibrinogen as fibrin when in contact with biomaterials which can lead to aggravation of the inflammatory response^{52,129}.

1.7.2 Biomaterials Active Leukocytes

Blood leukocytes consist of neutrophils and monocytes that differentiate into phagocytes and macrophages. However, when in contact with a biomaterial, size disparity between the surface of the material and the leukocyte means that the material is unable to be engulfed by the cell. Instead phagocytes can only release their metabolites and enzymes in an attempt to degrade the biomaterial surface in a process known as *frustrated phagocytosis* (**Fig. 1.7.2**)^{137,185–187}. Under normal conditions, the half-life of these leukocytes is very short (6-8hrs), but upon tissue injury it can be increased by several days¹³⁷. During activation, alterations in membrane receptor affinities occur and inflammatory mediators are released which act as chemo-attractants and

activators for other leukocytes, increasing cell adhesion to surfaces, and activating platelets ¹³⁷. Because foreign surfaces specifically activate platelets and leukocytes, it is important to understand how they interact with biomaterial surfaces as greater adhesion and activation can lead to adverse physiological responses. Evidence has suggested that biomaterials which mimic the extracellular matrix may better modulate the immune response by enhancing or suppressing the normal cell functions dependent upon the biomaterial design. HA is a key component of the ECM and thus HA-LLDPE may serve as an appropriate biomaterial surfaces for the modulation of the immune response in prosthetic heart valve leaflets and other cardiovascular medical devices.

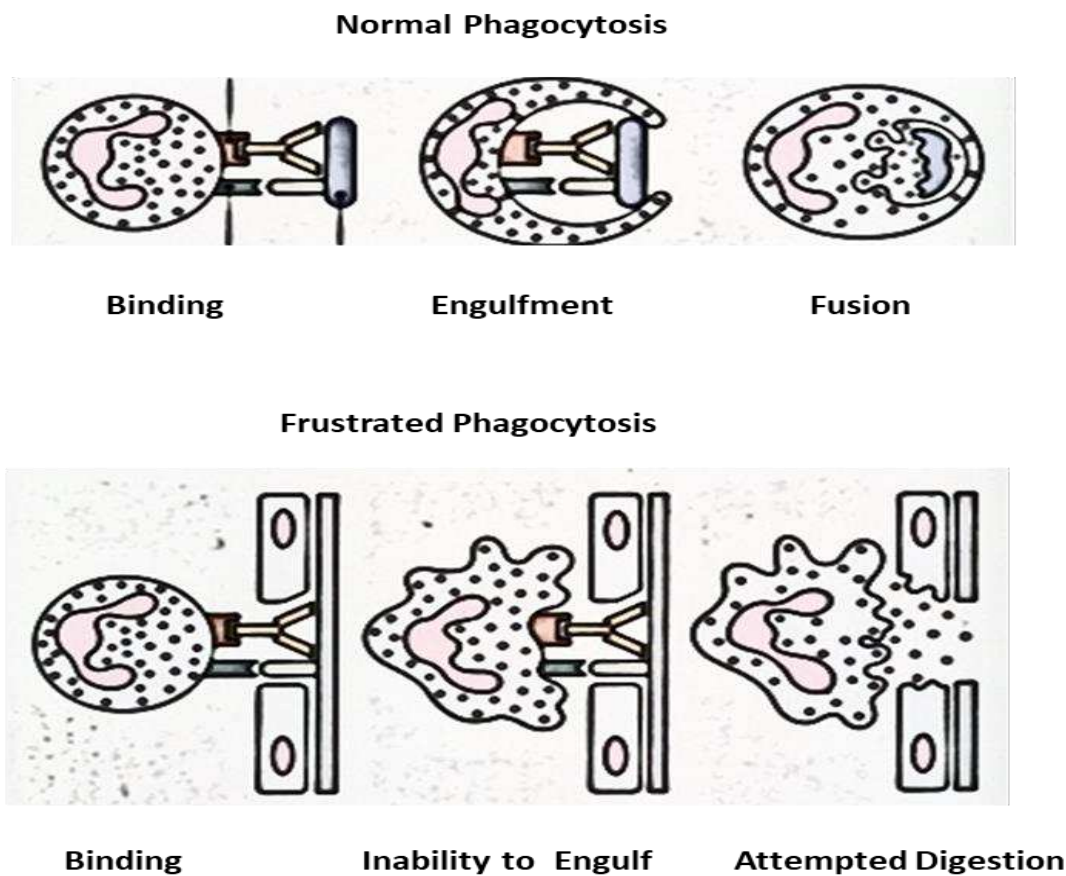


Figure 1.7.2: Frustrated phagocytosis of leukocytes unable to engulf biomaterial due to size disparity.

1.7.3 Complement Activation

Hemocompatibility of biomaterials is predominantly studied in terms of platelet and leukocyte aggregation and activation, although biomaterials are also known agonists of the complement system¹⁵⁹. The complement system is part of the immune response and utilizes both platelet and leukocyte activation to initiate cascades. Complement activation promotes inflammation and assists antibodies and phagocytic cells in the removal of antigens by attacking the cell membrane. The complement system consists of over 30 proteins and protein fragments which include cell membrane receptors and blood serum proteins. Protein interactions opsonize antigens and pathogens and induce a series of inflammatory responses to aid in the healing response¹³².

When in contact with a biomaterial, complement activation is triggered by the alternative pathway with the proteins C3 and C5 being its most critical components. However, some research has indicated that the classical pathway of complement activation may also be involved^{159,147}. Three biochemical pathways are implicated in the complement system: the classical complement pathway, the alternative pathway, and the lectin pathway. The classical pathway is triggered by antigen-antibody immune complexes (specified immune response)^{188,189}. The lectin pathway can be activated by C3 hydrolysis or antigens absent the presence the antibodies (non-specific immune response). Lectin pathway activation uses mannose-binding lectins and lectin ficolins found in plasma which recognize carbohydrate patterning found on microorganisms¹⁹⁰. Unlike the classical and lectin pathways which are activated primarily through the identification of exogenous microorganisms, alternative pathway activation can occur via spontaneous C3 hydrolysis, foreign bodies, biomaterials, pathogens, or damaged cells^{188,189}.

Alternative pathway activation is unique. At normal levels of non-distress the alternative pathway remains operative at low levels to ensure efficient and rapid actuation known as the “tick-over mechanism”^{191,192}. Each complement cascade shares the eventual cleavage and activation of the protein C3, creating C3a and C3b. Alternative pathway C3b is later complexed to protease which cleaves protein C5, shared by the classical pathway. C5a is an important chemotactic protein, helping to recruit inflammatory cells^{188,189}.

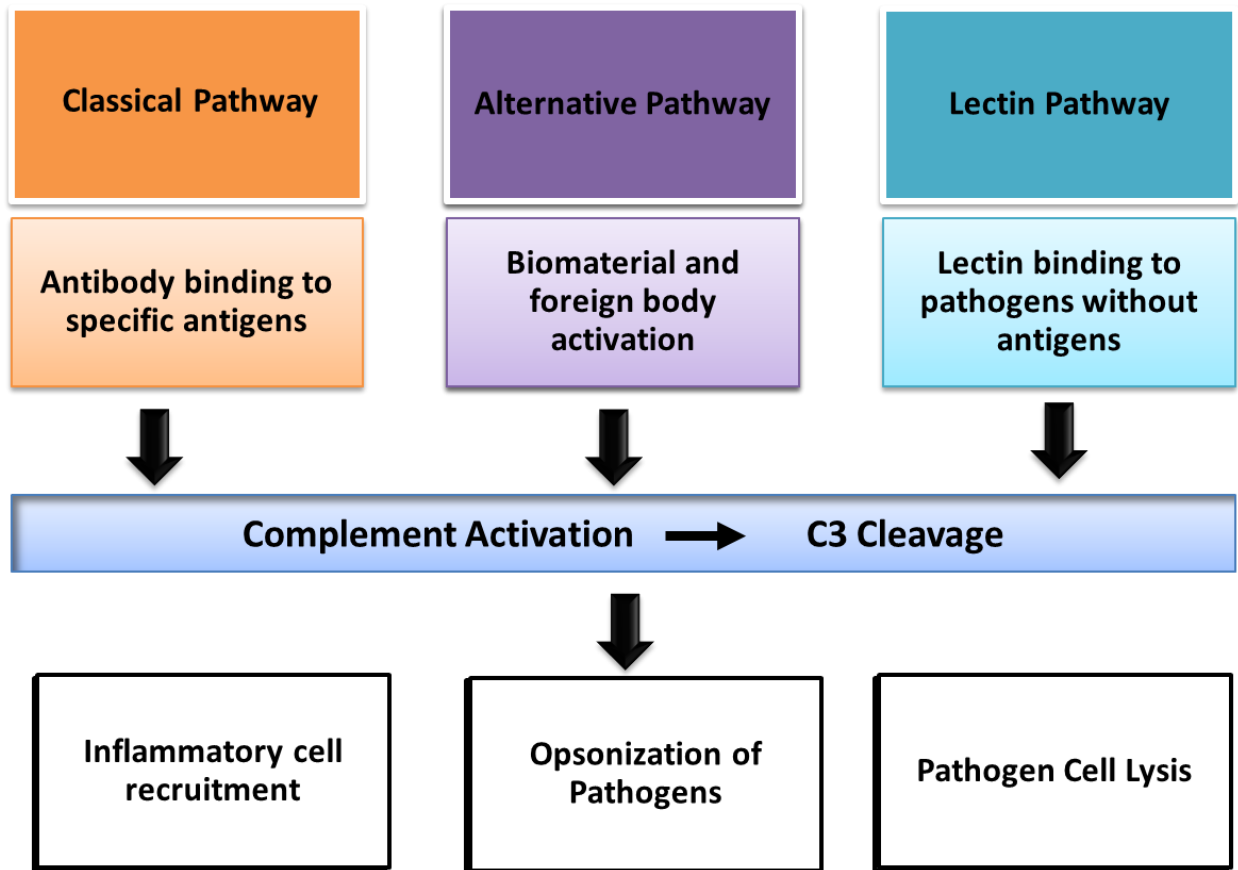


Figure 1.7.3: The biochemical pathways of the complement system¹³²

1.8 Cytotoxicity of Biomaterials

1.8.1 Lactate Dehydrogenase Assays Determine Cell Death by Biomaterial Surfaces

Mammalian lactate dehydrogenase (LDH) is a tetrameric enzyme found in human and animal tissues. LDH converts pyruvate to lactate using NADH and NAD⁺, thus representing the anaerobic metabolism of glucose¹⁹³. All tissues contain at least one of five LDH isozymes however, muscle, liver, and hematocytes are the dominant sources of serum LDH activity. LDH₂ is the primary isozyme found in serum and has long been used as a clinical marker for both *in vitro* and *in vivo* hemolysis resulting from disease or toxic substances^{47,193}. LDH concentrations rise significantly after organ infarction and elevated cell death exemplified in cases of hepatitis, shock, hypoxia, extreme hypothermia, and meningitis¹⁹⁴. Consequently, LDH can be used as a marker to determine cell viability after prolonged contact with a biomaterial. Cellular exposure to cytotoxic materials induces cytoplasmic and organelle swelling resulting in cellular necrosis. Organelle dissolution and rupture of the plasma membrane correspond to rises in cytosolic LDH. Loss of membrane integrity allows intercellular contents to spill into the extracellular milieu allowing for *in vitro* assessment of liberated LDH^{47,195,196}. Cytotoxicity of a material can thus be determined by inferring the magnitude of cell death through quantification of freed LDH.

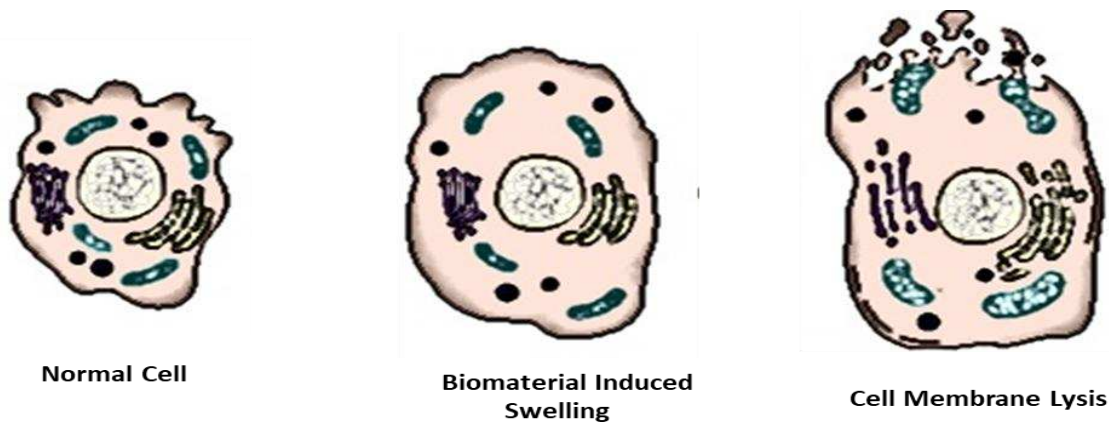


Fig 1.8.1: Biomaterial induced necrosis due to toxic effects imparts internal organelle swelling, membrane disintegration, and cell death¹⁹⁷.

1.8.2 Hemolysis Must Be Quantified for Medical Device Approval

In order for a blood-contacting material to be approved for a medical device, hemolytic activity i.e. the magnitude of the membranous breakdown of red-blood cells due to toxic material effects must be assessed. Hemolysis can occur due to a number of factors including chemicals or toxins present within the material, shear forces, leachables, or inherent properties of the material itself such as surface charge ¹⁸². Common hemolytic assays determine the amount of hemoglobin release in whole blood plasma or erythrocytes after exposure to biomaterial surfaces for a prescribed time period.

1.9 Endothelial Cell Assessments

1.9.1 Endothelial Cells Function to Maintain Optimal Hemocompatibility

The vasculature of the cardiovascular system is formulated by three layers composed of endothelial cells (EC; tunica intima), smooth muscle cells (tunica media), and fibroblasts (tunica adventitia). The tunica intima is a semi-permeable membrane composed of a mono-layer of EC which actively maintains blood flow throughout the cardiovascular system. Endothelium lines

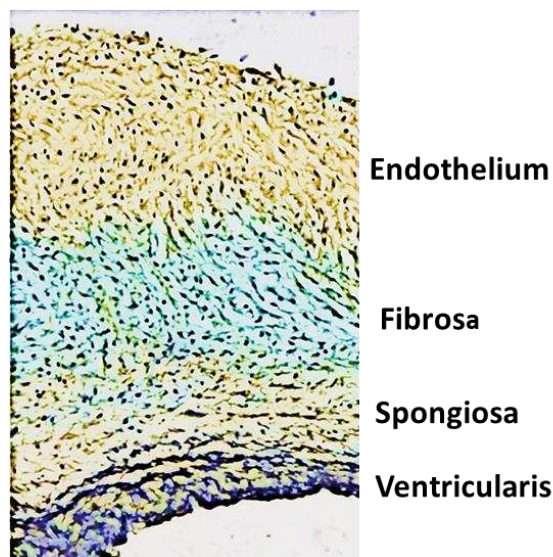


Figure 1.9.1: *Layers of the aortic valve leaflet*

the walls of the vasculature (arteries, veins, and microvessels), and the surface of heart valve leaflets. Heart valve leaflets have their own unique composition consisting of the endothelial layer, the fibrosa (composed mainly of interstitial cells), the spongiosa (mainly comprised of proteoglycans), and the ventricularis (composed mainly of elastin, **Fig.1.9.1**)¹⁹⁸. While EC possess features which are specific to their locational milieu, all EC function to maintain optimal hemocompatibility, regulate underlying tissues and cells, and assist in the removal of unwanted agents from the blood^{199,200}. In addition, all EC are effected by shear stress, and are implicated in the development of cardiovascular pathologies^{199,201}. The expression and secretion of regulatory molecules are found in both the healthy and pathogenic states of the endothelium and govern tone, permeability, inflammation, fibrinolysis, and thrombosis, and calcification^{141,201}. EC plays a dynamic role in regulating hemostatic events and tightly regulates the coagulation response. Uninjured endothelial cells express anti-thrombotic factors (Ex: anti-thrombin, thrombomodulin, TFP1, heparin co-factors, C1 inhibitors, and protein C pathways, NO) to prevent unwarranted clot formation²⁰¹. Once tissue damage is incurred, the EC layer becomes an active component in facilitating the wound healing process.

1.9.2 Endothelial Assessment on Different Surfaces

Just as hemocompatibility testing must ensure applicability to the desired application so must investigations which assess the ability of a material to promote or deter endothelialization. In this work it is hypothesized that endothelial attachment will be mitigated due to the HMW and hydrophilicity of HA-LLDPE. In order to ascertain the impact of HA-LLDPE on endothelial cells the following methods were employed:

- Lactate Dehydrogenase Assay: determines any potential toxicity to endothelial cells

- Fluorescent Staining (Actin/Dapi): to visualize amount of endothelial attachment to the surface
- SEM imaging: to assess morphology
- Alamarblue: to determine viability of cells attached to substrate surfaces
- CD31 Staining: to establish phenotype of adhered cells
- VEGF Staining: to ascertain potential for cellular proliferation

LDH assaying was chosen to ensure that any mitigation of cellular adhesion was not due to cytotoxic effects of substrates on endothelial cells. Next it was important to assess if cellular adhesion was affected by the treatment group and thus staining and SEM imaging were applied. This was followed by viability investigations and endogenous protein evaluations to determine if any cells which did adhere to surfaces were healthy, expressed the endothelial phenotype, and were able to proliferate. These last studies are particularly important as partial endothelialization of heart valve leaflets can lead to immune response and thrombus^{77,202}.

1.9.2 Endothelialization is a Key Objective in Cardiovascular Biomaterial Engineering

Exposure to the endothelial layer is the native state for blood and represents the “gold standard” that cardiovascular biomaterial research seeks to achieve *in vivo*²⁰³. This has made investigations into surface modifications for endothelializing biomaterials surfaces a popular subject. Endothelialization of biomaterial surfaces function under the assumption that EC interfaces will express a non-thrombogenic phenotype¹⁴¹. The majority of challenges concerning negative inflammatory and thrombotic responses of EC surfaces are often based in a biomaterial’s inability to provide an optimal environment which supports a confluent, mature,

quiescent, and non-thrombotic EC state^{203,204}. These often stem from a lack of bio-recognition and/or specific interaction at the cell-biomaterial interface²⁰⁵. Furthermore, mechanical properties (Ex: elasticity, hardness, density), bulk/surface properties (Ex: wettability, roughness, topography, porosity, softness, chemical composition), or design (Ex: diameter, hinge inclusion, thickness)^{126,204,206–214} of the implant can promote or deter healthy endothelialization. Cells sense cues from their environments and convert them into chemical stimuli which regulate their phenotype and function. Lack of biocompatibility between EC and biomaterial surfaces can lead to EC activation, ablation, and, phenotypic change which can result in platelet and leukocyte activation and thrombosis²⁰⁴. A large portion of cardiovascular biomaterials research is spent developing material interfaces which mimic or otherwise deliver an environment which is suitable to endothelial growth. Examples of this include pre-seeding an implant with endothelial cells to “mask” the implant from the native physiology^{215–217} and/or facilitating EC growth post-implantation. Both measures require EC exposure to the biomaterial interface.

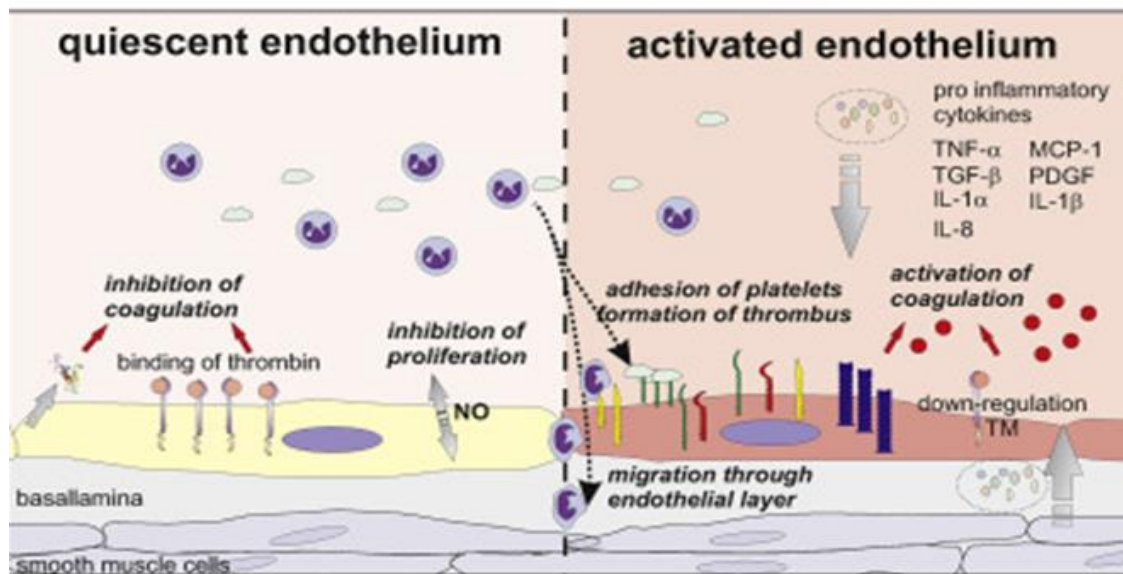


Figure 1.9.2: Quiescent endothelium is required to achieve hemocompatible surfaces. Reproduced with permission © Elsevier Ltd.

1.9.3 Permanent Endothelialization of Biomaterials Has Proven Quite Complex

While endothelialization of cardiovascular biomaterials has been widely investigated, the process has proven quite complex. Factors which must be considered when seeking to promote endothelialization on biomaterial surfaces include; 1) the ability of the material to promote angiogenesis and vasculogenesis to ensure nutrient supply to the local area 2) the ability to achieve a mono-layer of mature, quiescent EC that are non-thrombotic 3) the effect of local hemodynamics on EC phenotype, leukocyte attachment, and trans-endothelial migration (turbulent flow increases endothelial permeability to leukocytes) 4) The prevention of EC ablation (denuding) due to shear stress to prevent blood from exposure to the biomaterial surfaces 5) The creation of a material that supports biochemical cues to preserve EC phenotype and function 6) The effect of the material's composition and surface properties on the target EC behavior and angiogenic potential 7) EC source (Ex: small diameter vs large diameter vessels vs valvular phenotypes) behaviors on angiogenic potential, molecular permeability, leukocyte transmigration, hemostasis, vascular tone, humidification, thermoregulation, and immune tolerance 8) The potential need for co-culturing of different cell lines to support EC adhesion, proliferation etc. 9) The time and cost needed to endothelialize the surface^{43,200,204,218}. These examples are not inclusive of all the considerations necessary to attend to but represent the level of difficulty characteristic of endothelializing biomaterial surfaces.

In general, endothelialization of implants is considered beneficial as it potentiates a native surface for blood exposure, protects implants from mechanical degradation, and supports bio-functionality²¹⁹. However, while endothelialized surfaces are considered optimal, a permanent solution to endothelialization of biomaterials has proven difficult^{43,220}. In addition, endothelializing biomaterial surfaces requires extracorporeal culture which is time consuming

and negates its use in emergency surgeries ¹⁴¹. Thus, an alternative may be essential. Developing a surface that is hemocompatible without endothelialization may offer another choice to the current drawbacks which have been experienced in attempting to endothelialize biomaterial surfaces.

1.9.4 Hyaluronan and Endothelialization

Hyaluronan (HA) enhanced cardiovascular biomaterials have gained popularity for their potential to promote endothelialization, mitigate blood cell and protein adhesion, and reduce adverse inflammation ^{103,106,112,113,221–223}. HA is a highly hemocompatible polysaccharide whose chain lengths are easily manipulated, allowing for biomaterial surfaces to become finely tuned to impart bio-modulating properties. This alone broadens its potential for use in a wide variety of cardiovascular biomaterial applications such as vascular grafts, stents, heart valve leaflets, vascular patches, and other implants ^{224–229}. HMW-HA has been found to reduce endothelial cell attachment and the potential for angiogenesis, while low molecular weight HA has been found to be more amenable to endothelialization (See Table **1.5.2**). Depending upon the target goal for biomaterial use, modifying chain length can facilitate the functional aims of an implant. In this thesis we explore the hypothesis that HMW-HA will mitigate endothelialization on HA-LLDPE surfaces. Permanent endothelialization of heart valve leaflets would be ideal but has proven difficult. While these applications have been somewhat successful in a laboratory environment they have not proved to be translational to the market ²³⁰. Thus, limiting endothelialization while providing a hemocompatible and highly durable interface may offer an alternative to endothelialized surfaces.

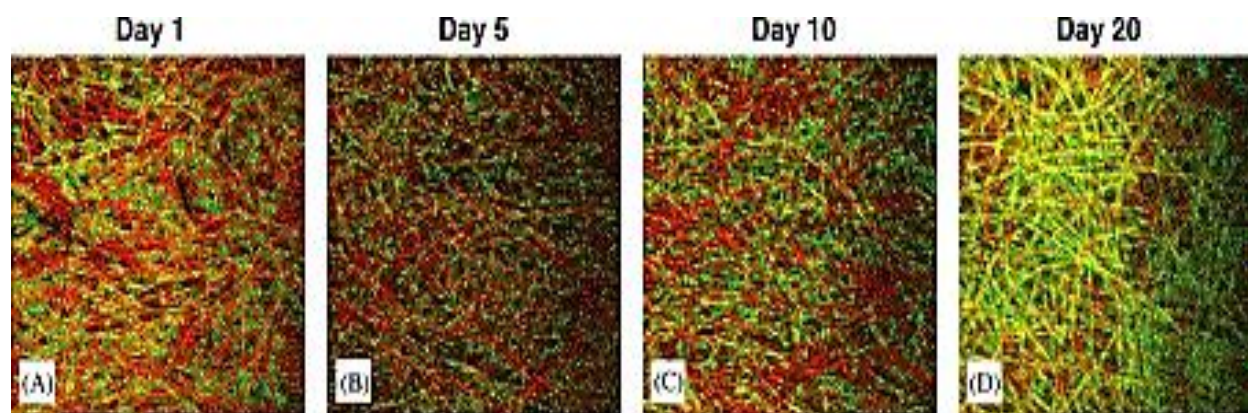


Fig. 1.9.4. Confocal microscopy illustrating endothelial cell growth (green) on hyaluronan enhanced benzyl ester scaffolds at up to 20 days of cell growth. All images are $\times 10$ magnification, scale bar = 200 μm . Reproduced with permission © Elsevier Ltd.

1.10 Conclusions

Heart valve replacement therapy (HVRT) has become a crucial method of treatment to enhance survival and improve the quality of life of the patients with valvular diseases. Heart valves are broadly placed into two categories: mechanical heart valves and tissue-based valves. Despite the overall success with MHVs and TBVs they are still plagued with durability and/or hemocompatibility issues which often result in the need for subsequent replacement and/or life-long anticoagulation therapy. Thus, there is a significant interest in developing HV leaflets that can address these issues. Polymeric based materials have been proposed for use HV leaflets due to their ability to be finely tuned through manufacturing and surface modification to enhance durability, and hemocompatibility.

Due to their high durability, flexible nature, and tunable surface properties, polyethylenes have been highly sought after for their potential to be used as prosthetic heart valve leaflets. Nevertheless, in defiance of these multiple structural and facial benefits, polyethylene-based cusps have remained susceptible to host response actuation and thrombosis as a result of their innate hydrophobicity which attracts blood proteins, platelets, and leukocytes.

To address this, a novel material for use as prosthetic heart valve leaflet was by forming an interpenetrating polymer network of high molecular weight HA in LLDPE. By enhancing LLDPE with a naturally occurring, hydrophilic, polysaccharide present within human tissues, we hope to mitigate foreign body effects and enhance hemocompatibility.

It is essential to develop exceptional hemocompatible biomaterials to ensure that adverse thrombosis and immune response are mitigated to reduce device related consequences. To create an ideal implant surface which reduces inflammation, thrombosis, and promotes proper integration with the native physiology it is essential to understand the mechanisms by which blood and vascular tissue components interact with the material surfaces of implants. The purpose of this research is to introduce and investigate the effects of a novel material, hyaluronan enhanced linear low-density polyethylene, as a potential interface for cardiovascular applications. Because of its superior biocompatibility, chain size malleability, and ease of conjugation with other polymers, HA has gained popularity for use in cardiovascular biomaterials. Studies investigating immobilized HA coatings, multifunctional surface HA coatings, HA based hydrogel-antibody amalgamates, and HA scaffolds for cardiovascular applications have pointed to its ability to reduce plasma protein binding, platelet/leukocyte adhesion and activation, and facilitate tissue restoration ^{124,133,221}. Recently, the addition of HA to polymer bases have produced promising results that may assist in achieving surfaces for use in heart valves and other cardiovascular applications that are highly durable and mitigate the coagulation and immune responses ^{41,99}. The aim of this study was to evaluate the hemocompatibility of the HA-LLDPE surface and compare it to that of the untreated LLDPE surface by assessing cytotoxicity, blood protein adhesion, cellular adhesion and activation,

whole blood clotting kinetics, and specific biochemical markers involved in the coagulation and immune responses.

REFERENCES:

1. Benjamin EJ, Blaha MJ, Chiuve SE, et al. Heart Disease and Stroke Statistics'2017 Update: A Report from the American Heart Association. *Circulation*. 2017;135(10):e146-e603. doi:10.1161/CIR.0000000000000485
2. Sidney S, Quesenberry CP, Jaffe MG, et al. Recent trends in cardiovascular mortality in the United States and public health goals. *JAMA Cardiol*. 2016;1(5):594-599. doi:10.1001/jamacardio.2016.1326
3. Jaffe RB. Explaining the decrease in U.S. deaths from coronary disease, 1980-2000: Commentary. *Obstet Gynecol Surv*. 2007;62(10):664-665. doi:10.1097/01.ogx.0000282009.19829.c3
4. Kramer DB. Cardiovascular Devices. In: *Cardiovascular Therapeutics: A Companion to Braunwald's Heart Disease: Fourth Edition*. ; 2012:747-760. doi:10.1016/B978-1-4557-0101-8.00050-3
5. Erglis A. Coronary guidewires. *EuroIntervention*. 2010;6(1):168-169. doi:10.4244/EIJV6I1A24
6. Vlahakes GJ. Mechanical heart valves: The test of time... *Circulation*. 2007;116(16):1759-1760. doi:10.1161/CIRCULATIONAHA.107.729582
7. Pratt AK, Shah NS, Boyce SW. Left ventricular assist device management in the ICU. *Crit Care Med*. 2014;42(1):158-168. doi:10.1097/01.ccm.0000435675.91305.76
8. Kumar R, Kumar A, Sharma R, Baruwa A. Pharmacological review on Natural ACE inhibitors. *ScholarsresearchlibraryCom*. 2010;2(2):273-293. <http://scholarsresearchlibrary.com/DPL-vol2-iss2/DPL-2010-2-2-273-293.pdf>.

9. Briet M, Schiffrin EL. Aldosterone: Effects on the kidney and cardiovascular system. *Nat Rev Nephrol*. 2010;6(5):261-273. doi:10.1038/nrneph.2010.30
10. Wiysonge CS, Bradley HA, Volmink J, Mayosi BM, Opie LH. Beta-blockers for hypertension. *Cochrane Database Syst Rev*. 2017;2017(1). doi:10.1002/14651858.CD002003.pub5
11. Elliott WJ, Ram CVS. Calcium channel blockers. *J Clin Hypertens*. 2011;13(9):687-689. doi:10.1111/j.1751-7176.2011.00513.x
12. Khvorova A. Oligonucleotide Therapeutics — A New Class of Cholesterol-Lowering Drugs. *N Engl J Med*. 2017;376(1):4-7. doi:10.1056/NEJMp1614154
13. Dhanani NM, Caruso TJ, Carinci AJ. Complementary and alternative medicine for pain: An evidence-based review. *Curr Pain Headache Rep*. 2011;15(1):39-46. doi:10.1007/s11916-010-0158-y
14. Lin MC, Nahin R, Gershwin ME, Longhurst JC, Wu KK. State of complementary and alternative medicine in cardiovascular, lung, and blood research: Executive summary of a workshop. *Circulation*. 2001;103(16):2038-2041. doi:10.1161/01.CIR.103.16.2038
15. Rogers JG, Aaronson KD, Boyle AJ, et al. Continuous Flow Left Ventricular Assist Device Improves Functional Capacity and Quality of Life of Advanced Heart Failure Patients. *J Am Coll Cardiol*. 2010;55(17):1826-1834. doi:10.1016/j.jacc.2009.12.052
16. Thomas SA, Friedmann E, Kao C-W, et al. Quality of life and psychological status of patients with implantable cardioverter defibrillators. *Am J Crit Care*. 2006;15(4):389-398. <http://www.ncbi.nlm.nih.gov/pubmed/16823016>.
17. Walther T, Falk V, Metz S, et al. Pain and quality of life after minimally invasive versus conventional cardiac surgery. *Ann Thorac Surg*. 1999;67(6):1643-1647. doi:10.1016/S0003-

4975(99)00284-2

18. Barnhorst DA, Oxman HA, Connolly DC, et al. Long-term follow-up of isolated replacement of the aortic or mitral valve with the Starr-Edwards prosthesis. *Am J Cardiol.* 1975;35(2):228-233. doi:10.1016/0002-9149(75)90006-5
19. Koski R, Lay C. Medications associated with implantable cardiac devices. *US Pharmacist.* 2016;41(2):30-34.
http://www.embase.com/search/results?subaction=viewrecord&from=export&id=L608516620%5Cnhttp://elinks.library.upenn.edu/sfx_local?sid=EMBASE&issn=01484818&id=doi:&atitle=Medications+associated+with+implantable+cardiac+devices&stitle=U.S.+Pharm.&title=U.S.+
20. Garg S, Serruys PW. Coronary stents: Looking forward. *J Am Coll Cardiol.* 2010;56(10 SUPPL.). doi:10.1016/j.jacc.2010.06.008
21. Garg S, Serruys PW. Coronary stents: Current status. *J Am Coll Cardiol.* 2010;56(10 SUPPL.). doi:10.1016/j.jacc.2010.06.007
22. Mani G, Feldman MD, Patel D, Agrawal CM. Coronary stents: A materials perspective. *Biomaterials.* 2007;28(9):1689-1710. doi:10.1016/j.biomaterials.2006.11.042
23. Ormiston JA, Serruys PWS. Bioabsorbable coronary stents. *Circ Cardiovasc Interv.* 2009;2(3):255-260. doi:10.1161/CIRCINTERVENTIONS.109.859173
24. Pibarot P, Dumesnil JG. Prosthetic heart valves: Selection of the optimal prosthesis and long-term management. *Circulation.* 2009;119(7):1034-1048.
doi:10.1161/CIRCULATIONAHA.108.778886
25. Butany J, Fayet C, Ahluwalia MS, et al. Biological replacement heart valves: Identification and evaluation. *Cardiovasc Pathol.* 2003;12(3):119-139. doi:10.1016/S1054-8807(03)00002-4

26. Hopkins RA. Tissue engineering of heart valves: Decellularized valve scaffolds. *Circulation*. 2005;111(21):2712-2714. doi:10.1161/CIRCULATIONAHA.104.527820
27. Ghanbari H, Viatge H, Kidane AG, Burriesci G, Tavakoli M, Seifalian AM. Polymeric heart valves: new materials, emerging hopes. *Trends Biotechnol*. 2009;27(6):359-367. doi:10.1016/j.tibtech.2009.03.002
28. Kowligi RR, Taylor HH, Wollner SA. Physical Properties and Testing Methods for PTFE Cardiovascular Patches. *J Biomater Appl*. 1993;7(4):353-361. doi:10.1177/088532829300700403
29. Mendelson K, Aikawa E, Mettler BA, et al. Healing and remodeling of bioengineered pulmonary artery patches implanted in sheep. *Cardiovasc Pathol*. 2007;16(5):277-282. doi:10.1016/j.carpath.2007.03.008
30. Bristow MR, Feldman AM, Saxon LA. Heart failure management using implantable devices for ventricular resynchronization: Comparison of Medical Therapy, Pacing, and Defibrillation in Chronic Heart Failure (COMPANION) trial. *J Card Fail*. 2000;6(3):276-285. doi:10.1054/jcaf.2000.9501
31. Burri H. Cardiac resynchronization therapy for mild-to-moderate heart failure. *Expert Rev Med Devices*. 2011;8(3):313-317. doi:10.1586/erd.11.6
32. Braunschweig F. Therapeutic and diagnostic role of electrical devices in acute heart failure. *Heart Fail Rev*. 2007;12(2):157-166. doi:10.1007/s10741-007-9019-0
33. Timms D. A review of clinical ventricular assist devices. *Med Eng Phys*. 2011;33(9):1041-1047. doi:10.1016/j.medengphy.2011.04.010
34. Fynn-Thompson F, Almond C. Pediatric ventricular assist devices. *Pediatr Cardiol*. 2007;28(2):149-155. doi:10.1007/s00246-006-1453-6

35. Defibrillator Image.
https://commons.wikimedia.org/wiki/File:Implantable_cardioverter_defibrillator_with_lead.jpg.
36. Vascular Patch. <http://www.terumo-cvs.com/products/ProductDetail.aspx?groupId=68&familyID=773&country=1>.
37. Heart Valve. <https://www.cryolife.com/products/on-x-heart-valves/>.
38. Coronary Stent. :<https://www.xiencestent.com/us/stent-design/>.
<https://www.xiencestent.com/us/stent-design/>.
39. Pace Maker. :<http://www.medtronic.com/us-en/patients/treatments>.
<http://www.medtronic.com/us-en/patients/treatments-therapies/pacemakers/options-types.html>.
40. Ventricular Assist Device. <http://cirtecmed.com/product-categories/ventricular-assist/>.
41. Prawel DA, Dean H, Forleo M, et al. Hemocompatibility and Hemodynamics of Novel Hyaluronan-Polyethylene Materials for Flexible Heart Valve Leaflets. *Cardiovasc Eng Technol*. 2014;5(1):70-81. doi:10.1007/s13239-013-0171-5
42. Sacks MS, Schoen FJ, Mayer JE. Bioengineering Challenges for Heart Valve Tissue Engineering. *Annu Rev Biomed Eng*. 2009;11:289-313. doi:10.1146/annurev-bioeng-061008-124903
43. Heath DE. Promoting Endothelialization of Polymeric Cardiovascular Biomaterials. *Macromol Chem Phys*. 2017;218(8). doi:10.1002/macp.201600574
44. Kolandaivelu K, Swaminathan R, Gibson WJ, et al. Stent thrombogenicity early in high-risk interventional settings is driven by stent design and deployment and protected by polymer-drug coatings. *Circulation*. 2011. doi:10.1161/CIRCULATIONAHA.110.003210
45. Peppas NA. Handbook of Biomaterial Properties. *J Control Release*. 2000;65(3):439. doi:10.1016/S0168-3659(99)00208-4

46. Dasi LP, Simon HA, Sucusky P, Yoganathan AP. Fluid mechanics of artificial heart valves. *Clin Exp Pharmacol Physiol*. 2009;36(2):225-237. doi:10.1111/j.1440-1681.2008.05099.x
47. Kato GJ, McGowan V, Machado RF, et al. Lactate dehydrogenase as a biomarker of hemolysis-associated nitric oxide resistance, priapism, leg ulceration, pulmonary hypertension, and death in patients with sickle cell disease. *Blood*. 2006;107(6):2279-2285. doi:10.1182/blood-2005-06-2373
48. Xu L-C, Wo Y, Meyerhoff ME, Siedlecki CA, Xu L-C. Inhibition of bacterial adhesion and biofilm formation by dual functional textured and nitric oxide releasing surfaces. *Acta Biomater*. 2017;51:53-65. doi:10.1016/j.actbio.2017.01.030
49. Scott RD. The direct medical costs of healthcare-associated infections in U.S. hospitals and the benefits of prevention. *Cdc*. 2009;(March):13.
doi:http://www.cdc.gov/hai/pdfs/hai/scott_costpaper.pdf
50. Bernard ML, Shotwell M, Nietert PJ, Gold MR. Meta-analysis of bleeding complications associated with cardiac rhythm device implantation. *Circ Arrhythmia Electrophysiol*. 2012;5(3):468-474. doi:10.1161/CIRCEP.111.969105
51. Fujiwara R, Yoshida A, Takei A, et al. "Heparin bridging" increases the risk of bleeding complications in patients undergoing anticoagulation therapy and device implantation. *J Arrhythmia*. 2012;28(2):96-99. doi:10.1016/j.joa.2012.03.005
52. Hu WJ, Eaton JW, Tang L. Molecular basis of biomaterial-mediated foreign body reactions. *Blood*. 2001. doi:10.1182/blood.V98.4.1231
53. Siedlecki CA. *Hemocompatibility of Biomaterials for Clinical Applications: Blood-Biomaterials Interactions*.; 2017.

54. Jaganathan SK, Supriyanto E, Murugesan S, Balaji A, Asokan MK. Biomaterials in cardiovascular research: Applications and clinical implications. *Biomed Res Int.* 2014;2014. doi:10.1155/2014/459465
55. Buja LM, Schoen FJ. Chapter 14 – The Pathology of Cardiovascular Interventions and Devices for Coronary Artery Disease, Vascular Disease, Heart Failure, and Arrhythmias. In: *Cardiovascular Pathology.* ; 2016. doi:10.1016/B978-0-12-420219-1.00032-X
56. Jennings DL, Weeks PA. Thrombosis in continuous-flow left ventricular assist devices: Pathophysiology, prevention, and pharmacologic management. *Pharmacotherapy.* 2015. doi:10.1002/phar.1501
57. Yamaji K, Ueki Y, Souteyrand G, et al. Mechanisms of Very Late Bioresorbable Scaffold Thrombosis: The INVEST Registry. *J Am Coll Cardiol.* 2017. doi:10.1016/j.jacc.2017.09.014
58. Rozmus G, Daubert JP, Huang DT, Rosero S, Hall B, Francis C. Venous thrombosis and stenosis after implantation of pacemakers and defibrillators. *J Interv Card Electrophysiol.* 2005. doi:10.1007/s10840-005-1140-1
59. Pedersen SB, Hjortshøj SP, Bøtker HE, et al. Venous thromboembolism in patients with implantable cardioverter-defibrillators. *Europace.* 2017. doi:10.1093/europace/euw124
60. Ratner BD. The catastrophe revisited: Blood compatibility in the 21st Century. *Biomaterials.* 2007. doi:10.1016/j.biomaterials.2007.07.035
61. Blood Contacting Time.
<https://www.uweb.engr.washington.edu/research/tutorials/biomatforcardio.html>.
62. Stassen OMJA, Muylaert DEP, Bouten CVC, Hjortnaes J. Current Challenges in Translating Tissue-Engineered Heart Valves. *Curr Treat Options Cardiovasc Med.* 2017. doi:10.1007/s11936-017-0566-y

63. Bezuidenhout D, Williams DF, Zilla P. Polymeric heart valves for surgical implantation, catheter-based technologies and heart assist devices. *Biomaterials*. 2015.
doi:10.1016/j.biomaterials.2014.09.013
64. Cheung DY, Duan B, Butcher JT. Current progress in tissue engineering of heart valves: multiscale problems, multiscale solutions. *Expert Opin Biol Ther*. 2015.
doi:10.1517/14712598.2015.1051527
65. Roudaut R, Serri K, Lafitte S. Thrombosis of prosthetic heart valves: diagnosis and therapeutic considerations. *Heart*. 2007;93(1):137-142. doi:10.1136/hrt.2005.071183
66. Ball Valve.
https://commons.wikimedia.org/wiki/File:Prosthetic_Cardiac_Ball_Valves.jpg.
67. Open Hinge. :<http://www.medtronic.com/us-en/healthcare-professi>.
<http://www.medtronic.com/us-en/healthcare-professionals/products/cardiovascular/heart-valves-surgical/open-pivot-mechanical-heart-valve.html>.
68. Chondros TG. Fatigue fracture of the Björk-Shiley heart valve strut and failure diagnosis from acoustic signatures. *Theor Appl Fract Mech*. 2010. doi:10.1016/j.tafmec.2010.10.001
69. Fihn SD, McDonnell M, Martin D, et al. Risk factors for complications of chronic anticoagulation: A multicenter study. *Ann Intern Med*. 1993. doi:10.7326/0003-4819-118-7-199304010-00005
70. Jose J, Sulimov DS, El-Mawardy M, et al. Clinical Bioprosthetic Heart Valve Thrombosis After Transcatheter Aortic Valve Replacement: Incidence, Characteristics, and Treatment Outcomes. *JACC Cardiovasc Interv*. 2017. doi:10.1016/j.jcin.2017.01.045
71. Rozeik MM, Wheatley DJ, Gourlay T. Percutaneous heart valves; past, present and future. *Perfusion*. 2014. doi:10.1177/0267659114523464

72. Piazza N, Bleiziffer S, Brockmann G, et al. Transcatheter Aortic Valve Implantation for Failing Surgical Aortic Bioprosthetic Valve: From Concept to Clinical Application and Evaluation (Part 1). *JACC Cardiovasc Interv.* 2011. doi:10.1016/j.jcin.2011.03.016
73. Tissue Valve.
<https://www.fda.gov/medicaldevices/productsandmedicalprocedures/deviceapprovalsandclearances/recently-approveddevices/ucm561731.htm>.
74. Lee C, Lim HG, Lee CH, Kim YJ. Effects of glutaraldehyde concentration and fixation time on material characteristics and calcification of bovine pericardium: Implications for the optimal method of fixation of autologous pericardium used for cardiovascular surgery. *Interact Cardiovasc Thorac Surg.* 2017. doi:10.1093/icvts/ivw356
75. Schoen FJ, Levy RJ. Calcification of tissue heart valve substitutes: Progress toward understanding and prevention. *Ann Thorac Surg.* 2005;79(3):1072-1080.
doi:10.1016/j.athoracsur.2004.06.033
76. Maraj R, Jacobs LE, Ioli a, Kotler MN. Evaluation of hemolysis in patients with prosthetic heart valves. *Clin Cardiol.* 1998. doi:10.1002/clc.4960210604
77. VeDepo MC, Detamore MS, Hopkins RA, Converse GL. Recellularization of decellularized heart valves: Progress toward the tissue-engineered heart valve. *J Tissue Eng.* 2017. doi:10.1177/2041731417726327
78. Vesely I. Heart valve tissue engineering. *Circ Res.* 2005.
doi:10.1161/01.RES.0000185326.04010.9f
79. Mayo Clinic. <https://www.mayoclinic.org/medical-professionals/clinical-updates/cardiovascular/prosthetic-valve-thrombosis-time-is-critical>.
80. Simon-Walker R, Cavicchia J, Prawel DA, Dasi LP, James SP, Popat KC.

Hemocompatibility of hyaluronan enhanced linear low density polyethylene for blood contacting applications. *J Biomed Mater Res - Part B Appl Biomater*. 2018;106(5).

doi:10.1002/jbm.b.34010

81. Fujimoto K, Tadokoro H, Ueda Y, Ikada Y. Polyurethane surface modification by graft polymerization of acrylamide for reduced protein adsorption and platelet adhesion. *Biomaterials*. 1993;14(6):442-448. doi:10.1016/0142-9612(93)90147-T

82. Govindarajan T, Shandas R. A survey of surface modification techniques for next-generation shape memory polymer stent devices. *Polymers (Basel)*. 2014;6(9):2309-2331.

doi:10.3390/polym6092309

83. Engberg AE, Rosengren-Holmberg JP, Chen H, et al. Blood protein-polymer adsorption: Implications for understanding complement-mediated hemoincompatibility. *J Biomed Mater Res - Part A*. 2011;97 A(1):74-84. doi:10.1002/jbm.a.33030

84. Calderon L, Collin E, Velasco-Bayon D, Murphy M, O'Halloran D, Pandit A. Type II collagen-hyaluronan hydrogel--a step towards a scaffold for intervertebral disc tissue engineering. *Eur Cell Mater*. 2010;20:134-148. doi:vol020a12 [pii]

85. Xu LC, Bauer JW, Siedlecki CA. Proteins, platelets, and blood coagulation at biomaterial interfaces. *Colloids Surfaces B Biointerfaces*. 2014;124:49-68.

doi:10.1016/j.colsurfb.2014.09.040

86. Grill a. Diamond-like carbon coatings as biocompatible materials—an overview. *Diam Relat Mater*. 2003. doi:10.1016/S0925-9635(03)00018-9

87. Santos M, Bilek MMM, Wise SG. Plasma-synthesised carbon-based coatings for cardiovascular applications. *Biosurface and Biotribology*. 2015;1(3):146-160.

doi:10.1016/j.bsbt.2015.08.001

88. Silver JH, Lin JC, Lim F, Tegoulia VA, Chaudhury MK, Cooper SL. Surface properties and hemocompatibility of alkyl-siloxane monolayers supported on silicone rubber: Effect of alkyl chain length and ionic functionality. *Biomaterials*. 1999. doi:10.1016/S0142-9612(98)00173-2
89. De Somer F, François K, Van Oeveren W, et al. Phosphorylcholine coating of extracorporeal circuits provides natural protection against blood activation by the material surface. *Eur J Cardio-thoracic Surg*. 2000;18(5):602-606. doi:10.1016/S1010-7940(00)00508-X
90. Kottke-Marchant K, Anderson JM, Umemura Y, Marchant RE. Effect of albumin coating on the in vitro blood compatibility of Dacron® arterial prostheses. *Biomaterials*. 1989;10(3):147-155. doi:10.1016/0142-9612(89)90017-3
91. Simon-Walker R, Romero R, Staver JM, et al. Glycocalyx-inspired nitric oxide-releasing surfaces reduce platelet adhesion and activation on titanium. *ACS Biomater Sci Eng*. 2017;3(1):68-77. doi:10.1021/acsbomaterials.6b00572
92. Duraiswamy N, Choksi TD, Pinchuk L, Schoepfoerster RT. A phospholipid-modified polystyrene-polyisobutylene-polystyrene (SIBS) triblock polymer for enhanced hemocompatibility and potential use in artificial heart valves. *J Biomater Appl*. 2009. doi:10.1177/0885328208093854
93. Spear KE, Dismukes JP. Emerging CVD Science and Technology. *Synth Diam*. 1994.
94. Roy RK, Choi HW, Yi JW, et al. Hemocompatibility of surface-modified, silicon-incorporated, diamond-like carbon films. *Acta Biomater*. 2009. doi:10.1016/j.actbio.2008.07.031
95. Li F, Wang J, Huang N. In vitro blood compatibility of polyethylene terephthalate with covalently bounded hirudin on surface. *J Wuhan Univ Technol Mater Sci Ed*. 2011. doi:10.1007/s11595-011-0343-9

96. Park Y, Ryu E, Kim H, et al. Characterization of antithrombotic activity of lumbrokinase-immobilized polyurethane valves in the total artificial heart. *Artif Organs*. 1999.
doi:10.1046/j.1525-1594.1999.06013.x
97. McKeen LW. *3 - Plastics Used in Medical Devices.*; 2014.
doi:http://dx.doi.org/10.1016/B978-0-323-22805-3.00003-7
98. Wang M. Bioactive ceramic-polymer composites for tissue replacement. *Eng Mater Biomed Appl World Sci*. 2004;8-1-29. doi:10.1142/9789812562227_0008
99. Simon-Walker R, Cavicchia J, Prawel DA, Dasi LP, James SP, Popat KC.
Hemocompatibility of hyaluronan enhanced linear low density polyethylene for blood contacting applications. *J Biomed Mater Res Part B Appl Biomater*. September 2017.
doi:10.1002/jbm.b.34010
100. Laurent TC, Fraser JR. Hyaluronan. *FASEB J*. 1992;6(7):2397-2404. doi:10.1016/S0740-8315(82)80016-8
101. Fraser JR, Laurent TC, Laurent UB. Hyaluronan: its nature, distribution, functions and turnover. *J Intern Med*. 1997;242:27-33. doi:10.1046/j.1365-2796.1997.00170.x
102. Allison DD, Grande-Allen KJ. Review. Hyaluronan: A Powerful Tissue Engineering Tool. *Tissue Eng*. 2006;0(0):060913044658042. doi:10.1089/ten.2006.12.ft-153
103. Bonafè F, Govoni M, Giordano E, Caldarera C, Guarnieri C, Muscari C. Hyaluronan and cardiac regeneration. *J Biomed Sci*. 2014;21(1):100. doi:10.1186/s12929-014-0100-4
104. Laurent TC, Laurent UB, Fraser JR. The structure and function of hyaluronan: An overview. *Immunol Cell Biol*. 1996;74(2):A1-A7. doi:10.1038/icb.1996.32
105. Stern R. Devising a pathway for hyaluronan catabolism: Are we there yet? *Glycobiology*. 2003;13(12). doi:10.1093/glycob/cwg112

106. Laurent TC, Fraser JR. Hyaluronan. *FASEB J.* 1992;6(7):2397-2404. doi:10.1016/S0140-6736(01)35637-4
107. Bonafè F, Govoni M, Giordano E, Caldarera CM, Guarnieri C, Muscari C. Hyaluronan and cardiac regeneration. *J Biomed Sci.* 2014;21(1). doi:10.1186/s12929-014-0100-4
108. Chuang TW, Masters KS. Regulation of polyurethane hemocompatibility and endothelialization by tethered hyaluronic acid oligosaccharides. *Biomaterials.* 2009;30(29):5341-5351. doi:10.1016/j.biomaterials.2009.06.029
109. Li J, Wu F, Zhang K, et al. Controlling Molecular Weight of Hyaluronic Acid Conjugated on Amine-rich Surface: Toward Better Multifunctional Biomaterials for Cardiovascular Implants. *ACS Appl Mater Interfaces.* 2017. doi:10.1021/acsami.7b07444
110. Rayahin JE, Buhrman JS, Zhang Y, Koh TJ, Gemeinhart RA. High and Low Molecular Weight Hyaluronic Acid Differentially Influence Macrophage Activation. *ACS Biomater Sci Eng.* 2015. doi:10.1021/acsbiomaterials.5b00181
111. Ruiz A, Flanagan CE, Masters KS. Differential support of cell adhesion and growth by copolymers of polyurethane with hyaluronic acid. *J Biomed Mater Res - Part A.* 2013;101(10):2870-2882. doi:10.1002/jbm.a.34597
112. Amarnath LP, Srinivas A, Ramamurthi A. In vitro hemocompatibility testing of UV-modified hyaluronan hydrogels. *Biomaterials.* 2006;27(8):1416-1424. doi:10.1016/j.biomaterials.2005.08.008
113. Li L, Wang N, Jin X, et al. Biodegradable and injectable in situ cross-linking chitosan-hyaluronic acid based hydrogels for postoperative adhesion prevention. *Biomaterials.* 2014;35(12):3903-3917. doi:10.1016/j.biomaterials.2014.01.050
114. Ramamurthi A, Vesely I. Ultraviolet light-induced modification of crosslinked

- hyaluronan gels. *J Biomed Mater Res - Part A*. 2003. doi:10.1002/jbm.a.10588
115. Amarnath LP, Srinivas A, Ramamurthi A. In vitro hemocompatibility testing of UV-modified hyaluronan hydrogels. *Biomaterials*. 2006. doi:10.1016/j.biomaterials.2005.08.008
116. Chuang TW, Masters KS. Regulation of polyurethane hemocompatibility and endothelialization by tethered hyaluronic acid oligosaccharides. *Biomaterials*. 2009. doi:10.1016/j.biomaterials.2009.06.029
117. Li J, Zhang K, Wu F, He Z, Yang P, Huang N. Constructing bio-functional layers of hyaluronan and type IV collagen on titanium surface for improving endothelialization. *J Mater Sci*. 2015. doi:10.1007/s10853-015-8889-0
118. Maleki A, Kjøniksen AL, Nyström B. Characterization of the chemical degradation of hyaluronic acid during chemical gelation in the presence of different cross-linker agents. *Carbohydr Res*. 2007;342(18):2776-2792. doi:10.1016/j.carres.2007.08.021
119. Levett PA, Melchels FPW, Schrobback K, Hutmacher DW, Malda J, Klein TJ. A biomimetic extracellular matrix for cartilage tissue engineering centered on photocurable gelatin, hyaluronic acid and chondroitin sulfate. *Acta Biomater*. 2014;10(1):214-223. doi:10.1016/j.actbio.2013.10.005
120. Tomihata K, Ikada Y. Crosslinking of hyaluronic acid with glutaraldehyde. *J Polym Sci Part A Polym Chem*. 1997;35(16):3553-3559. doi:10.1002/(SICI)1099-0518(19971130)35:16<3553::AID-POLA22>3.0.CO;2-D
121. Palumbo FS, Pitarresi G, Albanese A, Calascibetta F, Giammona G. Self-assembling and auto-crosslinkable hyaluronic acid hydrogels with a fibrillar structure. *Acta Biomater*. 2010;6(1):195-204. doi:10.1016/j.actbio.2009.06.014
122. Sakurai K, Miyazaki K, Kodera Y, Nishimura H, Shingu M, Inada Y. Anti-inflammatory

- activity of superoxide dismutase conjugated with sodium hyaluronate. *Glycoconj J*. 1997;14(6):723-728. doi:10.1023/A:1018521501289
123. Huang B, Li CQ, Zhou Y, Luo G, Zhang CZ. Collagen II/hyaluronan/chondroitin-6-sulfate tri-copolymer scaffold for nucleus pulposus tissue engineering. *J Biomed Mater Res - Part B Appl Biomater*. 2010;92(2):322-331. doi:10.1002/jbm.b.31518
124. Wu F, Li J, Zhang K, et al. Multifunctional Coating Based on Hyaluronic Acid and Dopamine Conjugate for Potential Application on Surface Modification of Cardiovascular Implanted Devices. *ACS Appl Mater Interfaces*. 2016;8(1):109-121. doi:10.1021/acsami.5b07427
125. Briganti E, Losi P, Raffi A, Scoccianti M, Munaò A, Soldani G. Silicone based polyurethane materials: A promising biocompatible elastomeric formulation for cardiovascular applications. *J Mater Sci Mater Med*. 2006;17(3):259-266. doi:10.1007/s10856-006-7312-4
126. Ratner BD, Hoffman AS, Schoen FJ, Lemons JE. *Biomaterials Science: An Introduction to Materials in Medicine.*; 2004.
127. Gong F, Lu Y, Guo H, Cheng S, Gao Y. Hyaluronan immobilized polyurethane as a blood contacting material. *Int J Polym Sci*. 2010;2010. doi:10.1155/2010/807935
128. Tanaka KA, Key NS, Levy JH. Blood coagulation: Hemostasis and thrombin regulation. *Anesth Analg*. 2009;108(5):1433-1446. doi:10.1213/ane.0b013e31819bcc9c
129. Franz S, Rammelt S, Scharnweber D, Simon JC. Immune responses to implants - A review of the implications for the design of immunomodulatory biomaterials. *Biomaterials*. 2011. doi:10.1016/j.biomaterials.2011.05.078
130. Vogler EA, Siedlecki CA. Contact activation of blood-plasma coagulation. *Biomaterials*. 2009;30(10):1857-1869. doi:10.1016/j.biomaterials.2008.12.041

131. Hanson SR, Tucker EI. Blood Coagulation and Blood - Materials Interactions. In: *Biomaterials Science: An Introduction to Materials: Third Edition.* ; 2013:551-557.
doi:10.1016/B978-0-08-087780-8.00048-6
132. Janeway CA, Travers P, Walport M, Shlomchik M. Immunobiology: The Immune System In Health And Disease. *Immuno Biol* 5. 2001:892. doi:10.1111/j.1467-2494.1995.tb00120.x
133. Camci-Unal G, Aubin H, Ahari AF, Bae H, Nichol JW, Khademhosseini* A. Surface-modified hyaluronic acid hydrogels to capture endothelial progenitor cells. *Soft Matter*. 2010;6(20):5120. doi:10.1039/c0sm00508h
134. Pitt WG, Morris RN, Mason ML, Hall MW, Luo Y, Prestwich GD. Attachment of hyaluronan to metallic surfaces. *J Biomed Mater Res A*. 2004;68(1):95-106.
doi:10.1002/jbm.a.10170
135. Thierry B, Winnik FM, Merhi Y, Griesser HJ, Tabrizian M. Biomimetic hemocompatible coatings through immobilization of hyaluronan derivatives on metal surfaces. *Langmuir*. 2008;24(20):11834-11841. doi:10.1021/la801359w
136. Seyfert UT, Biehl V, Schenk J. In vitro hemocompatibility testing of biomaterials according to the ISO 10993-4. In: *Biomolecular Engineering.* ; 2002. doi:10.1016/S1389-0344(02)00015-1
137. Gorbet MB, Sefton M V. Biomaterial-associated thrombosis: Roles of coagulation factors, complement, platelets and leukocytes. In: *The Biomaterials: Silver Jubilee Compendium.* ; 2006:219-241. doi:10.1016/B978-008045154-1.50025-3
138. Solouk A, Cousins BG, Mirzadeh H, Seifalian AM. Application of plasma surface modification techniques to improve hemocompatibility of vascular grafts: A review. *Biotechnol*

Appl Biochem. 2011;58(5):311-327. doi:10.1002/bab.50

139. Tang L, Eaton JW. Inflammatory responses to biomaterials. *Am J Clin Pathol.* 1995;103(4):466-471.
140. Tang L, Lucas a H, Eaton JW. Inflammatory responses to implanted polymeric biomaterials: role of surface-adsorbed immunoglobulin G. *J Lab Clin Med.* 1993;122(3):292-300. doi:0022-2143(93)90076-B [pii]
141. McGuigan AP, Sefton M V. The influence of biomaterials on endothelial cell thrombogenicity. *Biomaterials.* 2007. doi:10.1016/j.biomaterials.2007.01.039
142. Colvin B. Essential Haematology. *J Clin Pathol.* 1993. doi:10.1136/jcp.46.7.687-e
143. Ratner BD, Horbett TA. Evaluation of Blood-Materials Interactions. In: *Biomaterials Science: An Introduction to Materials: Third Edition.* ; 2013:617-634. doi:10.1016/B978-0-08-087780-8.00055-3
144. Mackman N. Triggers, targets and treatments for thrombosis. *Nature.* 2008. doi:10.1038/nature06797
145. Sperling C, Fischer M, Maitz MF, Werner C. Blood coagulation on biomaterials requires the combination of distinct activation processes. *Biomaterials.* 2009. doi:10.1016/j.biomaterials.2009.05.044
146. Cool DE, Edgell CJ, Louie G V, Zoller MJ, Brayer GD, MacGillivray RT. Characterization of human blood coagulation factor XII cDNA. Prediction of the primary structure of factor XII and the tertiary structure of beta-factor XIIa. *J Biol Chem.* 1985;260(25):13666-13676.
147. Konings J, Govers-Riemslog JWP, Philippou H, et al. Factor XIIa regulates the structure of the fibrin clot independently of thrombin generation through direct interaction with fibrin.

Blood. 2011;118(14):3942-3951. doi:10.1182/blood-2011-03-339572

148. Schmaier AH. Contact activation: A revision. In: *Thrombosis and Haemostasis*. Vol 78. ; 1997:101-107.

149. Girey GJD, Talamo RC, Colman RW. The kinetics of the release of bradykinin by kallikrein in normal human plasma. *Transl Res*. 1972;80(4):496-505.

150. Citarella F, Ravon DM, Pascucci B, Felici a, Fantoni a, Hack CE. Structure/function analysis of human factor XII using recombinant deletion mutants. Evidence for an additional region involved in the binding to negatively charged surfaces. *Eur J Biochem*. 1996.

doi:10.1111/j.1432-1033.1996.0240q.x

151. McMillin CR, Saito H, Ratnoff OD, Walton AG. The secondary structure of human Hageman factor (factor XII) and its alteration by activating agents. *J Clin Invest*. 1974.

doi:10.1172/JCI107877

152. Zhuo R, Miller R, Bussard KM, Siedlecki CA, Vogler EA. Procoagulant stimulus processing by the intrinsic pathway of blood plasma coagulation. *Biomaterials*. 2005.

doi:10.1016/j.biomaterials.2004.08.008

153. Walsh PN. The Effects of Collagen and Kaolin on the Intrinsic Coagulant Activity of Platelets. EVIDENCE FOR AN ALTERNATIVE PATHWAY IN INTRINSIC

COAGULATION NOT REQUIRING FACTOR XII. *Br J Haematol*. 1972. doi:10.1111/j.1365-2141.1972.tb05687.x

154. Green RJ, Davies MC, Roberts CJ, Tendler SJB. Competitive protein adsorption as observed by surface plasmon resonance. *Biomaterials*. 1999;20(4):385-391. doi:10.1016/S0142-9612(98)00201-4

155. Huang J, Yue Y, Zheng C. [Vroman effect of plasma protein adsorption to biomaterials

surfaces]. *Sheng Wu Yi Xue Gong Cheng Xue Za Zhi*. 1999;16(3):371-376.

http://www.ncbi.nlm.nih.gov/entrez/query.fcgi?cmd=Retrieve&db=PubMed&dopt=Citation&list_uids=12552765.

156. Leonard EF, Vroman L. Is the Vroman effect of importance in the interaction of blood with artificial materials? *J Biomater Sci Polym Ed*. 1992;3(1):95-107.

doi:10.1163/156856292X00105

157. Roach P, Farrar D, Perry CC. Interpretation of protein adsorption: Surface-induced conformational changes. *J Am Chem Soc*. 2005;127(22):8168-8173. doi:10.1021/ja042898o

158. Anderson L, Anderson NG. High resolution two-dimensional electrophoresis of human plasma proteins. *Proc Natl Acad Sci U S A*. 1977;74(12):5421-5425. doi:VL - 74

159. Gorbet MB, Sefton M V. Biomaterial-associated thrombosis: Roles of coagulation factors, complement, platelets and leukocytes. In: *The Biomaterials: Silver Jubilee Compendium*. ; 2006:219-241. doi:10.1016/B978-008045154-1.50025-3

160. Wertz CF, Santore MM. Adsorption and relaxation kinetics of albumin and fibrinogen on hydrophobic surfaces: Single-species and competitive behavior. *Langmuir*. 1999;15(26):8884-8894. doi:10.1021/la990089q

161. Gibbins JM. Platelet adhesion signalling and the regulation of thrombus formation. *J Cell Sci*. 2004;117(16):3415-3425. doi:10.1242/jcs.01325

162. Ryu JK, Davalos D, Akassoglou K. Fibrinogen signal transduction in the nervous system. *J Thromb Haemost*. 2009;7(SUPPL. 1):151-154. doi:10.1111/j.1538-7836.2009.03438.x

163. Rubens F, Brash J, Weitz J, Kinlough-Rathbone R. Interactions of thermally denatured fibrinogen on polyethylene with plasma proteins and platelets. *J Biomed Mater Res*. 1992;26(12):1651-1663. doi:10.1002/jbm.820261209

164. Skarja GA, Brash JL, Bishop P, Woodhouse KA. Protein and platelet interactions with thermally denatured fibrinogen and cross-linked fibrin coated surfaces. *Biomaterials*. 1998;19(23):2129-2138. doi:10.1016/S0142-9612(98)00045-3
165. Nishiyama K, Okudera T, Watanabe T, et al. Basic characteristics of plasma rich in growth factors (PRGF): blood cell components and biological effects. *Clin Exp Dent Res*. 2016;2(2):96-103. doi:10.1002/cre2.26
166. Ko TM, Cooper SL. SURFACE-PROPERTIES AND PLATELET-ADHESION CHARACTERISTICS OF ACRYLIC-ACID AND ALLYLAMINE PLASMA-TREATED POLYETHYLENE. *J Appl Polym Sci*. 1993;47(9):1601-1619. doi:10.1002/app.1993.070470908
167. Li N, Hu H, Lindqvist M, Wikström-Jonsson E, Goodall a H, Hjemdahl P. Platelet-leukocyte cross talk in whole blood. *Arterioscler Thromb Vasc Biol*. 2000;20(12):2702-2708. doi:10.1161/01.ATV.20.12.2702
168. Goodman SL, Grasel TG, Cooper SL, Albrecht RM. Platelet shape change and cytoskeletal reorganization on polyurethaneureas. *J Biomed Mater Res*. 1989;23(1):105-123. doi:10.1002/jbm.820230109
169. Rendu F, Brohard-Bohn B. The platelet release reaction: Granules' constituents, secretion and functions. *Platelets*. 2001;12(5):261-273. doi:10.1080/09537100120068170
170. Plow EF, McEver RP, Collier BS, Woods VL, Marguerie GA, Ginsberg MH. Related binding mechanisms for fibrinogen, fibronectin, von Willebrand factor, and thrombospondin on thrombin-stimulated human platelets. *Blood*. 1985;66:724-727.
171. Conti E, Carrozza C, Capoluongo E, et al. Insulin-like growth factor-1 as a vascular protective factor. *Circulation*. 2004;110(15):2260-2265. doi:10.1161/01.CIR.0000144309.87183.FB

172. Ross R. PLATELET-DERIVED GROWTH FACTOR. *Lancet*. 1989;333(8648):1179-1182. doi:10.1016/S0140-6736(89)92760-8
173. Amiral J, Bridey E, Dreyfus M, et al. Platelet factor 4 complexed to heparin is the target for antibodies generated in heparin-induced thrombocytopenia [4]. *Thromb Haemost*. 1992;68(1):95-96.
174. André P. P-selectin in haemostasis. *Br J Haematol*. 2004;126(3):298-306. doi:10.1111/j.1365-2141.2004.05032.x
175. Van Der Zee PM, Biró É, Ko Y, et al. P-selectin- and CD63-exposing platelet microparticles reflect platelet activation in peripheral arterial disease and myocardial infarction. *Clin Chem*. 2006;52(4):657-664. doi:10.1373/clinchem.2005.057414
176. Lin H, Chen B, Sun W, Zhao W, Zhao Y, Dai J. The effect of collagen-targeting platelet-derived growth factor on cellularization and vascularization of collagen scaffolds. *Biomaterials*. 2006;27(33):5708-5714. doi:10.1016/j.biomaterials.2006.07.023
177. Chandler WL, Velan T. Estimating the rate of thrombin and fibrin generation in vivo during cardiopulmonary bypass. *Blood*. 2003;101(11):4355-4362. doi:10.1182/blood-2002-08-2400
178. Weitz JI, Hudoba M, Massel D, Maraganore J, Hirsh J. Clot-bound thrombin is protected from inhibition by heparin-antithrombin III but is susceptible to inactivation by antithrombin III-independent inhibitors. *J Clin Invest*. 1990;86(2):385-391. doi:10.1172/JCI114723
179. Hoek JA, Sturk A, Ten Cate JW, Lamping RJ, Berends F, Borm JJJ. Laboratory and clinical evaluation of an assay of thrombin-antithrombin III complexes in plasma. *Clin Chem*. 1988;34(10):2058-2062.
180. Williams DF. On the mechanisms of biocompatibility. *Biomaterials*. 2008.

doi:10.1016/j.biomaterials.2008.04.023

181. Brodbeck WG, Anderson JM. Giant cell formation and function. *Curr Opin Hematol.*

2009. doi:10.1097/MOH.0b013e32831ac52e.GIANT

182. Leszczak V, Popat KC. Improved in vitro blood compatibility of polycaprolactone nanowire surfaces. *ACS Appl Mater Interfaces.* 2014;6(18):15913-15924.

doi:10.1021/am503508r

183. Anderson JM, Rodriguez A, Chang DT. Foreign body reaction to biomaterials. *Semin Immunol.* 2008. doi:10.1016/j.smim.2007.11.004

184. Cassatella M a. The production of cytokines by polymorphonuclear neutrophils. *Immunol Today.* 1995;16(1):21-26. doi:10.1016/0167-5699(95)80066-2

185. Anderson JM. Chapter 4 Mechanisms of inflammation and infection with implanted devices. *Cardiovasc Pathol.* 1993;2(3 SUPPL.):33-41. doi:10.1016/1054-8807(93)90045-4

186. Henson PM. The immunologic release of constituents from neutrophil leukocytes. I. The role of antibody and complement on nonphagocytosable surfaces or phagocytosable particles. *J Immunol.* 1971;107:1535-1546.

187. Henson PM. Mechanisms of exocytosis in phagocytic inflammatory cells. Parke-Davis Award Lecture. *Am J Pathol.* 1980;101(3):494-511.

188. Noris M, Remuzzi G. Overview of complement activation and regulation. *Semin Nephrol.* 2013;33(6):479-492. doi:10.1016/j.semnephrol.2013.08.001

189. Murphy K, Travers P, Walport M. The complement system and innate immunity. *Janeway's Immunobiol.* 2008;7:61-81. doi:10.1086/596249

190. Matsushita M, Fujita T. Ficolins and the lectin complement pathway. *Immunol Rev.* 2001;180:78-85. doi:10.1034/j.1600-065X.2001.1800107.x

191. Nilsson B, Nilsson Ekdahl K. The tick-over theory revisited: Is C3 a contact-activated protein? *Immunobiology*. 2012;217(11):1106-1110. doi:10.1016/j.imbio.2012.07.008
192. Bexborn F, Andersson PO, Chen H, Nilsson B, Ekdahl KN. The tick-over theory revisited: Formation and regulation of the soluble alternative complement C3 convertase (C3(H₂O)Bb). *Mol Immunol*. 2008;45(8):2370-2379. doi:10.1016/j.molimm.2007.11.003
193. Howell BF, McCune S, Schaffer R. Lactate-to-pyruvate or pyruvate-to-lactate assay for lactate dehydrogenase: A re-examination. *Clin Chem*. 1979;25(2):269-272.
doi:10.1093/jac/dkr570
194. Washington IM, Van Hoosier G. Clinical Biochemistry and Hematology. In: *The Laboratory Rabbit, Guinea Pig, Hamster, and Other Rodents*. ; 2012:57-116. doi:10.1016/B978-0-12-380920-9.00003-1
195. Chan FKM, Moriwaki K, De Rosa MJ. Detection of necrosis by release of lactate dehydrogenase activity. *Methods Mol Biol*. 2013;979:65-70. doi:10.1007/978-1-62703-290-2-7
196. Wang MO, Etheridge JM, Thompson JA, Vorwald CE, Dean D, Fisher JP. Evaluation of the in vitro cytotoxicity of cross-linked biomaterials. *Biomacromolecules*. 2013;14(5):1321-1329. doi:10.1021/bm301962f
197. Janeway CA, Travers P, Walport M, Shlomchik M. Immunobiology: The Immune System In Health And Disease. *Immuno Biol* 5. 2001. doi:10.1111/j.1467-2494.1995.tb00120.x
198. Rippel RA, Ghanbari H, Seifalian AM. Tissue-engineered heart valve: Future of cardiac surgery. *World J Surg*. 2012. doi:10.1007/s00268-012-1535-y
199. Butcher JT, Nerem RM. Valvular endothelial cells and the mechanoregulation of valvular pathology. *Philos Trans R Soc B Biol Sci*. 2007. doi:10.1098/rstb.2007.2127
200. Hauser S, Jung F, Pietzsch J. Human Endothelial Cell Models in Biomaterial Research.

Trends Biotechnol. 2017. doi:10.1016/j.tibtech.2016.09.007

201. Yau JW, Teoh H, Verma S. Endothelial cell control of thrombosis. *BMC Cardiovasc Disord.* 2015. doi:10.1186/s12872-015-0124-z

202. Jansson K, Bengtsson L, Swedenborg J, Haegerstrand A. In vitro endothelialization of bioprosthetic heart valves provides a cell monolayer with proliferative capacities and resistance to pulsatile flow. *J Thorac Cardiovasc Surg.* 2001. doi:10.1067/mtc.2001.110251

203. Herklotz M, Hanke J, Hänsel S, et al. Biomaterials trigger endothelial cell activation when co-incubated with human whole blood. *Biomaterials.* 2016.
doi:10.1016/j.biomaterials.2016.07.022

204. Khan OF, Sefton M V. Endothelialized biomaterials for tissue engineering applications in vivo. *Trends Biotechnol.* 2011. doi:10.1016/j.tibtech.2011.03.004

205. Prasad CK, Krishnan LK. Regulation of endothelial cell phenotype by biomimetic matrix coated on biomaterials for cardiovascular tissue engineering. *Acta Biomater.* 2008.
doi:10.1016/j.actbio.2007.05.012

206. Califano JP, Reinhart-King CA. A Balance of Substrate Mechanics and Matrix Chemistry Regulates Endothelial Cell Network Assembly. *Cell Mol Bioeng.* 2008. doi:10.1007/s12195-008-0022-x

207. Wang Y-X, Robertson JL, Spillman Jr. WB, Claus RO. Effects of the chemical structure and the surface properties of polymeric biomaterials on their biocompatibility. *Pharm Res.* 2004.
doi:10.1023/B:PHAM.0000036909.41843.18

208. Chang H-I, Wang Y. Cell Responses to Surface and Architecture of Tissue Engineering Scaffolds. In: *Regenerative Medicine and Tissue Engineering - Cells and Biomaterials.* ; 2011.
doi:10.5772/21983

209. Rehfeldt F, Engler AJ, Eckhardt A, Ahmed F, Discher DE. Cell responses to the mechanochemical microenvironment-Implications for regenerative medicine and drug delivery. *Adv Drug Deliv Rev.* 2007. doi:10.1016/j.addr.2007.08.007
210. Ma PX. Biomimetic materials for tissue engineering. *Adv Drug Deliv Rev.* 2008. doi:10.1016/j.addr.2007.08.041
211. Kim HN, Jiao A, Hwang NS, et al. Nanotopography-guided tissue engineering and regenerative medicine. *Adv Drug Deliv Rev.* 2013. doi:10.1016/j.addr.2012.07.014
212. García AJ. Surface Modification of Biomaterials. In: *Principles of Regenerative Medicine.* ; 2011. doi:10.1016/B978-0-12-381422-7.10036-7
213. Greisler HP, Dennis JW, Endean ED, Ellinger J, Friesel R, Burgess W. Macrophage/biomaterial interactions: The stimulation of endothelialization. *J Vasc Surg.* 1989. doi:10.1016/0741-5214(89)90478-3
214. Tan CH, Muhamad N, Abdullah MMAB. Surface Topographical Modification of Coronary Stent: A Review. In: *IOP Conference Series: Materials Science and Engineering.* ; 2017. doi:10.1088/1757-899X/209/1/012031
215. Choi WS, Joung YK, Lee Y, et al. Enhanced Patency and Endothelialization of Small-Caliber Vascular Grafts Fabricated by Coimmobilization of Heparin and Cell-Adhesive Peptides. *ACS Appl Mater Interfaces.* 2016. doi:10.1021/acsami.5b12052
216. Williams SK. Endothelial cell transplantation. *Cell Transpl.* 1995.
217. Liu H, Li X, Niu X, Zhou G, Li P, Fan Y. Improved hemocompatibility and endothelialization of vascular grafts by covalent immobilization of sulfated silk fibroin on poly(lactic-co-glycolic acid) scaffolds. *Biomacromolecules.* 2011. doi:10.1021/bm200479f
218. Aird WC. Phenotypic heterogeneity of the endothelium: I. Structure, function, and

- mechanisms. *Circ Res*. 2007. doi:10.1161/01.RES.0000255691.76142.4a
219. Simon A, Wilhelmi M, Steinhoff G, Harringer W, Brucke P, Haverich A. Cardiac valve endothelial cells: Relevance in the long-term function of biologic valve prostheses. *J Thorac Cardiovasc Surg*. 1998. doi:10.1016/S0022-5223(98)70167-9
220. Liu T, Liu S, Zhang K, Chen J, Huang N. Endothelialization of implanted cardiovascular biomaterial surfaces: The development from in vitro to in vivo. *J Biomed Mater Res - Part A*. 2014. doi:10.1002/jbm.a.35025
221. Verheye S, Markou CP, Salame MY, et al. Reduced thrombus formation by hyaluronic acid coating of endovascular devices. *Arterioscler Thromb Vasc Biol*. 2000;20:1168-1172. doi:10.1161/01.ATV.20.4.1168
222. Tamer TM. Hyaluronan and synovial joint: function, distribution and healing. *Interdiscip Toxicol*. 2013;6(3). doi:10.2478/intox-2013-0019
223. Li J, Zhang K, Ma W, et al. Investigation of enhanced hemocompatibility and tissue compatibility associated with multi-functional coating based on hyaluronic acid and Type IV collagen. *Regen Biomaterials*. 2016:149-157. doi:doi: 10.1093/rb/rbv03
224. Turner NJ, Kielty CM, Walker MG, Canfield AE. A novel hyaluronan-based biomaterial (Hyaff-11®) as a scaffold for endothelial cells in tissue engineered vascular grafts. *Biomaterials*. 2004. doi:10.1016/j.biomaterials.2004.02.002
225. Bae IH, Jeong MH, Kim JH, et al. The control of drug release and vascular endothelialization after hyaluronic acid-coated paclitaxel multi-layer coating stent implantation in porcine coronary restenosis model. *Korean Circ J*. 2017. doi:10.4070/kcj.2016.0203
226. Bedair TM, ElNaggar MA, Joung YK, Han DK. Recent advances to accelerate re-endothelialization for vascular stents. *J Tissue Eng*. 2017. doi:10.1177/2041731417731546

227. Puperi DS, O'Connell RW, Punske ZE, Wu Y, West JL, Grande-Allen KJ. Hyaluronan Hydrogels for a Biomimetic Spongiosa Layer of Tissue Engineered Heart Valve Scaffolds. *Biomacromolecules*. 2016. doi:10.1021/acs.biomac.6b00180
228. Nazir R. Collagen–hyaluronic acid based interpenetrating polymer networks as tissue engineered heart valve. *Mater Sci Technol*. 2016. doi:10.1179/1743284715Y.0000000097
229. Pandis L, Zavan B, Bassetto F, et al. Hyaluronic acid biodegradable material for reconstruction of vascular wall: A preliminary study in rats. *Microsurgery*. 2011. doi:10.1002/micr.20856
230. Kluin J, Talacua H, Smits AIPM, et al. In situ heart valve tissue engineering using a bioresorbable elastomeric implant – From material design to 12 months follow-up in sheep. *Biomaterials*. 2017. doi:10.1016/j.biomaterials.2017.02.007

CHAPTER 2

CHARACTERIZATION AND HEMOCOMPATIBILITY OF SEQUENTIAL INTERPENETRATING POLYMER NETWORKS OF HYALURONAN AND LINEAR LOW-DENSITY POLYETHYLENE FOR HEART VALVE LEAFLET APPLICATIONS

2.1 Introduction

2.1.1 Current Heart Valve Designs Require Improvement to Meet Patient Needs

For the most severe cases of valvular disease, heart valve replacement therapy (HVRT) has become a crucial method of treatment to enhance survival and improve the quality of life of patients. However, despite the overall success of these surgical procedures, even the most advanced heart valves (HV) on the market are plagued with such issues as durability, hemolysis, pannus growth, and/or calcification resulting in the need for subsequent replacement and/or life-long anticoagulation therapy¹⁻³. HVs are broadly placed into two categories: mechanical heart valves (MHV) and tissue-based valves (TBV). MHVs made with synthetic leaflets have been used since the 1970's and have proven to be highly durable, usually lasting the life of the patient, but are also exceedingly thrombotic. While the leaflets in MHVs are now made of materials such as pyrolytic carbon that are resistant to thrombosis, the rigid leaflet design can result in hematocyte lysis, as well as localized regions of turbulent flow, and stasis facilitating thrombus formation (See **Fig. 2.1.1**)^{1, 3-6}.

As an alternative, TBVs are composed of bovine or equine pericardium or porcine aortic valve leaflets offering a thin, flexible, leaflet design similar to the native valve which is vastly

more hemocompatible than MHVs. As a result, patients may be able to reduce or eliminate the need for anticoagulation therapy after the first few months following surgery ¹³. Unfortunately, TBVs are prone to tissue degradation and mineralization (as seen in the native valve). Consequently, TBV need to be replaced approximately every 10-15 years ⁶. Due to the risks to morbidity and mortality associated with both MHVs and TBVs point to a critical need to develop a heart valve leaflet which is both biocompatible and highly durable.

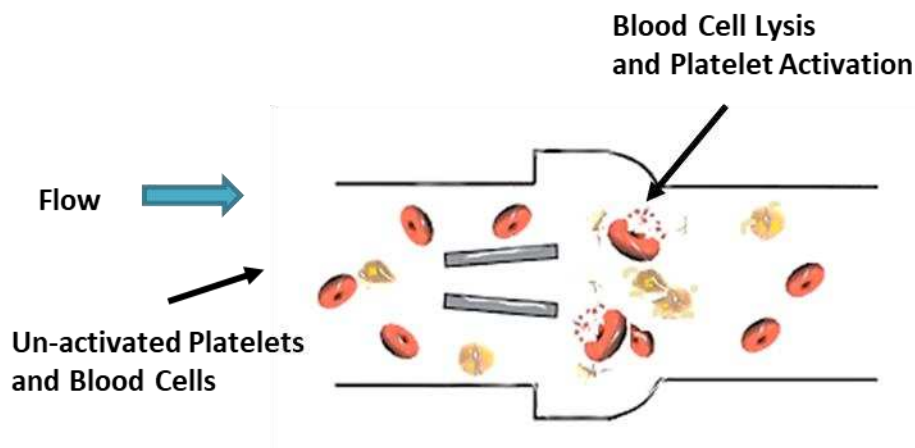


Figure 2.1.1: Red blood cell lysis and platelet activation due to sheer stress can occur as blood flows across mechanical heart valve leaflets.

2.1.2 Polymer Valves Offer the Durability of MHVs and the Hemocompatibility of TBVs

To this end, a vast amount of exploration has been done in the field of polymeric heart valve (PHV) leaflet development⁶. Advantages of PHVs are ultimately determined through the combination of the base material (polyurethane, PTFE, silicone, etc.) and method of fabrication. Although PHVs have all the physical properties present to lend themselves to the fabrication an ideal valve, they remain highly thrombotic similar to MHVs ^{6, 18}. Unlike MHVs whose proclivity for thrombosis is dependent upon valve profile and a rigid leaflet, the affinity for thrombosis in

PHVs is dependent on the inherent mechanical and surface properties such as bending stiffness, hardness, wettability, roughness, and topography¹⁻³.

2.1.3 Surface Properties of Biomaterials Affect Hemocompatibility

The relationship between hemocompatibility and surface properties on various implant surfaces is well documented²⁰⁻²⁴. Upon initial contact of an implant with the blood, proteins readily attach to the surface forming a bioactive interface that mediates between the implant and the hemostatic response. As blood proteins attach and spread, changing conformation, hydrophobic pockets are exposed. Hydrophobic surfaces tend to attract more proteins than their hydrophilic counterparts and can exacerbate healing responses such as platelet and leukocyte adhesion/activation leading to implant rejection and thrombosis and inflammation^{20,25}. However, it is well known that contact activation proteins are more attracted to hydrophilic surfaces⁴. The aim of creating a truly biocompatible PHVs therefore lies in the ability to control the interfacial adsorption of proteins through manipulation of surface chemistry, surface charge, and hydrophobicity in order to attenuate the provocation of these biological cascades²⁰.

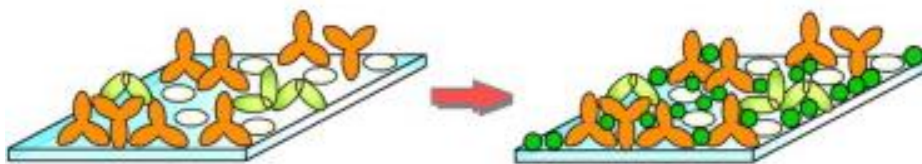


Figure 2.1.3: Protein competition on the surface determines future coagulation and immune events⁵. Reproduced with permission © Elsevier Ltd.

2.1.4 Hyaluronan Enhanced Linear Low-Density Polyethylene to Improve Hemocompatibility

To achieve this, we have developed a novel, hydrophilic, heart valve leaflet material comprised of an interpenetrating polymer network (IPN) of hyaluronan (HA) and linear low-density polyethylene (LLDPE). HA is a highly lubricious, anionic, glycosaminoglycan ubiquitously found in the human body. It is present throughout the extracellular matrix of almost all tissues, in the ocular viscera, the synovial fluid, and in the native heart valve leaflet. Because it is nontoxic, biodegradable, biocompatible, and non-immunogenic it is currently being investigated for a vast array of biomedical applications including cardiovascular therapies such as hydrogel based regenerative cell therapies for myocardial infarction, HA-coated stents, and surface modifications of polyurethane and metals for use in blood-contacting implants²⁶⁻³¹. Although HA is known to interact with some blood components, previous studies have shown that HA coated surfaces significantly reduce thrombosis, and high systemic concentrations of HA lead to extended bleeding times thereby giving credence to its antithrombotic properties³²⁻³⁴. LLDPE was chosen as our base material for its ability to be manufactured to be very thin similar to the native leaflet while maintaining a high tensile and tear strength, complemented by a low bending stiffness¹⁹. The aim of this study was to assess the ability of this novel material to reduce clotting mechanism to ascertain its feasibility to be used as a blood-contacting, flexible heart valve leaflet.

2.2 Materials and Methods

2.2.1 Fabrication and Characterization of HA-LLDPE Sequential IPNs

Dowlex 2056 LLDPE (Dow Corning) blown extruded films (80 μ m thickness) were cleaned in acetone, dried, and then immersed in xylene for 12hrs, followed by vacuum drying at 50°C to achieve constant weight prior to further use. Sodium hyaluronate (MW: 7.31 \times 10⁵Da) was

purchased from Lifecore Biomedical and stored at 2-8°C. Cetyltrimethylammonium bromide (CTAB) was obtained from Fisher Scientific. Poly (hexamethylene diisocyanate) (p (HMDI)), desmodur N3200, hexamethyldisilazane (HMDS, 99%), anhydrous dimethyl sulfoxide (DMSO, >99.9%) and acetone (ACS grade) were obtained from Sigma Aldrich. Xylene and 3A molecular sieves were purchased from EMD Millipore. Xylene was dried over molecular sieves for 24hrs then distilled into a silylated dry round bottom flask and stored under dry nitrogen atmosphere until further use. Ethanol (200 proof ACS/USP grade) was obtained from Pharmco (Brookfield, CT). All chemicals were used as received unless specified. Silylated hyaluronancetyltrimethylammonium (SilylHA-CTA) complex was synthesized as described elsewhere³⁵.

LLDPE films (3" diameter) were mounted onto an ultra-high molecular weight polyethylene holder and transferred to a dry N₂ atmosphere inside a glove-bag. The detailed fabrication process is described elsewhere¹⁹. In brief:

- LLDPE films were swollen for 60mins in 2.5% w/v SilylHA-CTA xylene solution at 50°C in a dry N₂ filled glove-bag.
- Films were then dried for approximately 2-3hrs in a vacuum oven at 50°C until no weight change was observed.
- SilylHA-CTA impregnated LLDPE films (SilylHA-CTA-LLDPE) were then crosslinked in 2% v/v p (HMDI) xylene solution for 60mins at 50°C in a dry N₂ filled glove-bag.
- Crosslinked SilylHA-CTA-LLDPE (xSilylHA-CTA-LLDPE) was cured in a vacuum oven for 15hrs at 50°C.
- Excess p (HMDI) was removed by soaking films in acetone for 1min and subsequently drying in a vacuum oven for 5-10mins at 50°C until no visible traces of acetone remained.

- A final step of hydrolysis to get rid of the Silyl and CTA groups was performed as described elsewhere. HA-LLDPE surfaces were then stored in a vacuum desiccator until further characterization.

2.2.2 Characterization of HA-LLDPE Surfaces

HA-LLDPE surfaces were characterized using attenuated total reflectance Fourier transform infrared spectroscopy (ATR-FTIR) and thermogravimetric analysis (TA). A Nicolet iS-50 FT-IR spectrometer with KBR beam splitter and diamond ATR crystal accessory was used to verify the presence of HA on the treated LLDPE films. Five spectra were taken with 4cm^{-1} resolution with 64 scans per spectra at different sections on the film. Spectra were averaged together for analysis.

A TGA 2950 (TA Instruments) was used for bulk-weight analysis of HA-LLDPE films. Between 4-6 mg of HA-LLDPE film was used per run and three runs were performed for each HA-LLDPE film. In a N_2 rich atmosphere, the samples were heated up to 600°C as follows:

A heating rate of $25^\circ\text{C}/\text{min}$ until a temperature of 110°C was reached followed by an isothermal hold for 5mins to ensure any adsorbed water was evaporated.

A heating rate of $10^\circ\text{C}/\text{min}$ until a temperature of 540°C was reached.

A heating rate of $25^\circ\text{C}/\text{min}$ until a temperature of 600°C was reached, followed by an isothermal hold for 5mins.

The resulting thermograms were analyzed for weight % changes occurring between 150°C to 350°C . The final true weight changes due to crosslinked HA were quantified as the difference between the mean HA-LLDPE weight % and LLDPE weight %. Fabrication of HA-LLDPE materials were performed by Dr. Sue James lab at Colorado State University.

2.2.3 Contact Angle

For contact angle measurements, HA-LLDPE substrates were hydrated in DI water overnight before being analyzed. The substrates were placed on a stage of a Rame-Hart Contact Angle goniometer. The dispensing needle was placed just above the substrate, and an initial drop was dispensed. For advancing angles, the volume of the drop was gradually increased; the tangent contact angle was measured as the contact line advanced outward, until a maximum angle stabilized as seen through plateauing of the angle value using DropImage Advanced software. The water was subsequently sucked back up slowly with the receding angle measured from the receding contact line until the angle stabilized or the angle was unmeasurable.

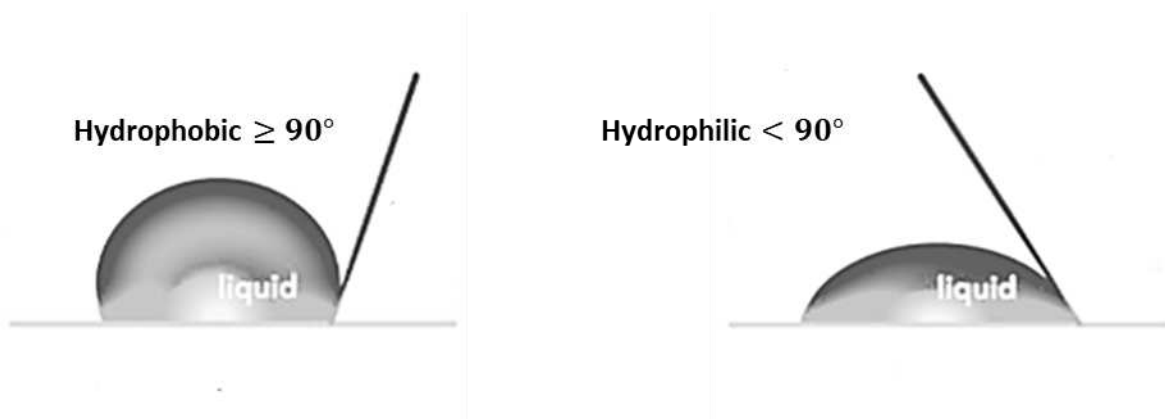


Figure 2.2.3: Contact angle measurements determine the wettability of a material surface.

2.2.4 Blood Plasma Isolation and Incubation on Different Surfaces

Whole human blood was drawn via venous phlebotomy from healthy donors who had refrained from taking thromboxane inhibitors (aspirin, ibuprofen, naproxen etc.) for at least 2 weeks. Blood was collected into 10ml EDTA coated vacuum tubes. Plasma was isolated through centrifugation at 100 g for 15mins and allowed to rest for 10mins prior to use. Plasma was pooled

into a sterilized 50ml conical tube. Tissue culture polystyrene (PS), LLDPE, and HALLDPE (all 8mm in size) were placed into a 24-well plate and incubated with 1ml of pooled plasma on a horizontal shaker plate (100rpm) for 2hrs at 37°C and 5% CO₂.

2.2.5 Material Cytotoxicity

Cytotoxicity was determined using a commercially available lactate dehydrogenase (LDH) assay kit (Cayman Chemical). After 2hrs of incubation in plasma, the substrates were further shaken on a horizontal shaker plate (1000rpm) for 5mins at room temperature. 100µL of substrate-exposed plasma and manufacturer supplied standards were transferred to a 96-well plate. A reaction solution consisting of 96% v/v assay buffer, 1% v/v NAD⁺, 1% v/v lactic Acid, 1% v/v INT, and 1% v/v LDH diaphorase was added in equal amounts (1:1) to all the standards and substrate-exposed plasma. This was followed by gentle shaking on horizontal shaker plate (100rpm) for 30mins at room temperature. The absorbance of this was immediately measured at a wavelength of 490nm using a plate reader.

2.2.6 Whole Blood Clotting on Different Surfaces

Whole blood clotting on different surfaces was evaluated by measuring the amount of free hemoglobin. Whole human blood from healthy donors who had refrained from taking thromboxane inhibitors for at least 2 weeks was drawn via venipuncture into vacuum tubes without any anticoagulants. 5µL of blood was immediately placed onto the surfaces and allowed to clot for up to 60mins. To measure the free hemoglobin in the un-clotted blood, the blood the substrates were transferred into a new 24-well plate containing 500µL of DI water after 15, 30 and 60mins. The surfaces were then gently agitated for 30secs and allowed to rest in DI water for

5mins to release the free hemoglobin from red blood cells that were not encapsulated in the clot. 200 μ L of the DI water/un-clotted blood solution was transferred to a 96-well plate and the absorbance was measured at a wavelength of 540nm using a plate reader.

2.2.7 Blood Cell Adhesion on Different Surfaces

Blood cell adhesion was investigated using fluorescence microscopy. After 2hrs of incubation in plasma, the surfaces were stained with Calcein-AM (Thermo-scientific). The un-adhered cells were gently aspirated and the surfaces were rinsed with PBS (2x). 1ml of a 5 μ M solution of Calcein-AM in PBS was added to the substrates. The substrates were allowed to incubate for 20mins in the stain solution. After 20mins, the stain solution was gently aspirated, and the substrates rinsed with PBS (2x). The surfaces were immediately imaged using a Zeiss Axiovision fluorescent microscope using a 493/514nm filter. All images were processed using Image J software.

2.2.8 Platelet Activation on Different Surfaces

Platelet activation was determined using scanning electron microscopy (SEM). After 2hrs of incubation in plasma, substrates were fixed with a primary fixative (6% glutaraldehyde (Sigma), 0.1M sodium cacodylate (Polysciences), and 0.1M sucrose (Sigma)) for 45 mins. The substrates were then transferred to a secondary fixative (primary fixative without glutaraldehyde) for 10mins. This was followed by exposing the substrates to consecutive solutions of ethanol (35%, 50%, 70% and 100%) for 10mins each followed by a final incubation in 97% hexamethyldisilazane (HMDS for 10mins at room temperature). The substrates were then air-

dried and stored in a desiccator until imaging by SEM. Prior to imaging; the surfaces were coated with a 10nm layer of gold and imaged at 5kV.

2.2.9 Platelet Factor 4 Expression on Different Surfaces

Platelet factor 4 (PF-4) expression was measured using an enzyme linked immunoabsorbant assay kit (ELISA, RayBio) to evaluate release from alpha granules during platelet activation. The protocol provided by the manufacturer was followed. After 2hrs of incubation, the substrate-exposed plasma was diluted (1:200) in the assay diluent. The diluted plasma and were transferred into the micro-assay well plate and incubated for 2.5hrs on a horizontal shaker plate (100rpm) at room temperature. The plasma and standards were aspirated, and the wells were washed (4x) with wash buffer and incubated with biotinylated antibody for 1hr on a horizontal shaker plate (100 rpm) at room temperature. The antibody was then aspirated, and the wells were washed (4x) to remove any unbound antibody. The wells were then incubated with a horseradish peroxidase (HRP)-streptavidin solution (1:25,000 in assay diluent) and incubated for 45mins on a horizontal shaker plate (100rpm) at room temperature. HRP was then aspirated and the wells were washed (4x) with wash buffer and incubated with TMB solution for 30mins on a horizontal shaker plate (100rpm) at room temperature in a dark environment. The reaction was stopped by adding stop solution and the optical density was measured using a plate reader at 450nm.

2.2.10 Contact Activation on Different Surfaces

Contact activation was assessed by an acid stop method (Chromogenix) to investigate prekallikrein expression. The protocol provided by the manufacturer was followed. After 2hrs of

incubation, the substrate-exposed plasma was diluted 10-fold in Tris buffer solution (pH 7.8). 100µl of the diluted plasma was transferred to a 96-well plate and incubated at 37°C and 5% CO₂ for 3-4mins. 100µl of pre-warmed (37°C) substrate solution was added to the wells and incubated at 37°C and 5% CO₂ for further 10mins. The reaction was stopped by adding 100µl of 20% acetic acid to the wells. Plasma blanks were prepared by adding reagents in reverse order, without incubation. The optical density of the solution was measured using a plate reader at 405nm.

2.2.11 Thrombin Anti-thrombin (TAT) Complex Formation on Different Surfaces

Thrombin anti-thrombin (TAT) complex formation was measured using a human thrombin anti-thrombin ELISA kit (HaemoScan). The protocol provided by the manufacturer was followed. A Nunc Maxisorp 96-well microtiter plate was coated with capture antibody and incubated in coating buffer overnight at 2-8°C. The plate was then washed (3x) with PBS-Tween wash buffer solution. After 2hrs of incubation, the substrate-exposed plasma was diluted (1:200). 100µL of diluted plasma and standards were transferred into the wells of the microtiter plate and incubated for 1hr at room temperature. The plasma and controls were then aspirated, and the wells were washed (3x) with wash buffer and incubated with 100µl of antibody solution 1hr at room temperature. The wells were washed (3x) and 100µl of substrate solution was added. After 20mins, the reaction was stopped with 50µl of stop solution and the optical density was measured using a plate reader at 450nm.

2.2.12 Thrombin Generation on Different Surfaces

The rate of thrombin generation was assessed using a thrombin generation assay (TGA, HaemoScan). The protocol supplied by the manufacturer was followed. The substrates were

incubated at 37°C with 350µl of diluted TGA plasma for 15mins in a sterilized centrifuge tube. 175µl of a mixture of TGA reagent A and TGA reagent B was added to each tube. After 1min, 10µl of this mixture was placed into a tube containing 490µl of buffer B and stored on ice. Tubes were immediately placed back in the water bath after sampling. This was repeated after 2mins, 4mins, and 6mins for each substrate. 150µl of samples from each substrate and standard was placed into a 96-well plate and incubated for 2mins at 37°C and 5% CO₂. 50µl of diluted substrate solution was added to each well and the covered well plate was incubated for 20mins at 37°C and 5% CO₂. 50µl of stop solution was added to each well and optical density was read immediately at 405nm, using 540nm as a reference wavelength. Thrombin generation rate was calculated by determining the highest velocity between the two measured time points and correcting for the dilution factor (50x).

2.2.13 Hemolytic Activity on Different Surfaces

Hemolytic activity was evaluated using a biomaterial hemolytic assay (HaemoScan). Sterilized substrates and reference material (positive control) provided by the manufacturer were placed in syringes with one syringe without any material (negative control). An erythrocyte suspension (500µl) provided by the manufacturer was added to each syringe containing substrates, reference material or the negative control. Air was removed and parafilm was used to close the outlet. Vials were incubated at 37°C for 24hrs while subjected to end over end rotating on a rotator plate. The erythrocyte suspension was carefully transferred to a centrifuge tube (1.5ml) followed by centrifugation at high speed (3600g) for 1min. 20µl of supernatant from each substrate, reference material and negative control was transferred into a 96-well plate along with 180µl of

assay buffer. The 96-well plate was mixed on a shaker plate and the optical density was measured using a plate reader at 415nm.

2.3 Statistical Analysis

Each qualitative experiment was performed to evaluate differences between PS, LLDPE and HA-LLDPE on at least three substrates ($n_{\min} = 9$), except for ELISA's which were performed on at least five substrate surfaces per group ($n_{\min} = 15$). Each assay was repeated at least three times with three different whole blood plasma populations. All results were evaluated using a one-way analysis of variance (ANOVA) with a Tukey's, Bonferroni, and Scheffé post-hoc tests.

2.4 Results and Discussion

2.4.1 Characterization Results of HA-LLDPE Surfaces

To ensure the presence of between HA on LLDPE, ATR-FTIR spectra were taken for HA-LLDPE and compared to that of plain LLDPE. The results indicate characteristic peaks for both HA and LLDPE on HA-LLDPE surfaces (**Fig. 2.4.1**). The characteristic peaks for LLDPE include: CH₃ and CH₂ asymmetric and symmetric stretching near 2914 and 2847cm⁻¹; CH₂ and CH₃ scissoring and stretching at 1472 and 1462cm⁻¹; and CH₂ rocking at 718cm⁻¹. The characteristics peaks for cross-linked HA include: OH and NH stretching near 3338cm⁻¹; carbonyl stretching of urethane linkages near 1765cm⁻¹; amide and carboxyl carbonyl stretching near 1685cm⁻¹; and CNH stretching characteristic of amides and urethanes due to HA and the HMDI cross-linker near 152cm⁻¹. Further, TA was used for bulk-weight analysis of HA-LLDPE surfaces. The results indicate a mean of 1.002 ± 0.194 w/v % of cross-linked HA in HA-LLDPE surfaces.

This result was comparable to the % HA in HA-LLDPE as reported by earlier study¹⁹. ATR-FTIR analysis was performed by Dr. Sue James lab at Colorado State University.

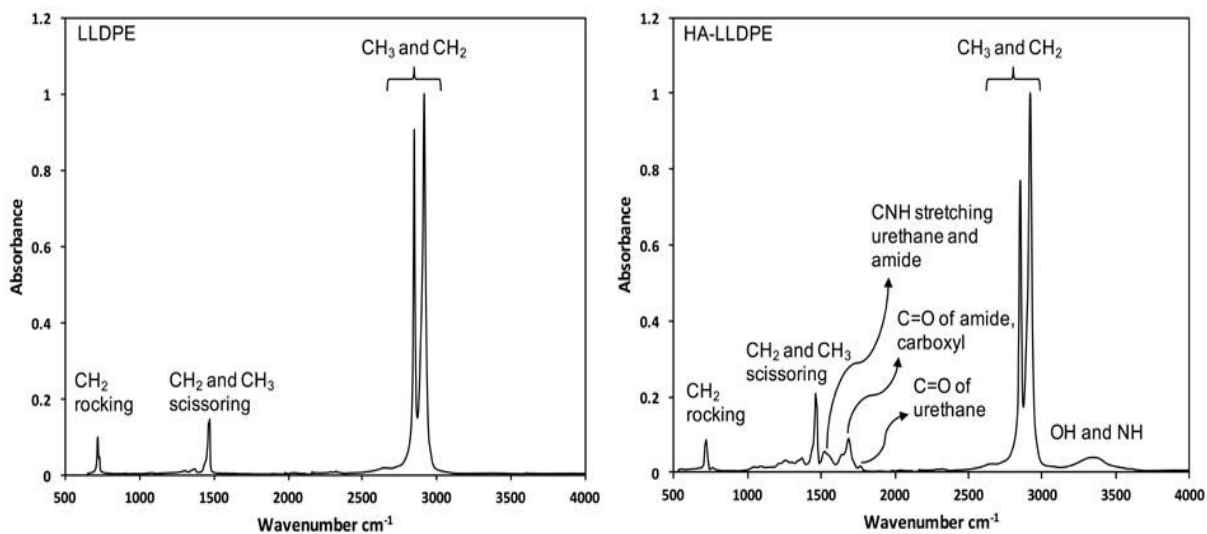


Figure 2.4.1: ATR-FTIR spectra for LLDPE and HA-LLDPE surfaces showing characteristic peaks of HA (OH and NH) and HA indicative carbonyl and urethane groups after impregnation.

2.4.2 Contact Angle Results

Contact angle goniometry was used to characterize the wettability of HA-LLDPE substrates (**Fig.2.4.2.**) The results indicate that due to high contact angle hysteresis (i.e. the difference between advancing and receding contact angles) of HA-LLDPE substrates, water droplets will not easily roll off and will spread on the surface, indicating that all the HA-LLDPE substrates are hydrophilic. In contrast, the contact angle hysteresis was lower for LLDPE substrates indicating the substrate is hydrophobic. Further, none of the advancing and receding contact angles for HA-LLDPE substrates were significantly different from each other, however, they were all significant different from LLDPE substrates ($p \leq 0.05$). Contact angle data was provided by James Lab at Colorado State University.

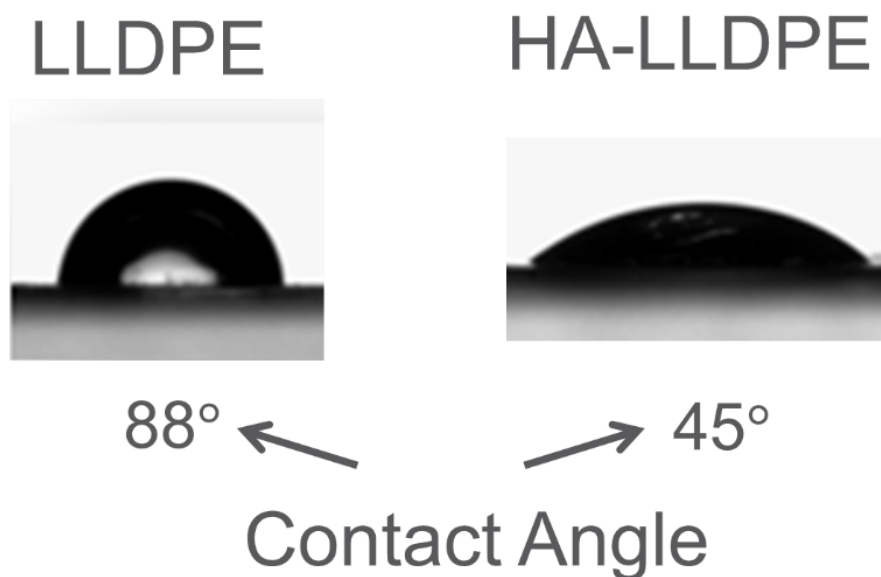


Figure 2.4.2 Contact angle measurements provided by James Lab at Colorado State University demonstrate that HA-LLDPE surfaces exhibit greater wettability than virgin LLDPE.

2.4.3 Lactate Dehydrogenase Results

To ensure that the inherent material properties of HA-LLDPE pose no threats to the blood and its components, cytotoxicity was assessed through use of a commercially available lactate dehydrogenase assay (LDH). An enzyme found abundantly in hematocytes, LDH has long been used as a clinical marker for both in vitro and in vivo hemolysis resulting from disease or toxic substances³⁶. Cytotoxic materials result in cell death by inducing cytoplasmic and organelle swelling, followed by organelle dissolution and rupture of the plasma membrane. These events correspond to a rise in cytosolic LDH which is then released into the extracellular milieu as loss of membrane integrity allows intercellular contents to spill into the environment^{37,38}. Cytotoxicity of a material is thus determined by inferring magnitude of cell death through quantification of freed LDH. Results of the study indicate similar levels of LDH expression after exposure to PS,

LLDPE, and HA-LLDPE surfaces (**Fig. 2.4.3**). PS was utilized in this study as a positive control as it is commonly used in cell culturing methods and is well known to exhibit low toxicity. Thus, a similar level of LDH expression on HA-LLDPE and LLDPE surfaces to that of PS indicates that LLDPE and HA-LLDPE share a similar cytotoxicity to that of PS.

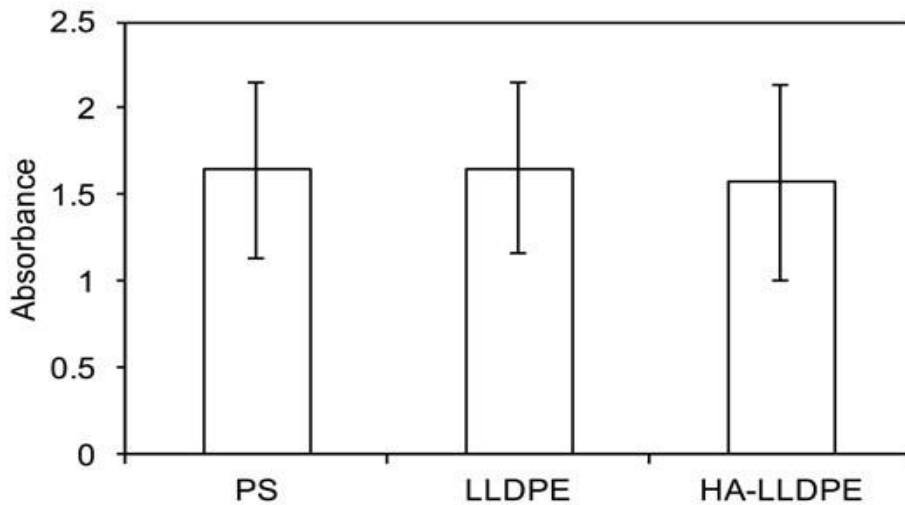


Figure 2.4.3: Cytotoxicity of different material surfaces assessed after 2hrs of incubation in whole blood plasma. Results indicate no significant difference in LDH activity for all surfaces. Experiments were replicated with at least three different human plasmas on at least five different samples ($n_{\min} = 9$). A one-way ANOVA was performed. Average values and standard deviations are as follows: PS (av=1.643; st.dev=.510); LLDPE (av=1.652; st.dev=.491); HA-LLDPE (av=1.574; st.dev =.570).

2.4.4 Whole Blood Clotting Results

Cytotoxicity is the primary measure of fitness in the assessment of all medical devices. In addition, for prosthetic heart valves, the rate and means by which blood clots on heart valve leaflet material surfaces is central its long-term performance. Exacerbated by low-hemocompatible materials, valve thrombosis can manifest clinically as pulmonary congestion, insufficient peripheral perfusion, systemic embolization, valve occlusion, stroke, and/or death ³⁹. The pathogenesis of intra-cardiac thrombus formation due to a material's surface is based on three

primary mechanisms: its proclivity to attract adhesive blood proteins such as von Willebrand factor, fibrinogen, and thrombospondin; subsequent platelet adhesion and activation; and the rate of clot formation⁴⁰. Thus, complementary anti-coagulant therapy is often required even with bio-prosthetics and points to the necessity to find a heart valve leaflet material that will completely exclude thrombosis if anticoagulants are to be eliminated as obligate therapies for prosthetic valves. Determining the time scale in which total whole blood clotting occurs in a static environment can assist in discerning a material's ability to promote or prevent thrombosis. Thus, to ascertain if HA-LLDPE surfaces affect blood coagulation, whole blood clotting was characterized. Human whole blood was placed on test surfaces and allowed to clot for a predetermined length of time and then rinsed in DI H₂O. As blood clots, hemoglobin is bound into the fibrin network and is unable to be released into its environment. Unbound hemoglobin is freed into the DI H₂O and can be analyzed via spectrophotometry to ascertain amount of overall clotting. All surfaces promoted some amount of clotting within 1hr of static exposure, but the rate of clotting was drastically reduced on HA-LLDPE surfaces (**Fig. 2.4.4**). At all-time points (15, 30, 60mins) free hemoglobin from blood in contact with HA-LLDPE surfaces was significantly greater than for both PS and LLDPE surfaces indicating that HA-LLDPE surfaces reduced clotting as compared to PS and LLDPE. Complete clotting was not seen on HA-LLDPE surfaces even after 1hr of exposure to blood. Both PS and LLDPE exhibited comparable levels clotting at all time points with almost full clotting reached after 1hr of exposure.

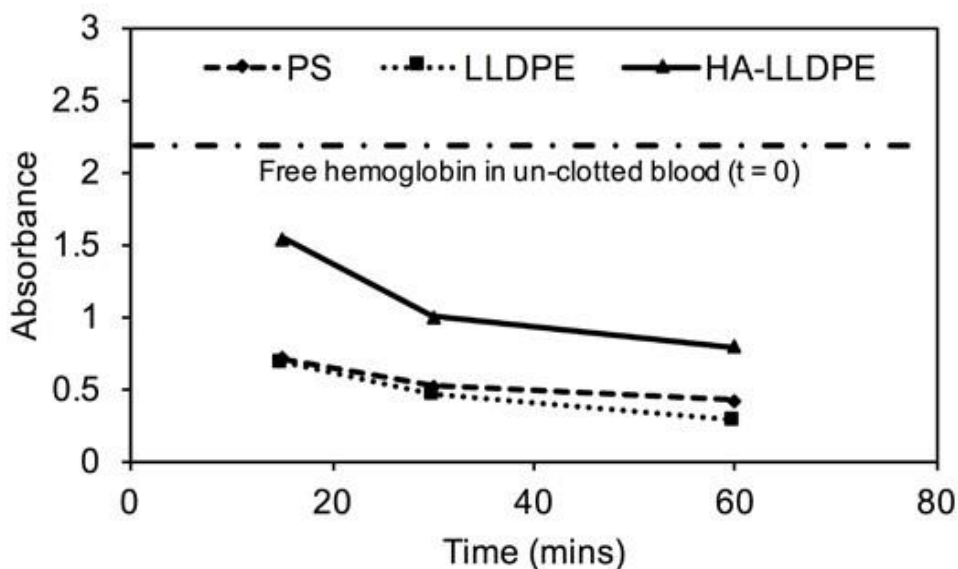


Figure 2.4.4: Free hemoglobin concentration as determined by absorbance on PS, LLDPE, and HA-LLDPE surfaces. Significant differences in free hemoglobin concentrations were seen between HA-LLDPE and all other surfaces at all time points at $p \leq .05$. Experiments were replicated with at least three different human whole bloods on at least five different samples ($n_{\min} = 15$). A one-way ANOVA was performed. No significance was seen between PS and LLDPE. Average values and standard deviations are as follows: PS (t=15; av=.710; st.dev=.124 t=30; av=.516; st.dev=.119; t=60; av=.418; st.dev=.151) LLDPE (t=15; av=.678; st.dev=.240; t=30; av=.457; st.dev=.279; t=60; av=.274; st.dev=.336); HA-LLDPE (t=15; av=1.535; st.dev=.1.38; t=30; av=.995; st.dev=.070; t=60; av=.788; st.dev=.502).

2.4.5 Platelet Adhesion and Activation on HA-LLDPE Surfaces

Once a biomaterial comes into contact with blood a provisional matrix of proteins adsorbs immediately onto the surface. This bioactive protein layer provides the foundation for coagulation/immune responses to take place; however, it is the binding and activation of cells to this film that are the key events in their stimulation. Adsorbed proteins are recognized by platelet and leukocyte receptors allowing them to bind, aggregate, activate, and spread across the biomaterial surface. To accomplish this, platelets must first be activated either through the binding of plasma proteins or by the molecular production and self-release of activating factors such as

platelet activating factor, cathespi-G, epinephrine, serotonin, ADP, ATP, and thromboxane ⁴¹. Upon platelet activation, conformational changes in the membrane lead to the exposure of high affinity binding sites for fibrinogen which further assists in platelet aggregation and the formation of platelet-leukocyte complexes ^{41,49}. In this study, cellular adhesion to surfaces was determined by visualization after Calcein-AM staining. After 2hr of incubation in human plasma, the surfaces were stained and imaged using fluorescence microscopy. The images were further analyzed using Image J to determine the cell coverage on all the surfaces. The results indicate significantly lower total cell adhesion on HA-LLDPE surfaces as compared to PS and LLDPE (**Fig. 2.4.5 (a)**). The HA-LLDPE surfaces had approximately 76% and 83% less cell adhesion as compared to PS and LLDPE respectively (**Fig. 2.4.5 (b)**).

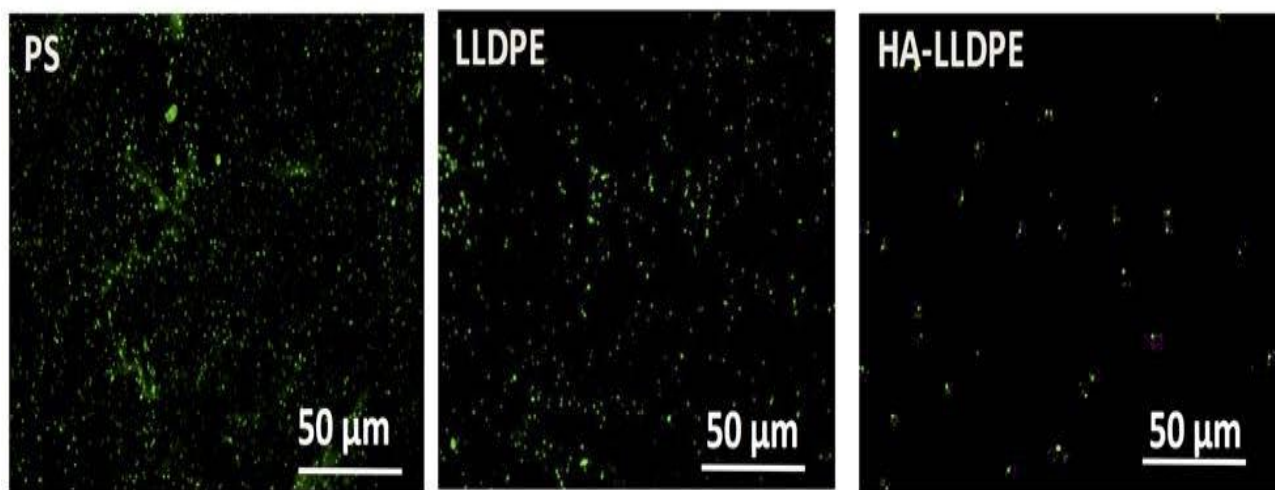


Figure 2.4.5 (a): Representative fluorescence microscopy images of adhered platelets and leukocytes stained with Calcein-AM on PS, LLDPE, and HA-LLDPE surfaces.

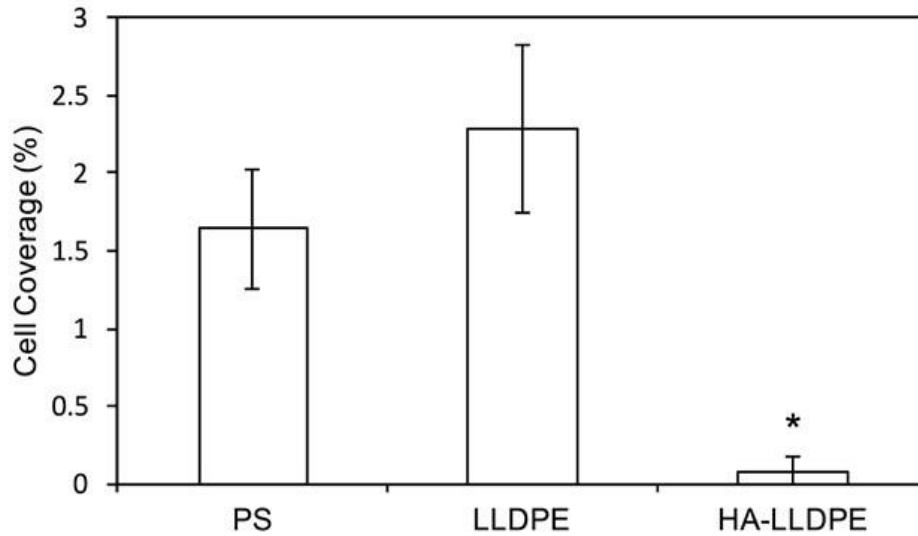


Figure 2.4.5 (b): Percent coverage analysis of adhered platelets and leukocytes after staining with Calcein-AM on PS, LLDPE, and HA-LLDPE surfaces. Experiments were replicated with at least three different cell populations on at least three different samples ($n_{\min} = 9$). A one-way ANOVA was performed. Results indicated significantly less cellular adhesion on HA-LLDPE as compared to other surfaces $p \leq 0.05$. Average values and standard deviations are as follows: PS (av=1.642; st.dev=.631); LLDPE (av=2.29; st.dev=.392); HA-LLDPE (av=.08; st.dev = .420).

2.4.6 Scanning Electron Microscopy Visualizes Platelet Activation

To characterize platelet activation, SEM imaging was used. During activation, platelets undergo cytoskeletal dependent membranous shape changes. This commences with the disassembly of the microtubule ring followed by actin polymerization to form dendritic extensions that are thought to release chemo-attractants and summon additional platelets to the area to aggregate and begin the formation of the platelet plug⁵⁵. Five morphological groups of dendritic expressions on implant surfaces have been identified and correspond with four levels of activation: *round* (un-activated): discoid shape with no pseudopodia present; *dendritic* (partially activated): early pseudopodia i.e. short reversible dendritic extensions; *spread dendritic* (moderately activated): irreversible long-dendritic extensions with some spreading, some pseudopodial flattening; *spreading* (fully activated): pseudopodia almost fully flattened, hyaloplasmic

spreading; and *fully spread* (fully activated): no pseudopodia present, hyaloplasm is well spread⁵⁶⁻⁵⁷. Similar to fluorescence microscopy images, the SEM images also indicate lower cell adhesion on HA-LLDPE surfaces as compared to LLDPE and PS surfaces (**Fig. 2.4.6**). The SEM images also indicated slight reversible *dendritic* extensions with no aggregation and lack of any specific morphological changes in platelets on HA-LLDPE surfaces as compared to LLDPE surfaces that exhibited *spread-dendritic*, *spreading* morphologies and platelet aggregation. Furthermore, neither LLDPE nor HA-LLDPE surfaces showed formation of platelet-leukocyte complexes.

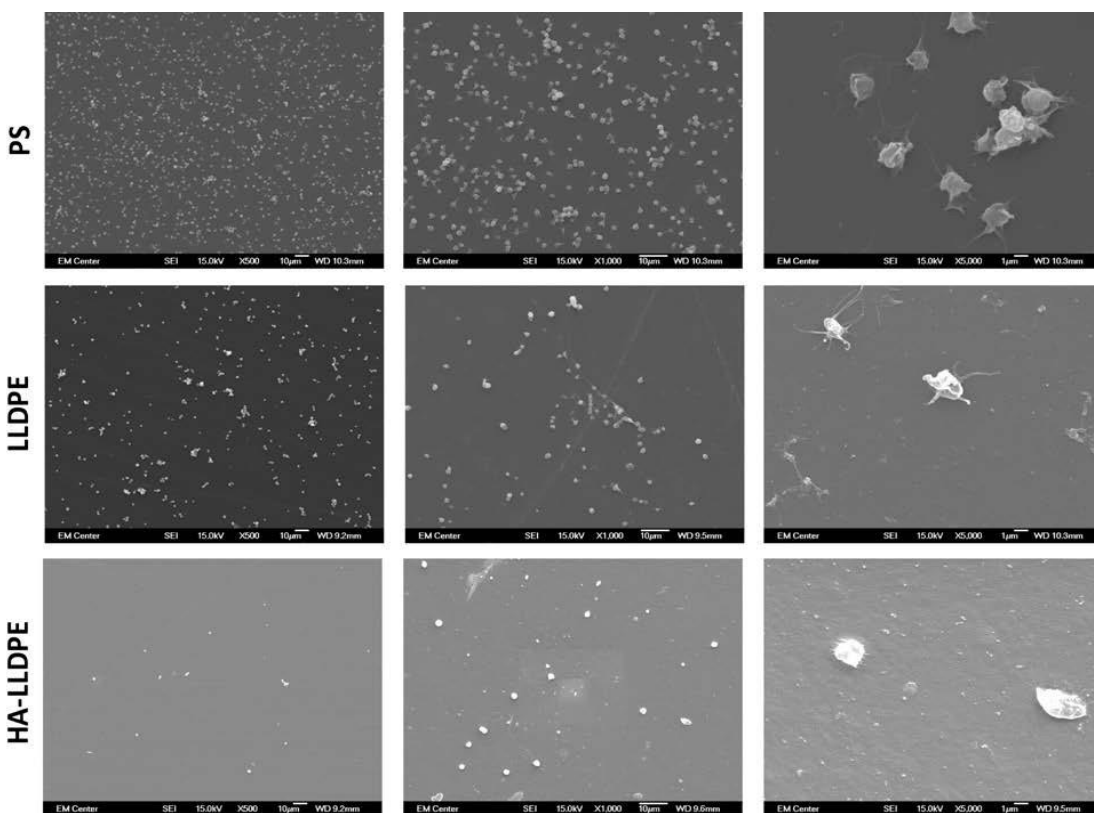


Figure 2.4.6: Representative SEM images of adhered platelets and leukocytes on PS, LLDPE, and HA-LLDPE surfaces. Results indicate HA-LLDPE surfaces promoted no activation of platelets as noted by the rounded morphology. By comparison PS and LLDPE both resulted in fully activated platelets as expressed by the spread-dendritic morphology of platelets on these surfaces. Experiments were replicated with at least three different cell populations on at least three different samples ($n_{\min} = 9$).

2.4.7 Platelet Factor 4 Expression on Different Surfaces

In conjunction with morphological changes, platelets also release dense and alpha granules both containing biomolecules (e.g. ADP, ATP, serotonin, and PF-4) that operate as chemokines and cytokines to similarly activate and degranulate leukocytes. Platelet-leukocyte complexes recruit immune cells and drive inflammation by helping leukocytes to perform many of their functions including chemotaxis, phagocytosis, and superoxide anion generation or inhibition ⁵⁸. Similarly, leukocytes enhance many platelet functions including increased adhesion, activation, and secretion of granules ⁵⁹. From alpha granules PF-4, a cytokine is released and is responsible for enhancing blood coagulation. Thus, PF-4 ELISA assay was performed to determine if HA-LLDPE surfaces activated platelets to release PF4 after incubation in whole blood plasma for 2hrs. Results indicated significant differences in PF-4 expression for platelets on LLDPE and HA-LLDPE surfaces at $p \leq .08$, however PF-4 expression was significantly higher on PS surfaces with a significance at $p \leq .05$ (**Fig. 2.4.7**). Platelet activation and subsequent release of its components such as PF-4 have been shown to increase in presence of leukocytes which can lead to pro-thrombotic surfaces.

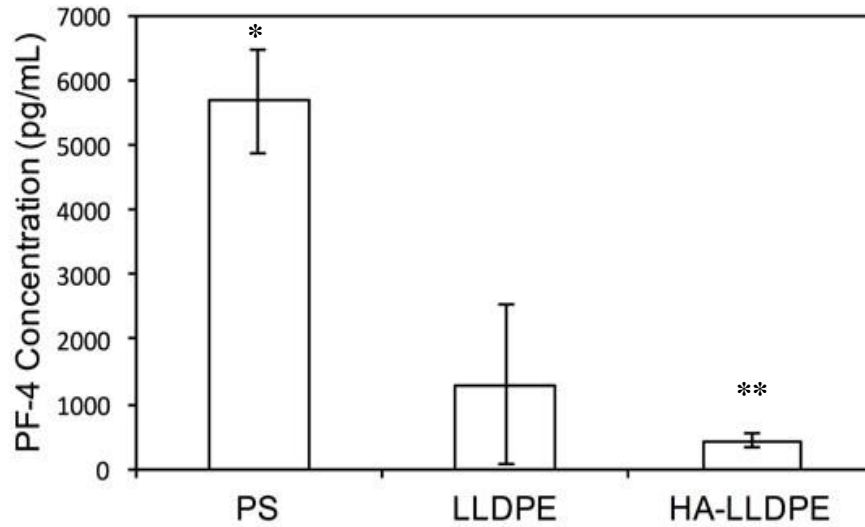


Figure 2.4.7: PF-4 expression of degranulated platelets after 2hrs of incubation in whole blood plasma. Results indicate a significant increase in PF-4 expression on PS surfaces compared to LLDPE and HA-LLDPE surfaces $p \leq .05$. Significant differences were noted between LLDPE and HA-LLDPE at $p \leq .08$. Experiments were replicated with at least three different human plasmas on at least five different samples ($n_{\min} = 15$). A one-way ANOVA was performed. Average values and standard deviations are as follows: PS (av=5663.087; st.dev=812.784); LLDPE (av=1290.386; st.dev=1226.414); HA-LLDPE (av=433.464; st.dev =109.620).

2.4.8 Contact Activation on Different Surfaces

When blood comes in contact with a biomaterial the intrinsic pathway, aptly named the contact activation pathway, is initiated. The intrinsic pathway is regulated by the binding of three proteins to the material surface: factor XII (the Hageman factor), which undergoes autocatalysis upon contact with a negatively charged surface triggering the cascade; prekallikrein, which interacts with factor XII initiating a positive feedback loop that further activates these factors and intensifies the contact activation scheme; and high molecular weight kininogen, which acts as a cofactor for the activation of prekallikrein and factor XII⁶⁰⁻⁶³. To investigate the effect of HA-LLDPE on the contact activation, an acid stop assay was used to determine the amount of prekallikrein expressed. The results indicate no significant differences in prekallikrein expression on all the surfaces (**Fig. 2.4.8**). Previous studies investigating the role of contact activation on

polymers used for cardiovascular implants (e.g. Dacron™, expanded polytetrafluoroethylene and polyethylene) have noted adsorption of all three contact proteins on the polymer surfaces, but factor XII was not found in its activated form, thus halting further activation of the coagulation cascade via the intrinsic pathway and thus likely retarding the expression of prekallikrein^{60, 62-63}. Furthermore, evaluations performed on UV modified HA gels also noted that factor XII was not found in its activated form⁵³. It should be noted that these HA gels utilized HMW-HA which may affect its interaction with factor XII, similar to its effect on fibrinogen binding. Based on these results, it can be hypothesized that both LLDPE and HA-LLDPE have a similar role in mitigating intrinsic coagulation activity.

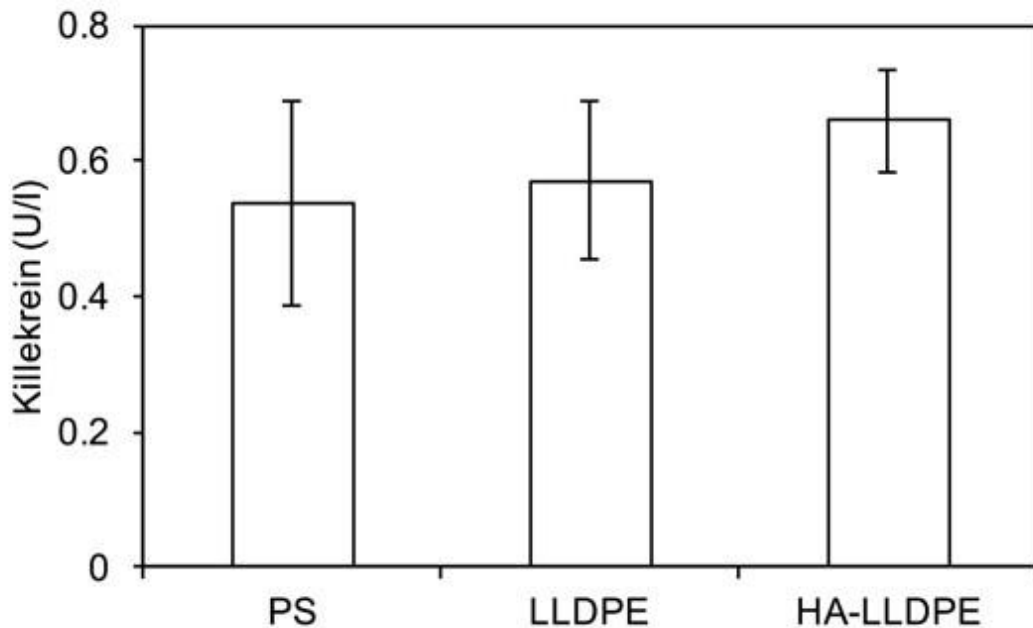


Figure 2.4.8: Contact activation measured by the amount of pre-kallikrein on different surfaces after 2hrs of incubation in whole plasma. The results indicate no significant difference in contact activation on the surfaces. Experiments were replicated with at least three different human plasmas on at least five different samples ($n_{\min} = 15$). A one-way ANOVA was performed. Average values and standard deviations are as follows: PS (av=.539; st.dev=.152); LLDPE (av=.570; st.dev=.116); HA-LLDPE (av=.660; st.dev =.076).

2.4.9 Thrombin Formation on Different Surfaces

Once platelets and leukocytes trigger the coagulation system, the protease thrombin (fibrinogenase) cleaves the protein fibrin causing it to polymerize and produce a gelatinous fibrin matrix clot. During this process, a sequence of biochemical markers are produced which can be measured to determine the extent to which these clotting factors are generated. These include prothrombin, which determines the amount of thrombin being generated; and the thrombin-antithrombin-complex (TAT), which determines the amount of thrombin that was inhibited ⁷⁰. The most accurate method of determining the amount of thrombin would be to test specifically for the protease itself; however, thrombin is rapidly bound and inactivated by antithrombin during the regulatory process. Thus, thrombin from unadulterated plasma can only be measured indirectly through quantification of the cleavage products produced by prothrombin or through the measurements of the TAT complex ⁷¹. Determining the amount of direct endogenous thrombin generation due to the material however can be accomplished using special plasmas which are absent anti-thrombin and platelets. To investigate the effect of HA-LLDPE on TAT and thrombin generation, an enzyme immunoassay was used. The results indicate significant differences between PS and LLDPE and HA-LLDPE at $p \leq .05$ and LLDPE and PS at $p \leq .08$ for TAT formation. Significant differences were seen at $p \leq .05$ in TGA evaluations for PS as compared to LLDPE and HA-LLDPE groups. No differences were seen in endogenous thrombin generation between LLDPE and HA-LLDPE groups (**Fig. 2.4.9 (a) and (b)**). Previous studies have found only small amounts of TAT and thrombin generation on biomaterial surfaces when exposed to undiluted plasma. However, in the same study these markers were found to be significantly present when in contact with whole blood suggesting that the presences of leukocytes may be needed for full activation of the coagulation cascade ^{41, 72-73}. This may explain the differences observed in the

TAT and TGA evaluations. No significant differences were observed in TGA evaluations between LLDPE and HA-LLDPE groups when in contact with the manufacturer's plasma absent anti-thrombin and plasma cells was utilized. However, when in contact with plasma including cells in TAT assaying, differences were noted, exhibiting the role of platelets and leukocytes in clotting mechanisms.

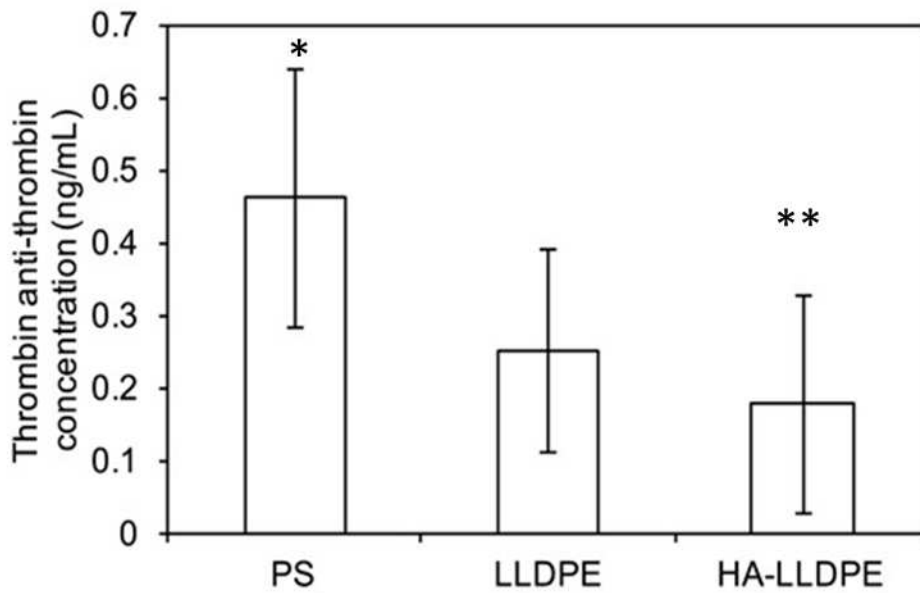


Figure 2.4.9 (a): TAT concentration determined after 2hrs of incubation of different surfaces in whole blood plasma. Experiments were replicated with at least three different human plasmas on at least five different samples ($n_{\min} = 15$). A one-way ANOVA was performed. Results indicate significant difference in TAT concentration between PS and LLDPE and HA-LLDPE at $p \leq .05$ and significant differences between LLDPE and PS at $p \leq .08$. Average values and standard deviations are as follows: PS (av=.463; st.dev=.098); LLDPE (av=.250; st.dev=.082); HA-LLDPE (av=.212; st.dev =.078).

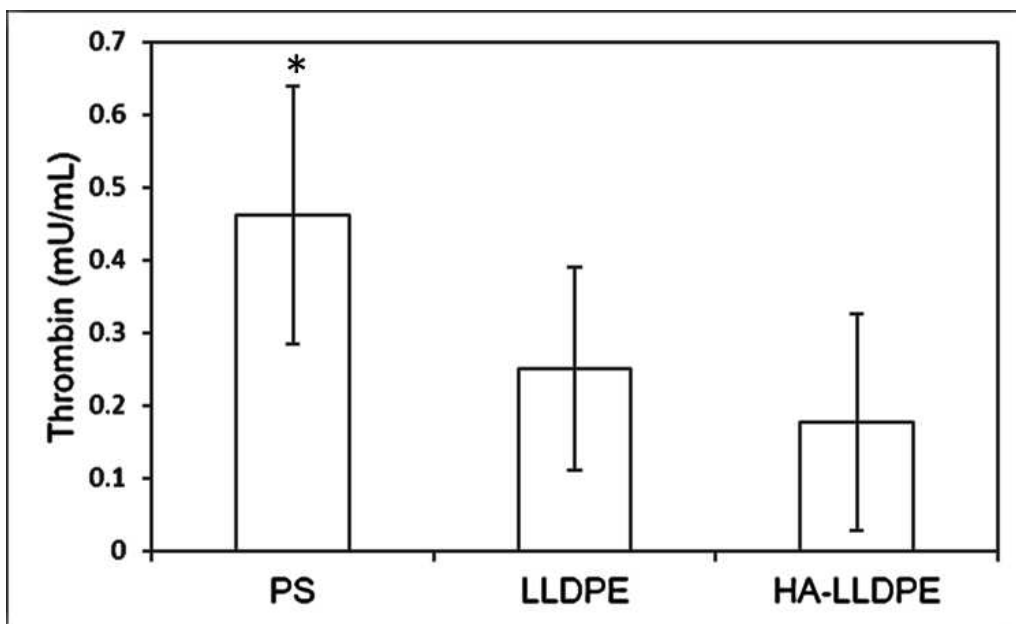


Figure 2.4.9 (b): Thrombin generation velocity on different surfaces calculated as the greatest difference between two time points and normalized to the area of each surface. Experiments were replicated with at least three different human plasmas on at least five different samples ($n_{\min} = 15$). A one-way ANOVA was performed. No significant differences were seen between LLDPE and HA-LLDPE groups however PS was significantly different at $p \leq .05$. Average values and standard deviations are as follows: PS (av=.462; st.dev=.177); LLDPE (av=.251; st.dev=.140); HA-LLDPE (av=.177; st.dev =.149).

2.4.10 Hemolysis on Different Surfaces

For a blood-contacting material to be approved for a medical device, hemolytic activity (the magnitude of the membranous breakdown of red-blood cells due toxic material) must be assessed. Hemolysis can occur due to a number of factors including chemicals or toxins present within the material, shear forces, leachables, or inherent properties of the material itself such as surface charge ⁷⁴. To evaluate the hemolytic activity, erythrocytes were exposed to material surfaces for 24hrs, and hemoglobin released by the cells was measured via spectrophotometry. The results indicate no significant differences between hemoglobin released on LLDPE, HA-

LLDPE, and PS surfaces (**Fig. 2.4.10**). Since PS is known to exhibit low levels of factors which can lead to hemolysis, the results suggest that that HA-LLDPE surfaces exhibit negligible hemolytic effects on erythrocytes as well.

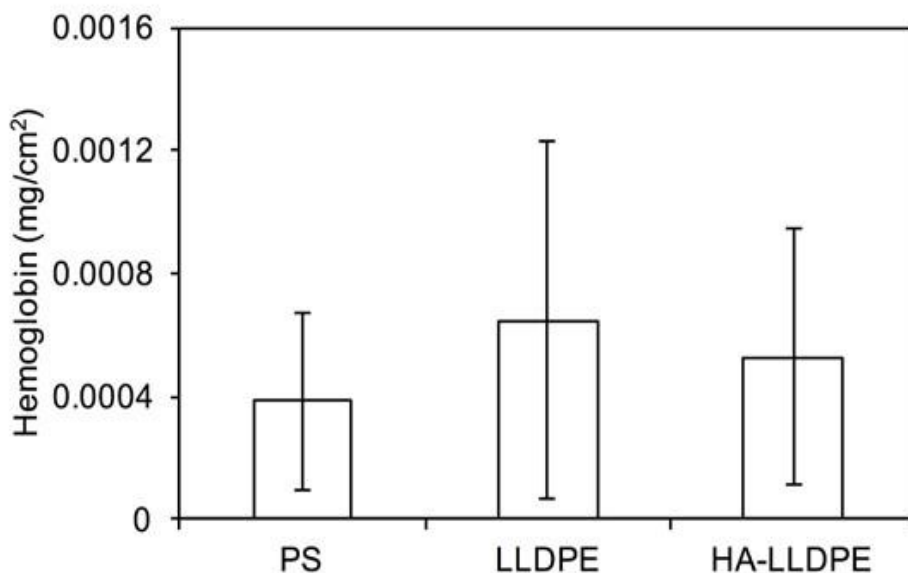


Figure 2.4.10: Hemoglobin release from a human erythrocyte suspension measured by spectrophotometry after 24hrs of substrate-erythrocyte incubation. Results indicate no significant differences between all the surfaces. Experiments were replicated with at least three different cell populations on at least five different samples ($n_{\min} = 9$). Average values and standard deviations are as follows: PS (av=.00039; st.dev=.00029); LLDPE (av=.00065; st.dev=.00058); HA-LLDPE (av=.00053; st.dev =.00042).

2.5 Conclusions

Hemocompatible and long-lasting flexible HV leaflets are the sought-after gold standard for HVRT. To this end, polymer-based leaflets have been widely investigated as they have the potential to offer highly durable base materials which can be chemically and physically modified to improve hemocompatibility. Unfortunately, no polymer-based heart valve leaflet has proven viable for prolonged implantation as historically, they are fraught with structural degradation and thrombotic complications. One of the main obstacles is the natural hydrophobic nature of polymeric surfaces which attracts hydrophobic blood proteins and thus exacerbates coagulation

and immune response cascades. However, advances in polymer science and surface modification techniques have ushered in a new era in polymeric heart valve technology.

In this study, we assessed the thrombogenic impact of hydrophilic polymer surface, HA-LLDPE for future potential use as flexible heart valve leaflets. The results indicate that HA-LLDPE exhibits low toxicity similar to that of PS commonly used in cell culture. In addition, the results demonstrate that HA may reduce the thrombogenic potential of virgin LLDPE surfaces. Cytotoxicity studies measuring the release of LDH showed no significant differences when compared with PS, a substance used widely in tissue culture and known to exhibit low toxicity. SEM imaging demonstrated only partially activated platelets on HA-LLDPE surfaces noted by their reversible dendritic extensions and mostly round appearance. Reduced platelet activation was further confirmed through the use of PF-4 assay that showed less PF-4 expression on HA-LLDPE surfaces although significant differences were not noted in PF-4 expression between LLDPE and HA-LLDPE. However, LLDPE did exhibit greater platelet coverage. Overall, the results indicate that HA-LLPE may reduce whole blood clotting *in vivo*. Additional verification of this hypothesis was tested using TAT and thrombin generation assays. No significant differences were noted between any of the surfaces. Finally, a hemolytic assay was performed to evaluate the potential for red blood lysing due to contact with the material with no significant differences as compared to PS. While these results are not clinically relevant, they do provide compelling data to suggest that future studies using animal models may exhibit successful results.

REFERENCES:

1. Sacks, M. S.; Schoen, F. J.; Mayer, J. E. Bioengineering Challenges for Heart Valve Tissue Engineering. *Annu Rev Biomed Eng* **2009**, *11*, 289-313.
2. Schoen, F. J.; Levy, R. J. Founder's Award, 25th Annual Meeting of the Society for Biomaterials, Perspectives. Providence, Ri, April 28-May 2, 1999. Tissue Heart Valves: Current Challenges and Future Research Perspectives. *J Biomed Mater Res* **1999**, *47* (4), 439-465.
3. Seiler, C. Management and Follow up of Prosthetic Heart Valves. *Heart* **2004**, *90* (7), 818-824.
4. Hammermeister, K.; Sethi, G. K.; Henderson, W. G.; Grover, F. L.; Oprian, C.; Rahimtoola, S. H. Outcomes 15 Years after Valve Replacement with a Mechanical Versus a Bioprosthetic Valve: Final Report of the Veterans Affairs Randomized Trial. *J Am Coll Cardiol* **2000**, *36* (4), 1152-1158.
5. Hauert, R. A Review of Modified Dlc Coatings for Biological Applications. *Diamond and Related Materials* **2003**, *12* (3-7), 583-589.
6. Yee Han, K.; Lakshmi Prasad, D.; Ajit, Y.; Hwa Liang, L. Recent Advances in Polymeric Heart Valves Research. *International Journal of Biomaterials Research and Engineering (IJBRE)* **2011**, *1* (1), 1-17.
7. Makkar, R. R.; Fontana, G.; Jilaihawi, H.; Chakravarty, T.; Kofoed, K. F.; de Backer, O.; Asch, F. M.; Ruiz, C. E.; Olsen, N. T.; Trento, A.; Friedman, J.; Berman, D.; Cheng, W.; Kashif, M.; Jelnin, V.; Kliger, C. A.; Guo, H.; Pichard, A. D.; Weissman, N. J.; Kapadia, S.;

- Manasse, E.; Bhatt, D. L.; Leon, M. B.; Sondergaard, L. Possible Subclinical Leaflet Thrombosis in Bioprosthetic Aortic Valves. *N Engl J Med* **2015**, *373* (21), 2015-2024.
8. Roudaut, R.; Serri, K.; Lafitte, S. Thrombosis of Prosthetic Heart Valves: Diagnosis and Therapeutic Considerations. *Heart* **2007**, *93* (1), 137-142.
 9. Cannegieter, S. C.; Rosendaal, F. R.; Briet, E. Thromboembolic and Bleeding Complications in Patients with Mechanical Heart Valve Prostheses. *Circulation* **1994**, *89* (2), 635-641.
 10. Pollard, J. W.; Hamilton, M. J.; Christensen, N. A.; Achor, R. W. Problems Associated with Long-Term Anticoagulant Therapy. Observations in 139 Cases. *Circulation* **1962**, *25*, 311317.
 11. Scarff, C. E.; Baker, C.; Hill, P.; Foley, P. Late-Onset Warfarin Necrosis. *Australas J Dermatol* **2002**, *43* (3), 202-206.
 12. Stults, B. M.; Dere, W. H.; Caine, T. H. Long-Term Anticoagulation. Indications and Management. *West J Med* **1989**, *151* (4), 414-429.
 13. Heras, M.; Chesebro, J. H.; Fuster, V.; Penny, W. J.; Grill, D. E.; Bailey, K. R.; Danielson, G. K.; Orszulak, T. A.; Pluth, J. R.; Puga, F. J.; et al. High Risk of Thromboemboli Early after Bioprosthetic Cardiac Valve Replacement. *J Am Coll Cardiol* **1995**, *25* (5), 11111119.
 14. Pathak, C. P.; Adams, A. K.; Simpson, T.; Phillips, R. E., Jr.; Moore, M. A. Treatment of Bioprosthetic Heart Valve Tissue with Long Chain Alcohol Solution to Lower Calcification Potential. *J Biomed Mater Res A* **2004**, *69* (1), 140-144.
 15. Pibarot, P.; Dumesnil, J. G. Prosthetic Heart Valves: Selection of the Optimal Prosthesis and Long-Term Management. *Circulation* **2009**, *119* (7), 1034-1048.
 16. Schoen, F. J.; Levy, R. J. Pathology of Substitute Heart Valves: New Concepts and Developments. *J Card Surg* **1994**, *9* (2 Suppl), 222-227.

17. Smith, C. R.; Leon, M. B.; Mack, M. J.; Miller, D. C.; Moses, J. W.; Svensson, L. G.; Tuzcu, E. M.; Webb, J. G.; Fontana, G. P.; Makkar, R. R.; Williams, M.; Dewey, T.; Kapadia, S.; Babaliaros, V.; Thourani, V. H.; Corso, P.; Pichard, A. D.; Bavaria, J. E.; Herrmann, H. C.; Akin, J. J.; Anderson, W. N.; Wang, D.; Pocock, S. J.; Investigators, P. T. Transcatheter Versus Surgical Aortic-Valve Replacement in High-Risk Patients. *N Engl J Med* **2011**, *364* (23), 2187-2198.
18. Ghanbari, H.; Viatge, H.; Kidane, A. G.; Burriesci, G.; Tavakoli, M.; Seifalian, A. M. Polymeric Heart Valves: New Materials, Emerging Hopes. *Trends Biotechnol* **2009**, *27* (6), 359-367.
19. Prawel, D. A.; Dean, H.; Forleo, M.; Lewis, N.; Gangwish, J.; Popat, K. C.; Dasi, L. P.; James, S. P. Hemocompatibility and Hemodynamics of Novel Hyaluronan-Polyethylene Materials for Flexible Heart Valve Leaflets. *Cardiovasc Eng Technol* **2014**, *5* (1), 70-81.
20. Hlady, V. V.; Buijs, J. Protein Adsorption on Solid Surfaces. *Curr Opin Biotechnol* **1996**, *7* (1), 72-77.
21. Ito, E.; Suzuki, K.; Yamato, M.; Yokoyama, M.; Sakurai, Y.; Okano, T. Active Platelet Movements on Hydrophobic/Hydrophilic Microdomain-Structured Surfaces. *J Biomed Mater Res* **1998**, *42* (1), 148-155.
22. Lee, J. H.; Khang, G.; Lee, J. W.; Lee, H. B. Platelet Adhesion onto Chargeable Functional Group Gradient Surfaces. *J Biomed Mater Res* **1998**, *40* (2), 180-186.
23. Lee, J. H.; Khang, G.; Lee, J. W.; Lee, H. B. Interaction of Different Types of Cells on Polymer Surfaces with Wettability Gradient. *J Colloid Interface Sci* **1998**, *205* (2), 323-330.
24. Lee, J. H.; Lee, H. B. Platelet Adhesion onto Wettability Gradient Surfaces in the Absence and Presence of Plasma Proteins. *J Biomed Mater Res* **1998**, *41* (2), 304-311.

25. Stroncek, J. D.; Reichert, W. M., Overview of Wound Healing in Different Tissue Types. In *Indwelling Neural Implants: Strategies for Contending with the in Vivo Environment*, Reichert, W. M., Ed. Boca Raton (FL), **2008**.
26. Esposito, E.; Menegatti, E.; Cortesi, R. Hyaluronan-Based Microspheres as Tools for Drug Delivery: A Comparative Study. *Int J Pharm* **2005**, *288* (1), 35-49.
27. Laurent, T. C.; Fraser, J. R. Hyaluronan. *FASEB J* **1992**, *6* (7), 2397-2404.
28. Laurent, T. C.; Laurent, U. B.; Fraser, J. R. The Structure and Function of Hyaluronan:
29. An Overview. *Immunol Cell Biol* **1996**, *74* (2), A1-7.
30. Yoo, H. S.; Lee, E. A.; Yoon, J. J.; Park, T. G. Hyaluronic Acid Modified Biodegradable Scaffolds for Cartilage Tissue Engineering. *Biomaterials* **2005**, *26* (14), 1925-1933.
31. Zawko, S. A.; Suri, S.; Truong, Q.; Schmidt, C. E. Photopatterned Anisotropic Swelling of Dual-Crosslinked Hyaluronic Acid Hydrogels. *Acta Biomater* **2009**, *5* (1), 14-22.
32. Bonafe, F.; Govoni, M.; Giordano, E.; Caldarera, C. M.; Guarnieri, C.; Muscari, C. Hyaluronan and Cardiac Regeneration. *J Biomed Sci* **2014**, *21*, 100.
33. Magnani, A.; Albanese, A.; Lamponi, S.; Barbucci, R. Blood-Interaction Performance of Differently Sulphated Hyaluronic Acids. *Thromb Res* **1996**, *81* (3), 383-395.
34. Pitt, W. G.; Morris, R. N.; Mason, M. L.; Hall, M. W.; Luo, Y.; Prestwich, G. D. Attachment of Hyaluronan to Metallic Surfaces. *J Biomed Mater Res A* **2004**, *68* (1), 95-106.
35. Verheye, S.; Markou, C. P.; Salame, M. Y.; Wan, B.; King, S. B., 3rd; Robinson, K. A.; Chronos, N. A.; Hanson, S. R. Reduced Thrombus Formation by Hyaluronic Acid Coating of Endovascular Devices. *Arterioscler Thromb Vasc Biol* **2000**, *20* (4), 1168-1172.
36. Zhang, M.; James, S. P. Silylation of Hyaluronan to Improve Hydrophobicity and Reactivity for Improved Processing and Derivatization. *Polymer* **2005**, *46* (11), 3639-3648.

37. Kato, G. J.; McGowan, V.; Machado, R. F.; Little, J. A.; Taylor, J. t.; Morris, C. R.; Nichols, J. S.; Wang, X.; Poljakovic, M.; Morris, S. M., Jr.; Gladwin, M. T. Lactate Dehydrogenase as a Biomarker of Hemolysis-Associated Nitric Oxide Resistance, Priapism, Leg Ulceration, Pulmonary Hypertension, and Death in Patients with Sickle Cell Disease. *Blood* **2006**, *107* (6), 2279-2285.
38. Chan, F. K.; Moriwaki, K.; De Rosa, M. J. Detection of Necrosis by Release of Lactate Dehydrogenase Activity. *Methods Mol Biol* **2013**, *979*, 65-70.
39. Wang, M. O.; Etheridge, J. M.; Thompson, J. A.; Vorwald, C. E.; Dean, D.; Fisher, J. P. Evaluation of the in Vitro Cytotoxicity of Cross-Linked Biomaterials. *Biomacromolecules* **2013**, *14* (5), 1321-1329.
40. Vongpatanasin, W.; Hillis, L. D.; Lange, R. A. Prosthetic Heart Valves. *N Engl J Med* **1996**, *335* (6), 407-416.
41. Caceres-Loriga, F. M.; Perez-Lopez, H.; Santos-Gracia, J.; Morlans-Hernandez, K. Prosthetic Heart Valve Thrombosis: Pathogenesis, Diagnosis and Management. *Int J Cardiol* **2006**, *110* (1), 1-6.
42. Gorbet, M. B.; Sefton, M. V. Biomaterial-Associated Thrombosis: Roles of Coagulation Factors, Complement, Platelets and Leukocytes. *Biomaterials* **2004**, *25* (26), 5681-5703.
43. Tang, L.; Eaton, J. W. Inflammatory Responses to Biomaterials. *Am J Clin Pathol* **1995**, *103* (4), 466-471.
44. Tang, L.; Lucas, A. H.; Eaton, J. W. Inflammatory Responses to Implanted Polymeric Biomaterials: Role of Surface-Adsorbed Immunoglobulin G. *J Lab Clin Med* **1993**, *122* (3), 292-300.

45. Ryu, J. K.; Davalos, D.; Akassoglou, K. Fibrinogen Signal Transduction in the Nervous System. *J Thromb Haemost* **2009**, *7 Suppl 1*, 151-154.
46. Rubens, F.; Brash, J.; Weitz, J.; Kinlough-Rathbone, R. Interactions of Thermally Denatured Fibrinogen on Polyethylene with Plasma Proteins and Platelets. *J Biomed Mater Res* **1992**, *26* (12), 1651-1663.
47. Skarja, G. A.; Brash, J. L.; Bishop, P.; Woodhouse, K. A. Protein and Platelet Interactions with Thermally Denatured Fibrinogen and Cross-Linked Fibrin Coated Surfaces. *Biomaterials* **1998**, *19* (23), 2129-2138.
48. Ruppert, S. M.; Hawn, T. R.; Arrigoni, A.; Wight, T. N.; Bollyky, P. L. Tissue Integrity Signals Communicated by High-Molecular Weight Hyaluronan and the Resolution of Inflammation. *Immunol Res* **2014**, *58* (2-3), 186-192.
49. Eriksson, C.; Nygren, H. Polymorphonuclear Leukocytes in Coagulating Whole Blood Recognize Hydrophilic and Hydrophobic Titanium Surfaces by Different Adhesion Receptors and Show Different Patterns of Receptor Expression. *J Lab Clin Med* **2001**, *137* (4), 296-302.
50. Cassatella, M. A. The Production of Cytokines by Polymorphonuclear Neutrophils. *Immunol Today* **1995**, *16* (1), 21-26.
51. Anderson, J. M. Chapter 4 Mechanisms of Inflammation and Infection with Implanted Devices. *Cardiovascular Pathology* **1993**, *2* (3, Supplement), 33-41.
52. Henson, P. M. The Immunologic Release of Constituents from Neutrophil Leukocytes. Ii. Mechanisms of Release During Phagocytosis, and Adherence to Nonphagocytosable Surfaces. *J Immunol* **1971**, *107* (6), 1547-1557.

53. Henson, P. M. Mechanisms of Exocytosis in Phagocytic Inflammatory Cells. Parke-Davis Award Lecture. *Am J Pathol* **1980**, *101* (3), 494-511.
54. Amarnath, L. P.; Srinivas, A.; Ramamurthi, A. In Vitro Hemocompatibility Testing of UvModified Hyaluronan Hydrogels. *Biomaterials* **2006**, *27* (8), 1416-1424.
55. Fujimoto, K.; Tadokoro, H.; Ueda, Y.; Ikada, Y. Polyurethane Surface Modification by Graft Polymerization of Acrylamide for Reduced Protein Adsorption and Platelet Adhesion. *Biomaterials* **1993**, *14* (6), 442-448.
56. Paul, B. Z.; Daniel, J. L.; Kunapuli, S. P. Platelet Shape Change Is Mediated by Both Calcium-Dependent and -Independent Signaling Pathways. Role of P160 Rho-Associated Coiled-Coil-Containing Protein Kinase in Platelet Shape Change. *J Biol Chem* **1999**, *274* (40), 28293-28300.
57. Goodman, S. L.; Grasel, T. G.; Cooper, S. L.; Albrecht, R. M. Platelet Shape Change and Cytoskeletal Reorganization on Polyurethaneureas. *J Biomed Mater Res* **1989**, *23* (1), 105123.
58. Ko, T.-M.; Cooper, S. L. Surface Properties and Platelet Adhesion Characteristics of Acrylic Acid and Allylamine Plasma-Treated Polyethylene. *Journal of Applied Polymer Science* **1993**, *47* (9), 1601-1619.
59. Deuel, T. F.; Senior, R. M.; Chang, D.; Griffin, G. L.; Heinrikson, R. L.; Kaiser, E. T. Platelet Factor 4 Is Chemotactic for Neutrophils and Monocytes. *Proc Natl Acad Sci U S A* **1981**, *78* (7), 4584-4587.
60. Li, N.; Hu, H.; Lindqvist, M.; Wikstrom-Jonsson, E.; Goodall, A. H.; Hjemdahl, P. PlateletLeukocyte Cross Talk in Whole Blood. *Arterioscler Thromb Vasc Biol* **2000**, *20* (12), 2702-2708.

61. Cool, D. E.; Edgell, C. J.; Louie, G. V.; Zoller, M. J.; Brayer, G. D.; MacGillivray, R. T. Characterization of Human Blood Coagulation Factor Xii Cdna. Prediction of the Primary Structure of Factor Xii and the Tertiary Structure of Beta-Factor Xiia. *J Biol Chem* **1985**, *260* (25), 13666-13676.
62. Konings, J.; Govers-Riemslog, J. W.; Philippou, H.; Mutch, N. J.; Borissoff, J. I.; Allan, P.; Mohan, S.; Tans, G.; Ten Cate, H.; Ariens, R. A. Factor Xiia Regulates the Structure of the Fibrin Clot Independently of Thrombin Generation through Direct Interaction with Fibrin. *Blood* **2011**, *118* (14), 3942-3951.
63. Schmaier, A. H. Contact Activation: A Revision. *Thromb Haemost* **1997**, *78* (1), 101-107.
64. Vogler, E. A.; Siedlecki, C. A. Contact Activation of Blood-Plasma Coagulation. *Biomaterials* **2009**, *30* (10), 1857-1869.
65. Gretzer, C.; Gisselalt, K.; Liljensten, E.; Ryden, L.; Thomsen, P. Adhesion, Apoptosis and Cytokine Release of Human Mononuclear Cells Cultured on Degradable Poly (Urethane Urea), Polystyrene and Titanium in Vitro. *Biomaterials* **2003**, *24* (17), 2843-2852.
66. Peerschke, E. I.; Ghebrehiwet, B. Platelet Receptors for the Complement Component C1q: Implications for Hemostasis and Thrombosis. *Immunobiology* **1998**, *199* (2), 239-249.
67. Engberg, A. E.; Rosengren-Holmberg, J. P.; Chen, H.; Nilsson, B.; Lambris, J. D.; Nicholls, I. A.; Ekdahl, K. N. Blood Protein-Polymer Adsorption: Implications for Understanding Complement-Mediated Hemoincompatibility. *J Biomed Mater Res A* **2011**, *97* (1), 74-84.
68. Roch, T.; Kruger, A.; Kratz, K.; Ma, N.; Jung, F.; Lendlein, A. Immunological Evaluation of Polystyrene and Poly(Ether Imide) Cell Culture Inserts with Different Roughness. *Clin Hemorheol Microcirc* **2012**, *52* (2-4), 375-389.

69. Jiang, D.; Liang, J.; Noble, P. W. Hyaluronan as an Immune Regulator in Human Diseases. *Physiol Rev* **2011**, *91* (1), 221-264.
70. Sengupta, A.; Banerjee, B.; Tyagi, R. K.; Datta, K. Golgi Localization and Dynamics of Hyaluronan Binding Protein 1 (Habp1/P32/C1qbp) During the Cell Cycle. *Cell Res* **2005**, *15* (3), 183-186.
71. Chandler, W. L.; Velan, T. Estimating the Rate of Thrombin and Fibrin Generation in Vivo During Cardiopulmonary Bypass. *Blood* **2003**, *101* (11), 4355-4362.
72. Hoek, J. A.; Sturk, A.; ten Cate, J. W.; Lamping, R. J.; Berends, F.; Borm, J. J. Laboratory and Clinical Evaluation of an Assay of Thrombin-Antithrombin Iii Complexes in Plasma. *Clin Chem* **1988**, *34* (10), 2058-2062.
73. Hong, J.; Nilsson Ekdahl, K.; Reynolds, H.; Larsson, R.; Nilsson, B. A New in Vitro Model to Study Interaction between Whole Blood and Biomaterials. Studies of Platelet and Coagulation Activation and the Effect of Aspirin. *Biomaterials* **1999**, *20* (7), 603-611.
74. van der Kamp, K. W.; Hauch, K. D.; Feijen, J.; Horbett, T. A. Contact Activation During Incubation of Five Different Polyurethanes or Glass in Plasma. *J Biomed Mater Res* **1995**, *29* (10), 1303-1306.
75. Leszczak, V.; Popat, K. C. Improved in Vitro Blood Compatibility of Polycaprolactone Nanowire Surfaces. *ACS Appl Mater Interfaces* **2014**, *6* (18), 15913-15924.

CHAPTER 3

NON-SPECIFIC IMMUNE RESPONSE OF HYALURONAN ENHANCED LINEAR LOW-DENSITY POLYETHYLENE

3.1 Introduction

3.1.1 Implantation of Medical Devices Results in Adaptive Immune Reactions

Due to their high durability, flexible nature, and tunable surface properties, polyethylenes have been highly sought after for their potential use in polymeric heart valve (PHV) leaflets ^{1,2}. Regardless of these multiple structural and facial benefits, polyethylene based cusps have remained susceptible to host response actuation and thrombosis as a result of their innate hydrophobicity which attracts blood proteins, platelets, and leukocytes ³⁻⁵. Upon implantation of a biomedical device, the innate and adaptive immune response of the host is initiated ⁶. While the immune response is essential to the healing of the injury site and subsequent tolerance of the implant, exacerbated responses can lead to acute and chronic inflammation, foreign body reactions, fibrous capsule development and implant rejection ⁷. Similar to the development of biomaterial surface related thrombosis, the non-specific immune response is initially governed by the facial characteristics of the implant which determine the amount and types of proteins which adsorb to its exterior in the formation of a provisional matrix (**Fig. 3.1.1**) ⁸⁻¹². These proteins facilitate communication between the implant and host. If unfavorable conditions to the host environment exist it can exacerbate non-specific immune reactions governed by the alternative pathways ^{8,13}. Examples of this may include (but are not limited to) surface characteristics, cellular components in hybrid biomaterials, and degradation products ¹⁴.

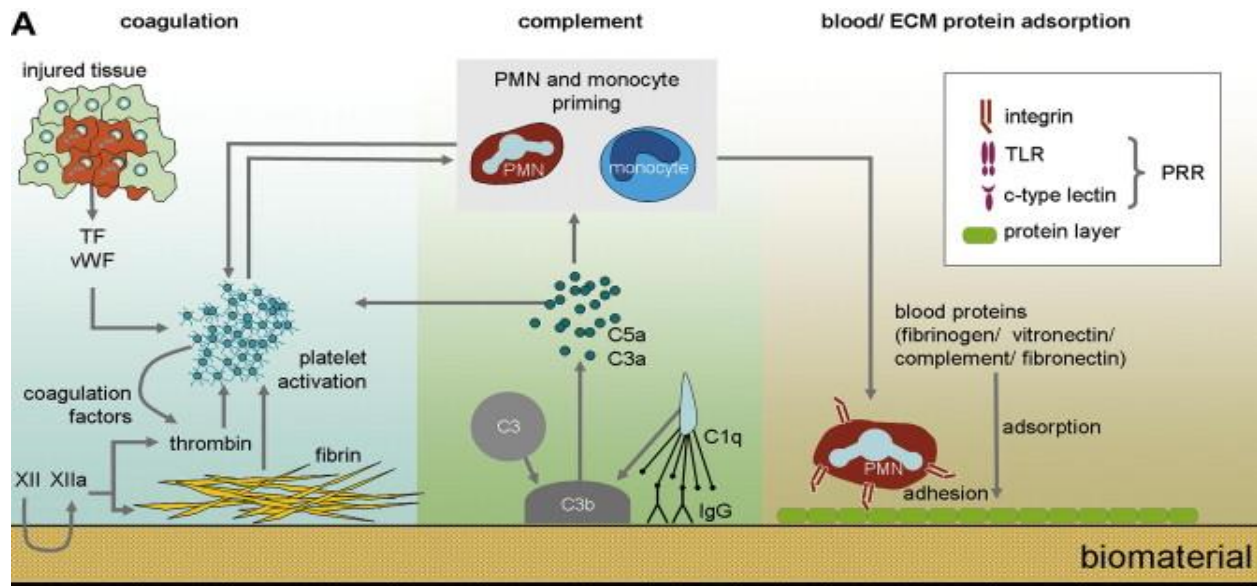


Figure 3.1.1: Like the coagulation cascade, the non-specific immune response is governed by the initial binding of proteins to the biomaterial surface which modulate its response to the host. Reproduced with permission © Elsevier Ltd.

3.1.2 Foreign Body Responses Can Affect the Tolerance of Biomedical Implants

Foreign body responses are responsible for promoting monocyte and macrophage adhesion, the fusion of macrophage into giant foreign body cells, inflammation, the provocation of hemostatic responses, and implant rejection⁷. Adverse immune reactions can negatively affect the tolerance and future success of the implant and lead to such end-points as intimal hyperplasia, fibrosis, and calcification which are impossible to treat pharmaceutically¹⁵. Thus the aim of creating a truly biocompatible PHVs includes the ability to control interfacial adsorption of proteins through manipulation of such mechanisms as surface chemistry, surface charge, and wettability in order to attenuate the provocation of the biological cascades which can lead to unwanted non-specific immune provocation⁸.

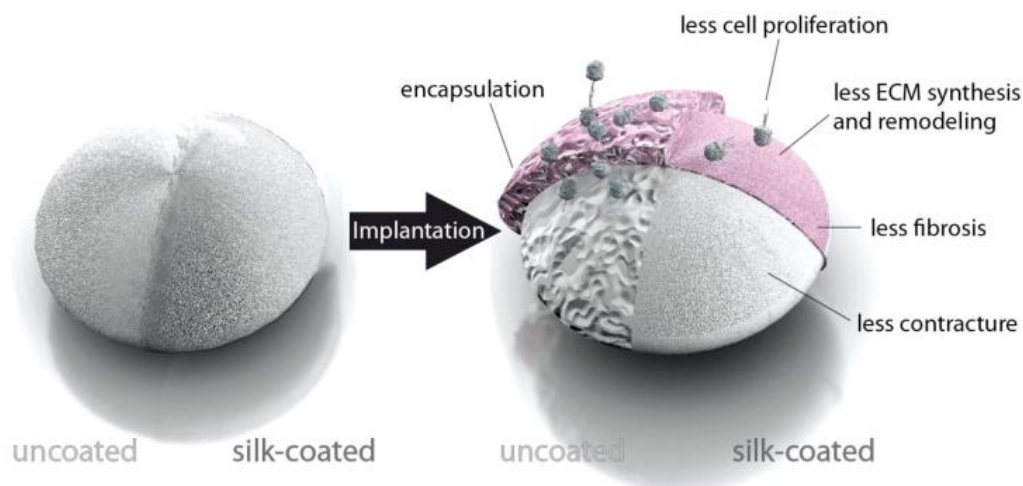


Figure 3.1.2: Illustration of biomaterial related fibrosis and attenuation of fibrosis by surface modification. Reproduced with permission © John Wiley and Sons.

3.1.3 Hyaluronan Enhanced Linear Low-Density for Non-Specific Immune Response Attenuation

To achieve this, a novel, hydrophilic, heart valve leaflet material comprised of a semi-interpenetrating polymer network (S-IPN) of hyaluronan (HA) and linear low-density polyethylene (LLDPE) was developed. HA is a highly lubricious, anionic, glycosaminoglycan ubiquitously found in the human body. It is present throughout the extracellular matrix of almost all tissues, in the ocular viscera, the synovial fluid, in the native heart valve leaflet, and blood serum^{16,17}. Because it is nontoxic, biodegradable, biocompatible, and non-immunogenic, it is currently being investigated for a vast array of biomedical applications including cardiovascular therapies such as hydrogel based regenerative cell therapies for myocardial infarction¹⁸, HA-coated stents^{19,20}, and surface modifications of polymers and metals for use in blood-contacting implants^{21–24}. LLDPE was chosen as the base material for its ability to be manufactured to be very thin, similar to the native leaflet, while maintaining a high tensile and tear strength, complemented by a low bending stiffness^{25,26}. HA-LLDPE has already demonstrated the ability to be non-toxic and thrombo-passivating²⁷. The aim of this study was to assess the non-specific immune response

after plasma exposure to this novel material to ensure its feasibility to be used as a blood-contacting, flexible heart valve leaflet material.

3.2 Materials and Methods

3.2.1 Fabrication and Characterization of HA-LLDPE IPNs

Fabrication and Characterization of HA-LLDPE is described in Chapter 2 sections 2.2.1, 2.2.2., and 2.2.3. Briefly, sodium HA (~750 kDa, Lifecore Biomedical) was complexed with cetyltrimethylammonium (CTA) bromide to create HA-CTA, which was then silylated to create silylHA-CTA. The silylHA introduced into the LLDPE films was crosslinked with a 2% (v/v) poly(hexamethylene diisocyanate) (HMDI) xylenes solution. Treated LLDPE films were swelled at 50°C in a 2% (v/v) poly(hexamethylene diisocyanate) xylenes solution (i.e. HA crosslinking solution) for 60 min, and the crosslinker was cured in a vacuum oven at 50°C for 3 hr (See **Section 2.2.1**). Materials were then characterized using ATR-FTIR to ensure HA was present (**Section 2.2.2**). Contact angle measurements were taken to determine changes in wettability after HA impregnation (**Section 2.2.3**).

3.2.2 Blood Plasma Isolation and Incubation on Different Surfaces

Whole human blood was drawn via venous phlebotomy from healthy donors by a trained phlebotomist who had refrained from taking thromboxane inhibitors (aspirin, ibuprofen, naproxen) for at least 2 weeks. The protocol for blood isolation from healthy individuals was approved by Colorado State University Institutional Review Board. Blood was collected into 10 ml EDTA coated vacuum tubes (BD). Plasma was isolated through centrifugation at 100 g for 15 mins and allowed to rest for 10 mins prior to use. Buffy coat and plasma (herein referred to as plasma) was

pooled into a sterilized 50ml conical tube. Polystyrene (PS), LLDPE, and HA-LLDPE (all 8mm in size) were placed into a 24-well plate and incubated with 1ml of pooled plasma on a horizontal shaker plate (100rpm) for 2hrs at 37°C and 5% CO₂.

3.2.3 Fibrinogen Binding on Different Surfaces

Fibrinogen binding on different surfaces was assessed using an enzyme linked immunoassay (ELISA, GenWay). The protocol from the manufacturer was followed. After 2 hrs of incubation, the surface-exposed plasma was diluted (1:200) in the assay diluent. The diluted plasma and standards were transferred into the micro-assay well plate provided by the manufacturer and incubated for 60mins at room temperature. The plasma and standards were then aspirated, and the wells were washed (4x) with wash buffer and incubated with enzyme antibody conjugate for 30 mins at room temperature in a dark environment. The conjugate was then aspirated, and the wells were washed (4x) with the wash buffer and incubated with a tetramethyl benzidine buffer (TMB) solution for 10 mins at room temperature in a dark environment. The reaction was stopped by adding stop solution and the optical density was immediately measured using a plate reader at 450nm.

Leukocyte adhesion on different surfaces Identification of platelets and leukocytes on different surfaces was investigated through fluorescence microscopy. After 2hrs of incubation in plasma, the surfaces were stained with rhodamine phalloidin cytoskeleton stain and 4'6-diamidino-2-phenylindole dihydrochloride nucleus stain (DAPI, Thermo-Scientific). The un-adhered cells were gently aspirated, and the surfaces were washed with PBS (2x). The adhered cells on the surfaces were fixed in 3.7 wt % formaldehyde in PBS for 15mins at room temperature and rinsed (3x, 5mins each) with PBS. The cell membranes were further permeabilized by 1 % Triton-X solution in PBS at room temperature for 3 mins. The surfaces were then transferred to a

new 24-well plate and incubated with 500 μ l of rhodamine phalloidin solution in PBS for 25 min at room temperature. After 25 min, 0.2 μ g/ml DAPI stain was added to each well and incubated for 5mins. The stain solution was gently aspirated, and the substrates rinsed with PBS (2x). The surfaces were immediately imaged using a Zeiss Axiovision fluorescent microscope using appropriate filters. All images were then processed using ImageJ Software.

3.2.4 Leukocyte Adhesion on Different Surfaces

Identification of platelets and leukocytes on different surfaces was investigated through fluorescence microscopy. After 2hrs of incubation in plasma, the surfaces were stained with rhodamine phalloidin cytoskeleton stain and 4'6-diamidino-2-phenylindole dihydrochloride nucleus stain (DAPI, Thermo-Scientific). The un-adhered cells were gently aspirated, and the surfaces were washed with PBS (2x). The adhered cells on the surfaces were fixed in 3.7 wt % formaldehyde in PBS for 15mins at room temperature and rinsed (3x, 5mins each) with PBS. The cell membranes were further permeabilized by 1 % Triton-X solution in PBS at room temperature for 3 mins. The surfaces were then transferred to a new 24-well plate and incubated with 500 μ l of rhodamine phalloidin solution in PBS for 25 min at room temperature. After 25 min, 0.2 μ g/ml DAPI stain was added to each well and incubated for 5mins. The stain solution was gently aspirated and the substrates rinsed with PBS (2x). The surfaces were immediately imaged using a Zeiss Axiovision fluorescent microscope using appropriate filters. All images were then processed using ImageJ Software.

3.2.5 Scanning Electron Microscopy of Leukocytes

Leukocyte adhesion was determined using scanning electron microscopy (SEM). After 2hrs of incubation in plasma, substrates were fixed with a primary fixative (6% glutaraldehyde (Sigma), 0.1M sodium cacodylate (Polysciences), and 0.1M sucrose (Sigma)) for 45 mins. The substrates were then transferred to a secondary fixative (primary fixative without glutaraldehyde) for 10mins. This was followed by exposing the substrates to consecutive solutions of ethanol (35%, 50%, 70% and 100%) for 10mins each followed by a final incubation in 97% hexamethyldisilazane (HMDS for 10mins at room temperature). The substrates were then air-dried and stored in a desiccator until imaging by SEM. Prior to imaging, the surfaces were coated with a 10nm layer of gold and imaged at 5kV.

3.2.6 Complement Activation on Different Surfaces

Complement activation was assessed using an enzyme immunoassay (EIA, Quidel Corporation) to evaluate the expression of terminal complex, SC5b-9. The protocol provided by the manufacturer was followed. After 2hrs of incubation, the substrate-exposed plasma was diluted (1:10) in the assay diluent. The dilute plasma, standards and controls were transferred into pre-washed and hydrated micro-assay wells and incubated for 60mins at room temperature. The plasma, standards and controls were then aspirated, and the wells were washed (5x) with wash buffer and incubated with SC5b-9 plus conjugate for 30mins at room temperature. The conjugate was then aspirated, and the wells were washed (4x) with the wash buffer and incubated with a TMB solution for 15mins at room temperature in a dark environment. The reaction was stopped by adding stop solution and the optical density was immediately measured using a plate reader at 450nm.

3.3 Statistical Analysis

A linear mixed model with a random intercept was fit to the data to compare treatment groups accounting for repeated measures of HA-LLDPE using the “lme4” package in the R open source statistical data software. Multiple comparisons of contact angles between treatments were analyzed using Tukey’s HSD post-hoc test using the “emmeans” package (<https://cran.rproject.org/web/packages/emmeans/vignettes/comparisons.html>). For the FTIR spectra, a log (x+1) transform of the peak area was used due to heavily skewed data and the presence of a zero for the virgin LLDPE. A linear mixed model and Tukey post-hoc test was also used for fitting. All models used Satterthwaite denominator degrees of freedom for significance testing.

Each qualitative experiment was performed to evaluate differences between PS, LLDPE and HA-LLDPE on at least three substrates. Each assay was repeated at least three times with three different whole blood plasma populations (n min = 9), except for ELISA’s that were performed on at least five surfaces (n min = 15). All results were evaluated using a one-way analysis of variance (ANOVA) with a Tukey’s, Bonferroni, and Scheffé post-hoc tests. Statistical significance was considered at $p < 0.05$.

3.4 Results and Discussion

To address the drawbacks of polymeric based heart valves, a novel material for use as PHV leaflet was fabricated by forming an S-IPN of HMW- HA in LLDPE. By enhancing LLDPE with the HMW naturally occurring, hydrophilic, glycosaminoglycan, it is hypothesized that it will mitigate non-specific immune effects and enhance hemocompatibility. The aim of this study was to evaluate the non-specific immune response on the HA-LLDPE surface and compare it to that of

the untreated LLDPE surface by assessing fibrinogen adsorption, leukocyte adhesion, and complement activation.

3.4.1 Fibrinogen Adsorption to HA-LLDPE Substrates

Blood permeates all tissues of the body and assists in providing essential nutrients, maintaining homeostasis, and providing protective and healing mechanisms upon tissue injury. Under normal physiological conditions, blood remains in contact with the endothelial layer of heart valve leaflets and vasculature which contains anticoagulant tissue factors, inhibitors, and receptors that suppress the protective functions of blood until an injury occurs ²⁸. Upon implantation of a medical heart valve, both an acute insult to the tissue in the region of implantation, and the introduction of a foreign body results in blood proteins being shuttled to the area as the primary host response. Plasma proteins operate as signaling mechanisms to cells in the host environment and form a bioactive surface on the implant for blood and immune cells to attach, governing the physiological response to the implant. Hemostasis and immune responses are intimately connected and thus must be described in conjunction with one another. Incompatible biomaterials exacerbate protein adhesion resulting in over-activation of host responses, thus the amount of plasma protein adhesion is an important indicator of a material's biocompatibility ²⁹.

Although over three-hundred distinct proteins exist in plasma, three proteins dominate and regulate the healing response: albumin, immunoglobulin-G (IgG), and fibrinogen. Neither albumin nor IgG play major roles in the activation of the coagulation or immune response cascades. Rather, these proteins act as carriers of anticoagulant factors and subdue acute inflammation after initial contact with the exterior of the implant ^{30,31}. Fibrinogen however does play a major role in the coagulation and immune response, forming hemostatic clots, facilitating the adhesion and

aggregation of platelets, and binding to the integrins of cells activated by the inflammatory system³². After adsorption on an implant surface, denaturation of fibrinogen promotes strong adherence to the implant surface thereby increasing the surface area to which platelets and leukocytes can bind. Platelets and leukocytes can co-activate, aggravating the host response. Previous studies have shown a strong correlation between the rate and amount of fibrinogen denaturation and the severity of inflammation^{30,31,33,34}.

Gaining insight into the nature of fibrinogen adsorption to biomaterial surfaces is thus essential to ascertaining overall hemocompatibility. Fibrinogen binding on surfaces was determined by measuring the amount of un-bound fibrinogen in plasma after 2hrs of exposure to substrates. More fibrinogen was present in HA-LLDPE exposed plasma as compared to LLDPE indicating less fibrinogen binding on the HA-LLDPE surfaces; however, this was not statistically significant (See **Fig. 3.4.1**). Statistically significant differences however were seen between the PS group and that of LLDPE and HA-LLDPE.

It is known that the molecular weight of HA significantly effects its interaction with various biochemical mechanisms. HA is found ubiquitously in uninjured tissue throughout the body as a high weight molecule (HMW-HA ~ 4000 kDa) and is known to be anti-inflammatory in this state^{35,36}. Upon cell or tissue injury, HA production increases and HMW-HA is cleaved by hyaluronidases into low molecular weight HA (LMW-HA ~ 100-500 kDa). LMW-HA stimulates Toll-like receptors summoning the migration of inflammatory cells to the damaged tissue changing their conformation to expose binding sites for fibrinogen³⁵. In this study, HMW-HA was used, and thus the surfaces may exhibit a lower binding affinity towards fibrinogen resulting in fewer proclivities for inflammation, and binding of platelets and leukocytes. Further, blood proteins in general have been shown to bind at a higher concentration to hydrophobic over hydrophilic

surfaces, thus the hydrophilic nature of HA-LLDPE may also reduce overall protein adhesion ³⁸. It is interesting to note that such a low amount of fibrinogen was discovered to be bound to virgin LLDPE surfaces as they present as hydrophobic interfaces. However, these results agree with those of Brash et al. who reported less fibrinogen binding to low-density polyethylene films than polystyrene substrates when immersed in water and protein solutions ³⁷. However, it is important to understand that all biomaterial surfaces are unique unto themselves. Protein competition at one surface can vary greatly from that of others. Thus, further investigations of protein adsorption on these different substrates is required.

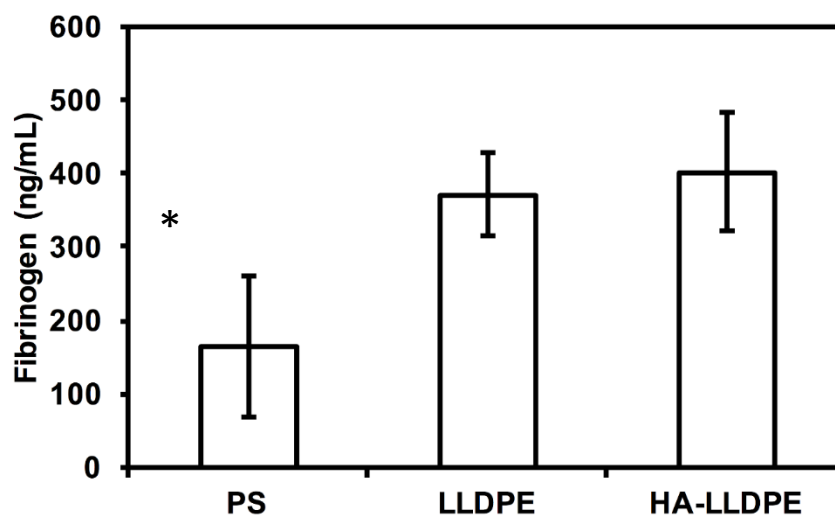


Figure 3.4.1: Fibrinogen adsorption to HA-LLDPE surfaces was not statistically different from that of virgin LLDPE but was significantly different from PS ($p \leq .05$) Results indicate greater free fibrinogen remained in plasma rather than adsorbed to LLDPE and HA-LLDPE surfaces. Experiments were replicated with at least three different human plasmas on at least five different samples ($n_{\min} = 15$). A one-way ANOVA was performed. Average values and standard deviations are as follows: PS (av=182.031; st.dev=180.454); LLDPE (av=390.919; st. dev=73.623); HA-LLDPE (av=429.804; st. dev=90.68).

3.4.2 *Leukocyte Adhesion to HA-LLDPE Substrates*

The bioactive protein layer on a material surface provides the foundation for coagulation/immune responses to take place; however, it is the binding and activation of cells to this film that are the key events in their stimulation. Adsorbed proteins are recognized by platelet and leukocyte receptors allowing them to bind, aggregate, activate, and spread across the biomaterial surface. Blood leukocytes consist of neutrophils and monocytes that differentiate into phagocytes and macrophages. However, when in contact with a biomaterial, size disparity between the surface of the material and the leukocyte means that the material is unable to be engulfed by the cell. Instead leukocytes can only release their metabolites and enzymes in an attempt to degrade the biomaterial surface^{7,28,39,40}. Under normal conditions, the half-life of these leukocytes is very short (6-8hrs), but upon tissue injury it can be increased by several days²⁸. During activation, alterations in membrane receptor affinities occur and inflammatory mediators are released which act as chemo-attractants and activators for other leukocytes, increasing cell adhesion to surfaces, and activating platelets²⁸. Because medical devices specifically activate both platelet and leukocytes, it is important to understand how they adhere to and activate on biomaterial surfaces as greater adhesion and activation can lead to adverse physiological responses.

Cellular adhesion was investigated by staining the cells with a rhodamine phalloidin cytoskeleton stain and a DAPI nucleus stain to identify adherent platelets and leukocytes. Activated platelets can bind to each other as well as interact with leukocytes, producing mixed aggregates. Platelet-leukocyte aggregation can be visualized using fluorescence microscopy. Rhodamine phalloidin stains the filamentous actin in the cytoskeleton which provides structure and locomotion to cells such as platelets and leukocytes whereas DAPI stains the nuclei in leukocytes. As platelets are anuclear this co-stain then allows for the discernment between the

leukocytes and platelets which have adhered to the surface. Results indicate lower cell adhesion and minimal platelet aggregation on HA-LLDPE surfaces as compared to LLDPE and PS surfaces (**Figure 3.4.2**). Further, the results also indicate lower leukocyte adhesion on HA-LLDPE surfaces as compared to LLDPE and PS surfaces. Since leukocytes are known co-activators of platelets, these results reinforce previous investigations noting lower platelet activation on the surface. both protein and cellular adhesion to biomaterials and attenuate the the non-specific immune response when exposed to whole blood or plasma ^{41,42}. Furthermore, leukocytes bind readily to fibrinogen. It has been demonstrated that leukocytes recognize fibrinogen as fibrin instigating inflammatory responses ¹⁴. Thus, the low levels of fibrinogen to HA-LLDPE and LLDPE surfaces may account for the reduced number of leukocytes present on surfaces.

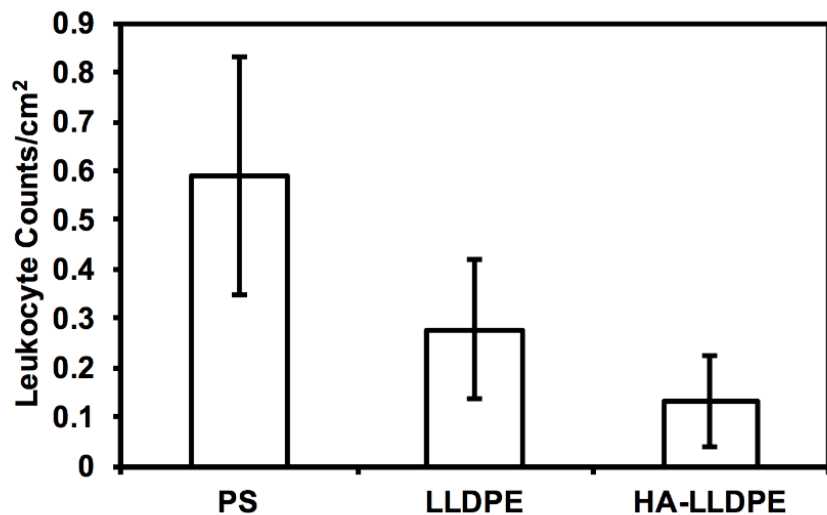


Figure 3.4.2 (a): Quantification of leukocyte adhesion through DAPI counting reveals significantly less cellular adhesion to HA-LLDPE surfaces compared to PS. Lower leukocyte adhesion is found as compared to LLDPE but results were not significant. Experiments were replicated with at least three different cell populations on at least three different samples ($n_{\min} = 9$). A one-way ANOVA was performed. Average values and standard deviations are as follows: PS (av=.589; st.dev=.214); LLDPE (av=.277; st.dev=1.43); HA-LLDPE (av=.130; st.dev=.092)

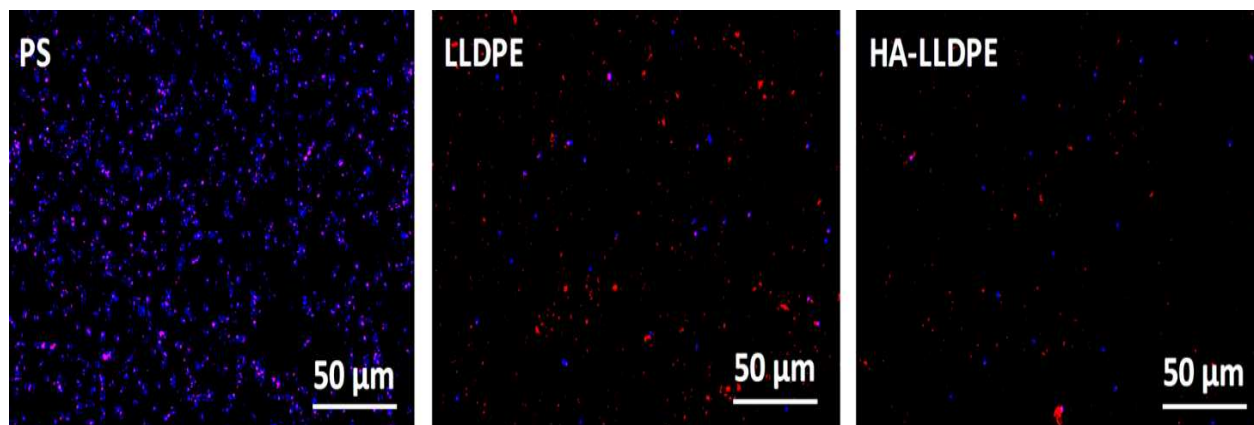


Figure 3.4.2 (b): Representative images of leukocyte staining demonstrating lower adhesion to HA-LLDPE surfaces. Experiments were replicated with at least three different cell populations on at least three different samples ($n_{min} = 9$).

3.4.3 Scanning Electron Microscopy

To confirm results of fluorescent imaging SEM was performed on substrates to visualize leukocyte adhesion. SEM imaging reinforced both fluorescent imaging results discussed above as well as those previously performed for platelet activation studies. Greater cell adhesion was noted on PS and LLDPE surfaced that HA-LLDPE. While some leukocyte adhesion was noted on LLDPE there was less observed than on PS surfaces. Again, this may be due to the lack of fibrinogen binding to LLDPE surfaces. Platelets which adhered to both PS and LLDPE exhibited less platelet adhesion as visualized in study results reported in Chapter 2: Section 2.4.6. HA-LLDPE surfaces followed previously observed trends. Less cellular adhesion was detected as well as less platelet activation. Very few leukocytes were found attached to HA-LLDPE surfaces.

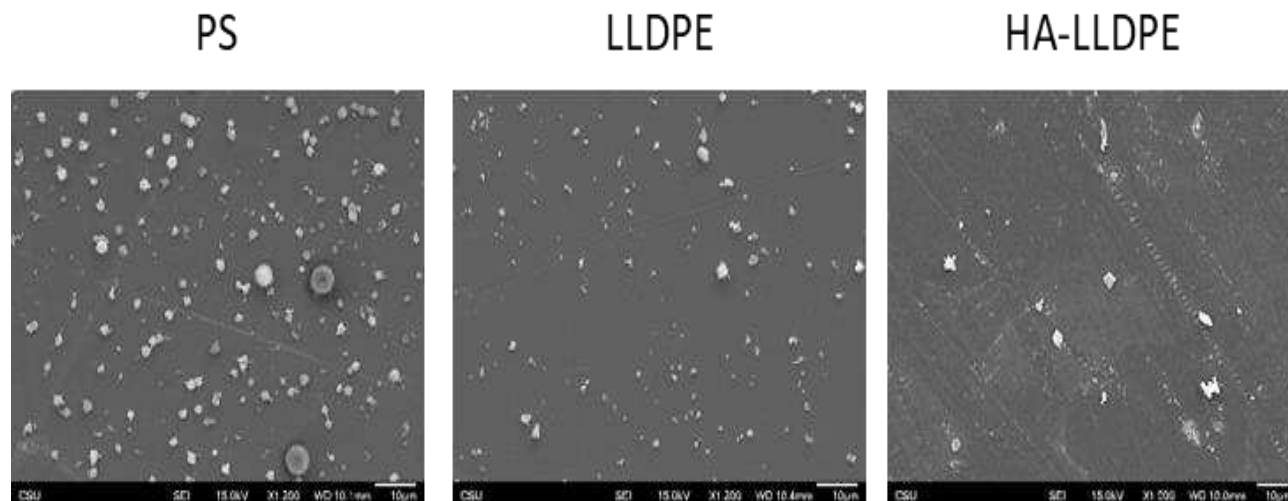


Figure 3.4.3: Representative SEM images of leukocyte adhesion on substrate surfaces. HA-LLDPE surfaces reduce leukocyte adhesion compared to PS and LLDPE.

3.3.4 Complement Activation on HA-LLDPE Surfaces

Hemocompatibility of biomaterials is mostly studied in terms of platelet and leukocyte aggregation and activation, although biomaterials are also known agonists of the complement system which can act as a precursor to platelet and leukocyte stimulation²⁸. The complement system is considered part of the immune response and assists antibodies and phagocytic cells in the removal of pathogens. When in contact with a biomaterial, complement activation is mostly triggered by the alternative pathway with the proteins C3 and C5 being its most critical components. However, some research has implicated that the classical pathway may also be involved^{28,43}.

To investigate the effect of HA-LLDPE on complement activation, an enzyme immunoassay was used to determine the expression of the terminal complex, SC5b-9. SC5b-9 is formed by the solubilization of proteins known as the terminal complement complex, a final step in the activation of the alternative pathway. The results indicate no significant differences in SC5b-9 expression on all the surfaces (**Figure 3.3.4**). This may be attributed to the base materials

themselves, as LLDPE and PS are both known to be weak activators of the complement system^{5,44}. Furthermore, HA is known to be anti-complementary. Some studies have found that hyaluronan binding protein 1, a hyaladherin implicated in cellular signaling and adhesion can bind to the globular heads of the C1q molecule effectively inhibiting C1 and thereby mitigating complement cascade activation^{45,46}.

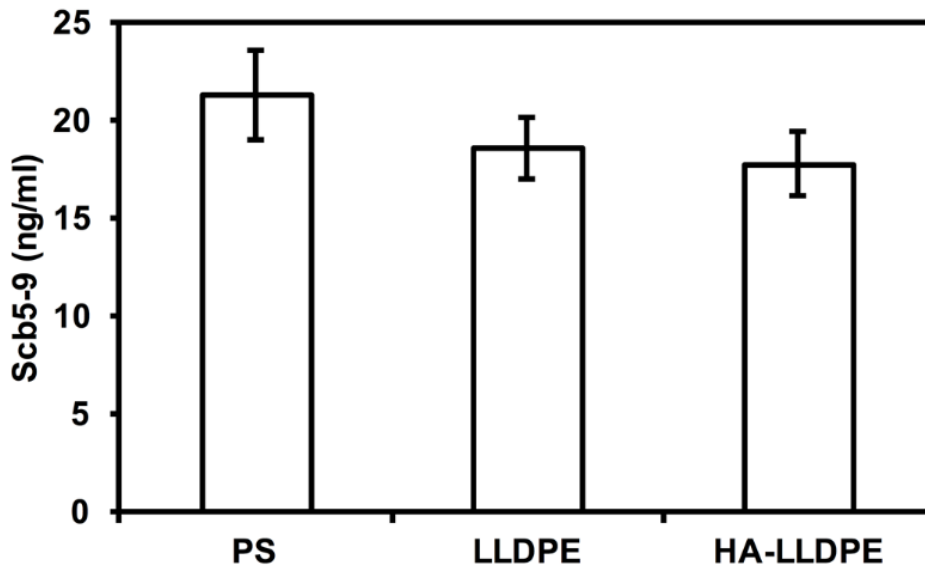


Figure 3.3.4: Complement activation measured by the amount of SC5b-9 activation on different surfaces after 2hrs of incubation in human plasma. The results indicate no significant difference in the level of complement activation. Experiments were replicated with at least three different human plasma on at least five different samples ($n_{\min} = 15$). A one-way ANOVA was performed. Average values and standard deviation are as follows: PS (av=21.265; st.dev=2.261); LLDPE (av=18.567; st.dev=1.587); HA-LLDPE(av=17.76; st.dev=1.632).

3.3.5 Conclusions

PHV technology requires the development of materials which will not only attenuate the coagulation cascade, but that of the immune response as well. Fibrinogen binding, leukocyte adhesion and complement system activation can all lead to exacerbated material induced non-specific immune responses. To determine how HA-LLDPE surface affect each of these

mechanisms fibrinogen and complement assays as well as fluorescent microscopy was performed. Results of this study indicated a reduction in fibrinogen binding on the HA-LLDPE surface as compared to control surfaces which may assist in reducing overall cellular adhesion; however, fibrinogen adsorption results were not significantly different between virgin LLDPE and HA-LLDPE. They were significantly different from PS however, demonstrating a lower affinity for fibrinogen binding. The reduction in platelet and leukocyte adhesion noted in the cellular studies is more likely due to the increased hydrophilicity of the HA-LLDPE material as compared to LLDPE, but further investigation is required. Because HA-LLDPE substrates showed a significant difference in leukocyte and platelet adhesion as well as anti-complementary effects it is asserted that HA-LLDPE surfaces may provide a beneficial material to help reduce immune response effects if used for the development of PHV technology. While these results may not be clinically significant they offer some depth in understanding how these materials may work *in vivo*.

REFERENCES:

1. Vongpatanasin W, Hillis LD, Lange RA. Prosthetic heart valves: A Review. *New Engl J Med.* 1996;335(6):407-416.
2. Pibarot P, Dumesnil JG. Prosthetic heart valves: Selection of the optimal prosthesis and long-term management. *Circulation.* 2009;119(7):1034-1048.
doi:10.1161/CIRCULATIONAHA.108.778886
3. Grunkemeier JM, Tsai WB, Horbett TA. Hemocompatibility of treated polystyrene substrates: Contact activation, platelet adhesion, and procoagulant activity of adherent platelets. In: *Journal of Biomedical Materials Research.* Vol 41. ; 1998:657-670. doi:10.1002/(SICI)1097-4636(19980915)41:4<657::AID-JBM18>3.0.CO;2-B
4. Fujimoto K, Tadokoro H, Ueda Y, Ikada Y. Polyurethane surface modification by graft polymerization of acrylamide for reduced protein adsorption and platelet adhesion. *Biomaterials.* 1993;14(6):442-448. doi:10.1016/0142-9612(93)90147-T
5. Engberg AE, Rosengren-Holmberg JP, Chen H, et al. Blood protein-polymer adsorption: Implications for understanding complement-mediated hemoincompatibility. *J Biomed Mater Res - Part A.* 2011;97 A(1):74-84. doi:10.1002/jbm.a.33030
6. Al-Maawi S, Orłowska A, Sader R, James Kirkpatrick C, Ghanaati S. In vivo cellular reactions to different biomaterials—Physiological and pathological aspects and their consequences. *Semin Immunol.* 2017. doi:10.1016/j.smim.2017.06.001
7. Anderson JM, Rodriguez A, Chang DT. Foreign body reaction to biomaterials. *Semin Immunol.* 2008. doi:10.1016/j.smim.2007.11.004
8. Hlady V, Buijs J. Protein adsorption on solid surfaces. *Curr Opin Biotechnol.*

1996;7(1):72-77. doi:10.1016/S0958-1669(96)80098-X

9. Ito E, Suzuki K, Yamato M, Yokoyama M, Sakurai Y, Okano T. Active platelet movements on hydrophobic/hydrophilic microdomain- structured surfaces. *J Biomed Mater Res.*

1998;42(1):148-155. doi:10.1002/(SICI)1097-4636(199810)42:1<148::AID-JBM18>3.0.CO;2-H

10. Lee JH, Khang G, Lee JW, Lee HB. Platelet adhesion onto chargeable functional group gradient surfaces. *J Biomed Mater Res.* 1998;40(2):180-186. doi:10.1002/(SICI)1097-4636(199805)40:2<180::AID-JBM2>3.0.CO;2-H [pii]

11. Lee J, Khang G, Lee J, Lee H. Interaction of Different Types of Cells on Polymer Surfaces with Wettability Gradient. *J Colloid Interface Sci.* 1998;205(2):323-330. doi:10.1006/jcis.1998.5688

12. Lee JH, Lee HB. Platelet adhesion onto wettability gradient surfaces in the absence and presence of plasma proteins. In: *Journal of Biomedical Materials Research.* Vol 41. ; 1998:304-311. doi:10.1002/(SICI)1097-4636(199808)41:2<304::AID-JBM16>3.0.CO;2-K

13. Stroncek JD, Reichert WM. Overview of Wound Healing in Different Tissue Types. In: *Indwelling Neural Implants: Strategies for Contending with the In Vivo Environment.* ; 2007:3-33. doi:NBK3938 [bookaccession]

14. Franz S, Rammelt S, Scharnweber D, Simon JC. Immune responses to implants - A review of the implications for the design of immunomodulatory biomaterials. *Biomaterials.* 2011. doi:10.1016/j.biomaterials.2011.05.078

15. Fioretta ES, Dijkman PE, Emmert MY, Hoerstrup SP. The future of heart valve replacement: recent developments and translational challenges for heart valve tissue engineering. *J Tissue Eng Regen Med.* 2016. doi:10.1002/term.2326

16. Fraser JR, Laurent TC, Laurent UB. Hyaluronan: its nature, distribution, functions and

turnover. *J Intern Med.* 1997;242:27-33. doi:10.1046/j.1365-2796.1997.00170.x

17. Laurent TC, Fraser JR. Hyaluronan. *FASEB J.* 1992;6(7):2397-2404. doi:10.1016/S0140-6736(01)35637-4
18. Esposito E, Menegatti E, Cortesi R. Hyaluronan-based microspheres as tools for drug delivery: A comparative study. *Int J Pharm.* 2005;288(1):35-49. doi:10.1016/j.ijpharm.2004.09.001
19. Vorpahl M, Nakano M, Acampado E, et al. Early maturation of endothelialisation on hyaluronan-coated stents in a rabbit model of ilio-femoral artery stenting. *EuroIntervention.* 2010.
20. Wu X, Zhao Y, Tang C, et al. Re-Endothelialization Study on Endovascular Stents Seeded by Endothelial Cells through Up- or Downregulation of VEGF. *ACS Appl Mater Interfaces.* 2016. doi:10.1021/acsami.6b00152
21. Chuang TW, Masters KS. Regulation of polyurethane hemocompatibility and endothelialization by tethered hyaluronic acid oligosaccharides. *Biomaterials.* 2009;30(29):5341-5351. doi:10.1016/j.biomaterials.2009.06.029
22. Gong F, Lu Y, Guo H, Cheng S, Gao Y. Hyaluronan immobilized polyurethane as a blood contacting material. *Int J Polym Sci.* 2010;2010. doi:10.1155/2010/807935
23. Thierry B, Winnik FM, Merhi Y, Griesser HJ, Tabrizian M. Biomimetic hemocompatible coatings through immobilization of hyaluronan derivatives on metal surfaces. *Langmuir.* 2008;24(20):11834-11841. doi:10.1021/la801359w
24. Pitt WG, Morris RN, Mason ML, Hall MW, Luo Y, Prestwich GD. Attachment of hyaluronan to metallic surfaces. *J Biomed Mater Res A.* 2004;68(1):95-106. doi:10.1002/jbm.a.10170
25. Prawel DA, Dean H, Forleo M, et al. Hemocompatibility and Hemodynamics of Novel

Hyaluronan-Polyethylene Materials for Flexible Heart Valve Leaflets. *Cardiovasc Eng Technol.* 2014;5(1):70-81. doi:10.1007/s13239-013-0171-5

26. Simon-Walker R, Cavicchia J, Prawel DA, Dasi LP, James SP, Popat KC. Hemocompatibility of hyaluronan enhanced linear low density polyethylene for blood contacting applications. *J Biomed Mater Res - Part B Appl Biomater.* 2018;106(5). doi:10.1002/jbm.b.34010

27. Simon-Walker R, Cavicchia J, Prawel DA, Dasi LP, James SP, Popat KC. Hemocompatibility of hyaluronan enhanced linear low density polyethylene for blood contacting applications. *J Biomed Mater Res Part B Appl Biomater.* September 2017. doi:10.1002/jbm.b.34010

28. Gorbet MB, Sefton M V. Biomaterial-associated thrombosis: Roles of coagulation factors, complement, platelets and leukocytes. In: *The Biomaterials: Silver Jubilee Compendium.* ; 2006:219-241. doi:10.1016/B978-008045154-1.50025-3

29. Peerschke EI, Ghebrehiwet B. Platelet receptors for the complement component C1q: implications for hemostasis and thrombosis. *Immunobiology.* 1998;199(2):239-249. doi:10.1016/S0171-2985(98)80030-2

30. Tang L, Eaton JW. Inflammatory responses to biomaterials. *Am J Clin Pathol.* 1995;103(4):466-471.

31. Tang L, Lucas a H, Eaton JW. Inflammatory responses to implanted polymeric biomaterials: role of surface-adsorbed immunoglobulin G. *J Lab Clin Med.* 1993;122(3):292-300. doi:0022-2143(93)90076-B [pii]

32. Ryu JK, Davalos D, Akassoglou K. Fibrinogen signal transduction in the nervous system. *J Thromb Haemost.* 2009;7(SUPPL. 1):151-154. doi:10.1111/j.1538-7836.2009.03438.x

33. Rubens F, Brash J, Weitz J, Kinlough-Rathbone R. Interactions of thermally denatured

- fibrinogen on polyethylene with plasma proteins and platelets. *J Biomed Mater Res.* 1992;26(12):1651-1663. doi:10.1002/jbm.820261209
34. Skarja GA, Brash JL, Bishop P, Woodhouse KA. Protein and platelet interactions with thermally denatured fibrinogen and cross-linked fibrin coated surfaces. *Biomaterials.* 1998;19(23):2129-2138. doi:10.1016/S0142-9612(98)00045-3
35. Bonafè F, Govoni M, Giordano E, Caldarera CM, Guarnieri C, Muscari C. Hyaluronan and cardiac regeneration. *J Biomed Sci.* 2014;21(1). doi:10.1186/s12929-014-0100-4
36. Ruppert SM, Hawn TR, Arrigoni A, Wight TN, Bollyky PL. Tissue integrity signals communicated by highmolecular weight hyaluronan and the resolution of inflammation. *Immunol Res.* 2014. doi:10.1007/s12026-014-8495-2
37. Brash JL, Lyman DJ. Adsorption of plasma proteins in solution to uncharged, hydrophobic polymer surfaces. *J Biomed Mater Res.* 1969. doi:10.1002/jbm.820030114
38. Eriksson C, Nygren H. Polymorphonuclear leukocytes in coagulating whole blood recognize hydrophilic and hydrophobic titanium surfaces by different adhesion receptors and show different patterns of receptor expression. *J Lab Clin Med.* 2001. doi:10.1067/mlc.2001.114066
39. Henson PM. Mechanisms of exocytosis in phagocytic inflammatory cells. Parke-Davis Award Lecture. *Am J Pathol.* 1980;101(3):494-511.
40. Henson PM. The immunologic release of constituents from neutrophil leukocytes. II. Mechanisms of release during phagocytosis, and adherence to nonphagocytosable surfaces. *J Immunol.* 1971;107:1547-1557.
41. Li B, Xie J, Yuan Z, et al. Mitigation of Inflammatory Immune Responses with Hydrophilic Nanoparticles. *Angew Chemie - Int Ed.* 2018. doi:10.1002/anie.201710068
42. Dai X, Wei Y, Zhang X, et al. Attenuating Immune Response of Macrophage by Enhancing

Hydrophilicity of Ti Surface. *J Nanomater.* 2015. doi:10.1155/2015/712810

43. Gretzer C, Gisselält K, Liljensten E, Rydén L, Thomsen P. Adhesion, apoptosis and cytokine release of human mononuclear cells cultured on degradable poly(urethane urea), polystyrene and titanium in vitro. *Biomaterials.* 2003;24(17):2843-2852. doi:10.1016/S0142-9612(03)00097-8
44. Roch T, Krüger A, Kratz K, Ma N, Jung F, Lendlein A. Immunological evaluation of polystyrene and poly(ether imide) cell culture inserts with different roughness. *Clin Hemorheol Microcirc.* 2012;52(2-4):375-389. doi:10.3233/CH-2012-1612
45. Jiang D, Liang J, Noble PW. Hyaluronan as an immune regulator in human diseases. *Physiol Rev.* 2011;91(1):221-264. doi:10.1152/physrev.00052.2009
46. Sengupta A, Banerjee B, Tyagi RK, Datta K. Golgi localization and dynamics of hyaluronan binding protein 1 (HABP1/p32/C1QBP) during the cell cycle. *Cell Res.* 2005;15(3):183-186. doi:10.1038/sj.cr.7290284

CHAPTER 4

ENDOTHELIAL CELL INTERACTIONS WITH HYALURONAN ENHANCED LINEAR LOW-DENSITY POLYETHYLENE

4.1 Introduction

4.1.1 The Properties of Hyaluronan Modulate Cellular Interactions

Hyaluronan (HA) is a highly biocompatible, non-immunogenic, mucopolysaccharide found ubiquitously in the connective tissue of higher order animals. It is especially abundant in the synovial fluids, ocular viscera, and the apical surface of endothelium¹⁻⁵. An essential component of the cardiovascular system, it is crucial to embryonic cardiac development, the facilitation of wound healing, tissue regeneration, repair, and angiogenesis¹⁻³. The architecture of the polymer consists of secured parallel hydrogen bonds running the length of the chain axis rendering an inflexible helix¹. The tightly coiled configuration allows it to mechanically trap up to one-hundred times its weight in water drawn in through the osmotic imbalance resulting from its high anionicity^{2,3,6,7}. The result is an exceedingly hydrophilic biomolecule.

Native HA exists as high molecular weight (HMW) chains which are cleaved in the presence of hyaluronidases located in the extracellular matrix and in platelet bodies^{8,9}. HA depolymerization increases bioactivity, promoting interaction with blood plasma constituents and other biomolecules present in the coagulation and immune response cascades. Due to its high anionicity and ability to modulate physiological processes through chain length, HA is capable of both enhancing cellular responses such as attachment and proliferation of cells, and reducing blood protein adsorption and cellular adhesion to biomaterial surfaces^{1,2,10-13}. Furthermore, HA can be

cross-linked to itself and other materials and has an easily controlled degradation profile ³. These qualities have made it particularly appealing as a target molecule for modification of cardiovascular biomaterials, and is currently being assessed for its usability in stents, heart-valve leaflets, drug-delivery hydrogels, scaffolds, and surrogate tissue designs among other applications ^{3,10,14,15}.

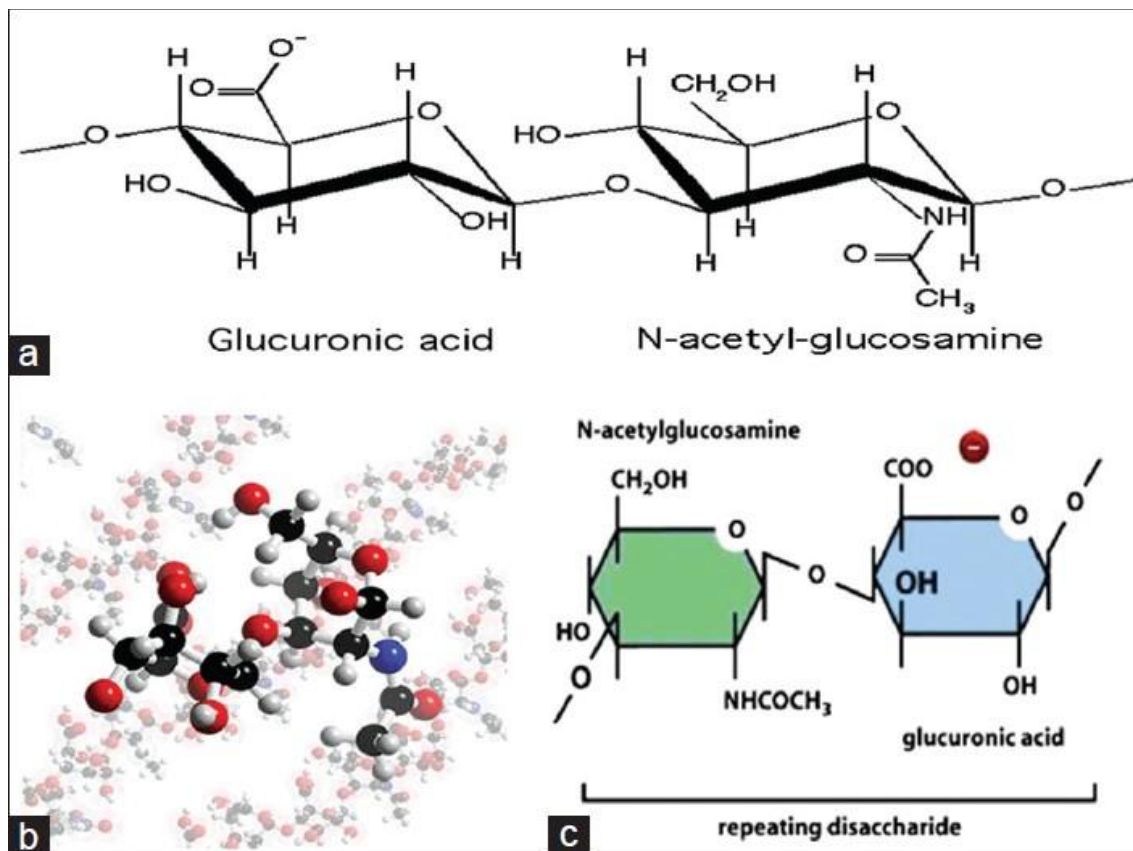


Figure 4.1.1: Structure of hyaluronan. Reprinted with Permission © North American Journal of Medical Sciences ¹⁶.

4.1.2 Endothelialization of Heart Valves

Endothelialization of cardiovascular biomaterials is considered the gold standard for achieving optimal hemocompatibility *in vivo*. Endothelialization subdues the attachment and activation of platelets and macrophage, reducing the risk of thrombosis, and can increase the

release of functional groups which support cellular proliferation¹⁷⁻²³. Because of this endothelialization of heart valve leaflets has been explored as an alternative to mechanical heart valves which are thrombotic due to their rigid leaflet design and tissue-based valves which are prone to calcification and degradation²⁴⁻²⁶. Approaches to endothelialized heart valves include seeding of base materials and subsequent conditioning in a bioreactor prior to implantation, and in situ population of constructs by progenitor cells (See **Fig. 4.1.2**)²⁷⁻²⁹.

However, this achievement has proven to be quite difficult. Endothelialization of biomaterials increases the complexity and cost of fabrication³⁰. To be effective, biomaterials must support a mono-layer of mature, quiescent endothelium. Implants pre-seeded with endothelial cells to support the native processes of transanastomotic and transmural growth, and the attachment of endothelial cells, utilize autologous isolation and *ex vivo* expansion acquired through biopsy of vascular tissue, or progenitor isolation from the patient's own blood^{30,31}. In addition, polymers used to promote the growth and proliferation of endothelium often require modification to ensure compatible compliance, reduce mechanical mismatch, modulate the behavior of cells, control protein deposition, and eliminate denuding under shear stress³⁰. If vascularization with the biomaterial is desired this dramatically increases the difficulty in engineering required³²⁻³⁵. Due to the vast array of complications that have arisen in endothelializing heart valves, the success of this technology has been limited³⁶⁻³⁸. Current approaches have turned to *in situ* endothelialization attempting to promote endothelial migration from other local tissue or the attachment of endothelial progenitor cells from the patient's blood³¹. Thus, mitigating the need for complex fabrication processes, and developing a simple interface that reduces protein, platelet, and cellular adhesion but still presents a biocompatible surface to the physiology can offer a cost-effective alternative.

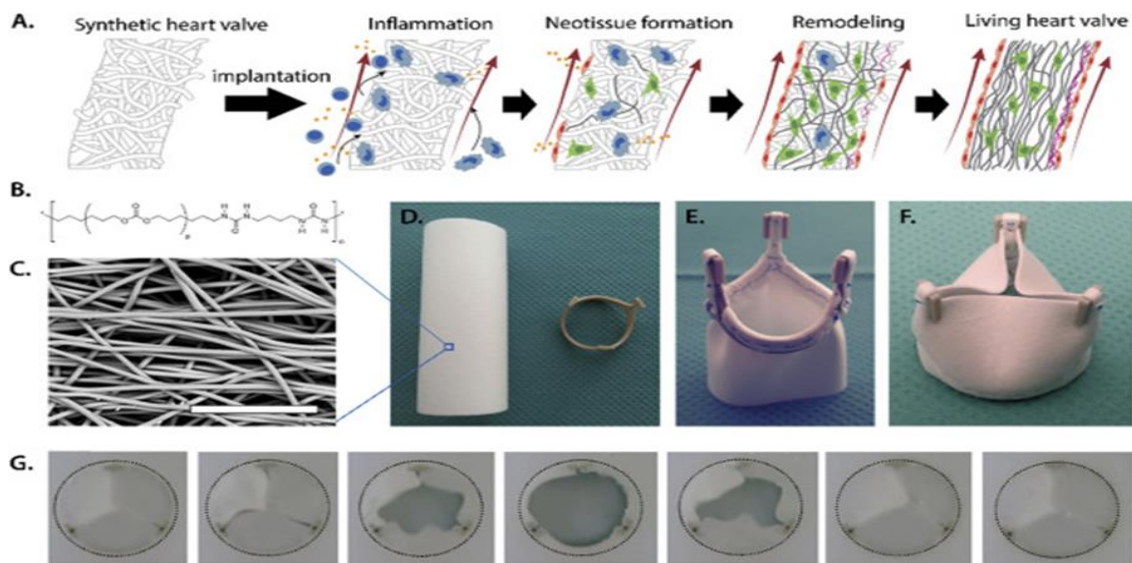


Figure 4.1.2: Example of endothelialization of heart valves using *in situ* approach on a bioresorbable elastomeric implant. Reproduced with permission Elsevier ©.

4.1.3 HMW-HA-LLDPE to Mitigate Endothelial Adhesion

In this study, we investigate the effects of HMW-HA enhanced linear low-density polyethylene (HA-LLDPE) on endothelial adhesion and proliferation. The hydrophilicity of HMW-HA is known to prohibit the adsorption of proteins to surfaces, limiting platelet interactions essential to endothelial attachment, migration, and proliferation. In addition, the molecular weight of the HA used to fabricate HA-LLDPE is anticipated to reduce proliferation, and cell growth^{10,11,14,15}. HA-LLDPE has been previously shown to reduce blood constituent adhesion and to be biocompatible and hemocompatible^{15,39}. Assessments include lactate dehydrogenase (LDH) assaying of cells after substrate exposure, scanning electron microscopy (SEM), rhodamine phalloidin (actin) and DAPI fluorescent staining to visualize cellular attachment, Alamar Blue viability investigations, and CD-31 and VEG-F protein stains to assess phenotype.

4.2 Methods

4.2.1 Human Umbilical Vein Endothelial Cell Culture

Human umbilical vein endothelial cells (HUVEC, Millipore Sigma) were removed from nitrogen storage and immediately thawed in a 37°C water bath. Media 199 (M199; Invitrogen) was used to dilute the cells and freeze media before centrifugation at 100g for 10 min to isolate the cell pellet. The supernatant was then gently aspirated followed by re-suspension of the cell pellet in M199. HUVECs were then plated in a T-75 tissue culturing flask at a density of 1×10^6 cells/flask. At 70% confluency HUVECs were disassociated using Trypsin/EDTA (Sigma) and seeded onto substrates at 10,000 cells/cm².

4.2.2 Porcine Aortic Valve Endothelial Cell Culture

Fresh porcine hearts were harvested from a local abattoir. The aortic root was excised aseptically. The aortic heart valve leaflets were then removed and placed in a 15 ml conical tube filled with PBS and gently oscillated on a shaker plate at 200rpm for 5min to remove any residual blood components. The heart valve leaflets were then transferred to a 15ml conical tube (3 leaflets/tube) filled with collagenase type II (Thermofisher) and placed on a shaker plate set at 200rpm in a 37°C incubator for 45min. After shaking, the tubes were centrifuged at 1000 rpm for 5min to isolate the cell pellet. The supernatant was aspirated off and 10ml of porcine endothelial cell media (Cell Applications Inc.; Sigma Aldrich) was added to the tube while pipetting up and down to resuspend the cell pellet. Cells were counted and plated at a density of 1×10^6 cells per T-75 flask which had been pre-coated with rat-tail collagen. At 70 % confluency cells were seeded onto samples at a density of 25,000 cells/8cm².

4.2.3 Progenitor Endothelial Cell Culture

Whole human blood was isolated via phlebotomy from volunteers who had refrained from taking thromboxane inhibitors for at least two weeks. Blood was collected in sodium heparin tubes (BD Vacutainer) and placed immediately on ice. It should be noted that blood was used within 2hrs of collection. Lymphoprep (Axis-shield; Proteogenix) was warmed to room temperature and distributed in 50ml conical tubes at a volume of 15ml per tube. 30ml of blood from sodium heparin tubes was gently layered over Lymphoprep with a pipette on a gravity setting to ensure that blood and Lymphoprep did not mix. The tubes were then centrifuged at 800 x g for 30min. Peripheral blood cells were then removed from the conical tubes and placed in a new 50ml conical tubes with a solution of 6% FBS in PBS until a volume of 50ml was obtained. The tubes were then centrifuged for 10min at 350 x g at ambient temperature. The supernatant was aspirated, and the cell pellet resuspended in human endothelial cell growth media (EGM-2; Cell Applications; Sigma Aldrich). Cells were plated at a density of 1×10^6 cells in a T-75 flask which had been pre-coated with fibronectin.

4.2.4 Lactate Dehydrogenase Release

A commercially available lactate dehydrogenase assay (LDH) was used to assess any cytotoxicity of different substrates on HUVECs. The protocol provided by the manufacturer was used (Pierce Biotechnology). In brief, a reaction mix was prepared by combining a substrate mixture (lyophilizate and ultrapure water) with an assay buffer provided by the manufacturer. The substrates were seeded with cells 24hrs prior to application of the LDH assay protocol, including a positive control group of lysis buffer added to a set of substrates to ensure maximal lysing of HUVECs and a negative control of HEPES buff. After incubation, 50 μ l of substrate media was

transferred to a 96 well plate. Fifty μl of reaction mix was then added to the media and mixed gently by tapping. Substrates were then incubated for 30min in a dark hood. After 30min absorbance was read at 490nm and 680nm on a spectrophotometer.

4.2.5 Cellular Visualization

Cells (either HUVECs or VECs) were seeded onto substrates at a density of 10,000 cells/cm² (HUVECs) or 25,000 cells/cm² (VECs) and allowed to grow for 24hrs and 7 days. After the prescribed time length of cell growth on substrates, the surfaces were stained with rhodamine phalloidin cytoskeleton stain (actin; Cytoskeleton) and 4'6-diamidino-2-phenylindole dihydrochloride nucleus stain (DAPI, Thermo-Scientific) to visualize cellular attachment. Any un-adhered cells were gently aspirated, and the surfaces were washed with PBS (2x). The adherent cells were fixed in 3.7 wt % formaldehyde in PBS for 15mins at room temperature and rinsed (3x, 5mins each) with PBS. The cell membranes were further permeabilized by 1 % Triton-X solution in PBS at room temperature for 3mins. The surfaces were then transferred to a new 24-well plate and incubated with 500 μl of rhodamine phalloidin solution in PBS for 25mins at room temperature. After 25mins, 0.2 $\mu\text{g}/\text{ml}$ DAPI stain was added to each well and incubated for 5mins. The stain solution was gently aspirated, and the surfaces rinsed with PBS (2x). The surfaces were immediately imaged using a Zeiss Axiovision fluorescent microscope using appropriate filters. All images were processed using ImageJ Software.

4.2.6 Scanning Electron Microscopy

Scanning electron microscopy (SEM) was used to visualize HUVEC attachment and morphology on HA substrates. After 24hrs and 7 days of cell growth, the substrates were gently rinsed twice with PBS, fixed, and dehydrated. The fixation process included 45 mins of incubation in a primary fixative of 6% glutaraldehyde (Sigma), 0.1M sodium cacodylate (Polysciences), and 0.1M sucrose (Sigma) in DI water. Afterwards, substrates were transferred to a buffer solution (primary fixative without glutaraldehyde) for 10mins. This was followed by incubating the substrates in consecutive solutions of ethanol (35%, 50%, 70% and 100%) for 10mins each to remove any excess water. Substrates were then stored in a desiccator until imaging. Prior to SEM visualization, the substrates were coated with 10nm layer of gold and imaged at 5 kV.

4.2.7 AlamarBlue Assaying

After 24 hrs and 7 days of cell growth on substrates media was gently aspirated from the well plates and fresh media was added to each well. AlamarBlue was added at 10% of the media volume as called for in the protocol (Thermo-Scientific). Substrates were allowed to incubate for up 8 hrs. After incubation 100 ul of media+alamarBlue was removed and transferred to a 96 well plate. Absorbance was read at 570nm and 600 nm on a spectrophotometer.

4.2.8 Protein expression

Protein expression and cellular adhesion was visualized using fluorescent imaging after 7 days of cell growth upon substrate surfaces. Cell media was gently aspirated and rinsed with PBS to remove non-adherent cells. Substrates were then transferred to a new 24 well plate. Cells were subsequently fixed with 3.7% w/v formaldehyde in PBS for 15min at room temperature and then

washed in PBS (3x). Immediately following, substrates were incubated with 1% bovine serum albumin (BSA) and 22.52 mg/mL glycine in PBST (PBS+ 0.1% Tween 20) for 30min to block unspecific binding of the antibodies. Cells were then incubated in diluted antibody (1:50 dilution in PBS; Anti-CD31 (rabbit polyclonal to CD-31; Abcam) or Anti-VEG-F (rabbit polyclonal to VEG-F; Abcam) in 1% BSA for 1hr at ambient temperature. Following incubation, the solution was decanted, and the cells were again washed (3x) in PBS for 5min. The cells were then incubated with the secondary antibody solution (Goat Anti-Rabbit IgG H&L (Alexa Fluor® 488, Abcam) in 1% BSA diluted in PBS (1:1000) for 1hr at room temperature in the dark. The secondary antibody solution was then decanted, and the cells were washed again for five minutes with PBS (3x) in the dark. Lastly, a DAPI nucleus stain was applied. Samples were then visualized using a Zeiss Axiovision fluorescent microscope.

4.2.9 Statistical Analysis

Each qualitative experiment was performed to evaluate differences between PS, LLDPE and HA-LLDPE on at least three substrates ($n_{\min} = 9$), except for ELISA's which were performed on at least five substrate surfaces per group ($n_{\min} = 15$). Each assay was repeated at least three times with three different whole blood plasma populations. All results were evaluated using a one-way analysis of variance (ANOVA) with a Tukey's, Bonferonni, and Scheffé post-hoc tests.

4.3 Results and Discussion

4.3.1 LDH Results after Endothelial Exposure to Different Surfaces

Endothelialization of biomaterials is generally considered the gold standard for which blood contacting material surfaces aspire, however achieving endothelialized biomaterial surfaces

that perform as well as the native endothelium is still a major challenge ⁴⁰ . A cardiovascular biomaterial surface that mitigates endothelial attachment, is compatible with the blood and surrounding tissues, can beneficially modulate the body's natural healing mechanisms, reduce production costs, and increase ease of fabrication etc. would offer a compelling alternative to current biomaterials. Previously, we assessed the hemocompatibility of blood components to HA-LLDPE surfaces ^{13,15}. It was determined that HA-LLDPE was non-toxic to blood constituents and reduced platelet and leukocyte adhesion and activation. In this investigation we look at the ability of HA-LLDPE to mitigate endothelial cell attachment, modulate morphology, and support phenotype.

It was of primary important to ensure that HA-LLDPE surfaces were non-toxic to endothelial cells so that any observed reduction in cellular attachment was not due to cytotoxic effects. To this end, an LDH assay was performed. LDH is an enzyme present within all cells. Because it is released during tissue damage it is commonly used as a marker for cell death and systemic injury ⁴¹⁻⁴⁴. Upon encountering a toxic substance, cellular necrosis is induced accompanied by the swelling of organelles and increases in LDH. This results in cell lysis and the spilling of internal contents into the extracellular milieu. LDH can then be assayed to determine the magnitude of cell death. In this study Triton-X was used at the negative control representing maximal lysis of HUVECs. HEPES buffer was used for the positive control as it maintains a physiological pH and is non-toxic to cells ⁴⁵. Results indicate that virgin LLDPE used as the base material for HA-LLDPE and HA-LLDPE are both non-toxic to HUVECs as there were no significant differences between the LDH expression of these and that of HEPES buffer (See **Fig. 4.3.1.**). These results are supported by previous evidence noting that LLDPE and HA-LLDPE were non-toxic to platelets ^{15,39}.

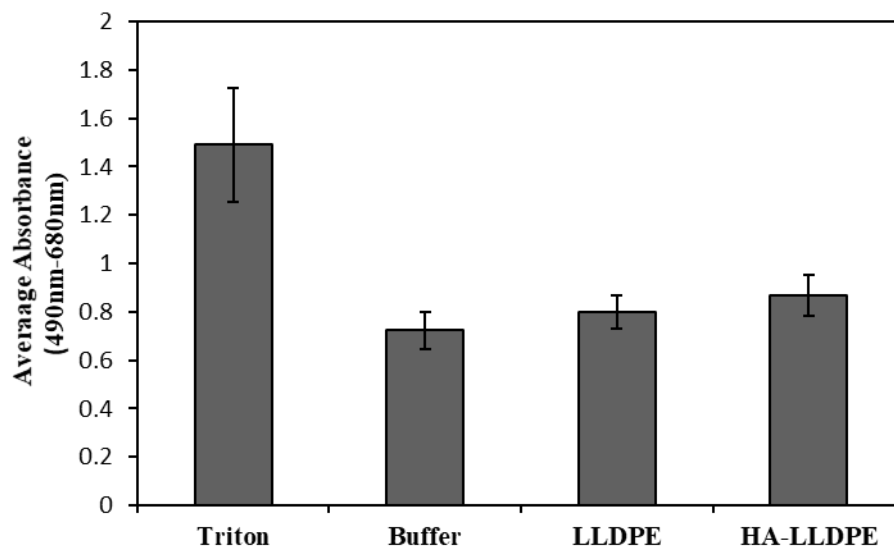


Figure 4.31: LDH assaying demonstrates low-toxicity of LLDPE and HA-LLDPE as compared to the maximal lysis Triton-X group $p \leq .05$. In addition, LLDPE and HA-LLDPE displayed no significant differences from HEPES buffer which is widely used in cell culturing. Experiments were replicated with at least three different cell populations on at least five different samples ($n_{\min} = 9$). A one-way ANOVA was performed. Average values and standard deviations are as follows: Triton-X(av=1.452; st.dev=.564); HEPES Buffer(av=.789; st.dev=.354); LLDPE(av=.826; st.dev=.312); HA-LLDPE(av=.953; st.dev=.421).

4.3.2 HUVEC Adhesion Results Using Fluorescent Imaging

To determine if HUVEC adhesion was mitigated on HA-LLDPE surfaces, actin/DAPI fluorescent co-staining were used to visualize and quantify cellular attachment. Rhodamine phalloidin is a fluorescent probe that assists in visualizing the F-actin filaments of cell bodies. Used in conjunction with the nuclear stain DAPI, it can be used to qualitatively assess the amount of cellular adhesion to surfaces as well as give information concerning the morphology of cells. Cell staining was applied after 24 hours and 7 days of cell growth upon sample substrates (See **Fig. 4.3.2a.**). DAPI counting was used to quantify the number of HUVECs present on the substrate surfaces. Results demonstrate that HA-LLDPE surfaces significantly reduced endothelial attachment by 52.1% compared to virgin LLDPE ($p \leq .05$) and 63.2% compared to PS ($p \leq .05$) after 7 days of cell growth. No significant differences were seen between PS and LLDPE groups

(See **Fig 4.2.3b.**) Actin/DAPI staining indicated that LLDPE surfaces resulted in agglomerates of HUVECS, likely due to the hydrophobicity of the polymer, an interaction commonly seen on surfaces with high contact angles ⁴⁶⁻⁵⁰. HUVECS on the surface of HA-LLDPE demonstrated cellular spreading and elongation of the cell body of the few cells that did attach, but proliferation and cell growth were greatly mitigated. Similar results have been noted by previous groups as the retention of water in hydrophilic materials greatly reduced the amount of proteins that can be adsorbed which facilitate cell adhesion ⁴⁶⁻⁴⁹. It should also be considered that these investigations were performed under static conditions, so the amount of cellular attachment will be at the upper limit as compared to what may be noted under flow conditions.

4.3.3 Porcine Aortic Valve Endothelial Adhesion to Different Surfaces

While HUVECs are the standard endothelial model used in most biomaterial endothelial investigations, there has been some question as to whether this model is the best to be used in most instances of endothelial research ³⁷. *In vivo* HUVECs are exposed to higher concentrations of oxygen which can affect cellular functioning. Thus, subsequent investigation of cellular adhesion sought to consider porcine valvular endothelial cells (VECs) upon substrate surfaces to address the more specific application of using HA-LLDPE for heart valve leaflet applications. Results utilizing VECs were found to be similar to those using HUVECs on substrate surfaces.

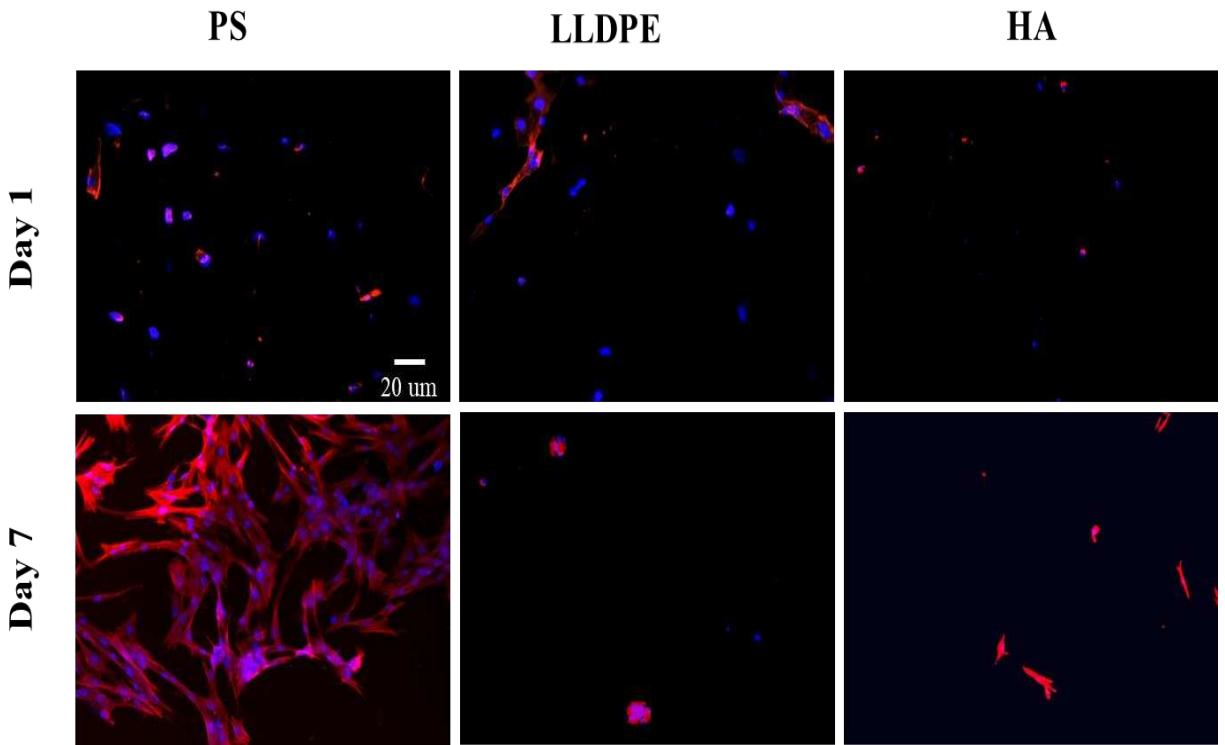


Figure 4.3.2a: Representative images of actin and DAPI staining demonstrating the amount of HUVEC attachment to surfaces after $t=24$ hrs and $t=7$ days. Results indicate less adhesion is displayed on HA surfaces as compared to PS and LLDPE. Images were taken at a magnification of 10x.

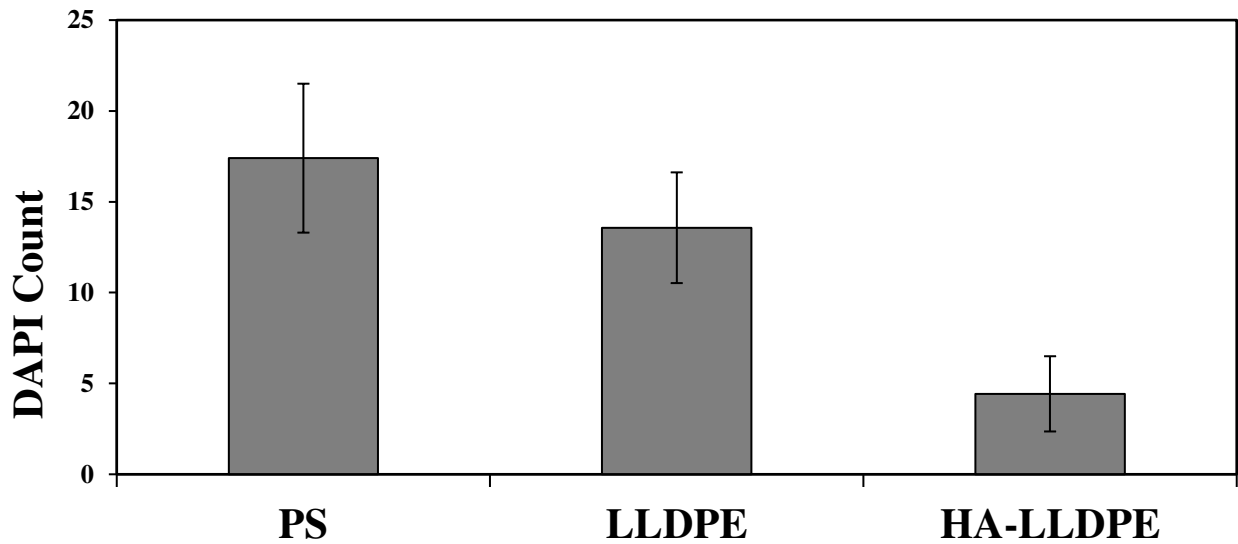


Figure 4.3.2b: Live cell DAPI staining indicates less adhesion displayed on HA surfaces at 7 days as compared to PS and LLDPE. This is likely due to the high hydrophilicity associated with hyaluronan as well as the high molecular weight utilized to fabricate HA-LLDPE materials (≈ 750 kDA). Experiments were replicated with at least three different cell populations on at least three different samples ($n_{\min} = 9$). A one-way ANOVA was performed. Average values and standard deviations are as follows: PS (av=17.4; st. dev=4.098); LLDPE (av=13.571; st.dev=3.04); HA-LLDPE (av=4.428; st. dev=2.070).

Qualitative assessments indicate that PS surfaces facilitated endothelial spreading and maturation noted by the spindle-like dendritic extensions projected from the cell bodies at 7 days of observation. Mono-layers of endothelium formed across the PS surface as observed in fluorescent imaging. By comparison, LLDPE promoted cell clustering across, and inhibited the formation of mono-layering across the surface as were seen in HUVEC investigations. Previous authors reporting on this phenomena note that this can be mitigated by pre-coating surfaces with adhesive proteins such as fibronectin⁵⁰⁻⁵³. HA-LLDPE followed previous trends noted in platelet adhesion studies limiting the amount of cellular adhesion to the surface. As previously discussed, this is most likely due to the enhanced hydrophilicity of the HA-LLDPE surface and the MW of the HA utilized. Further studies investigating cellular adhesion under flow conditions would offer more information on what may occur *in vivo* as flow and turbulence can result in cell shedding^{31,54,55}. Lastly, the culture of progenitor endothelial cells was attempted, but the process was found to be very time consuming. Progenitor endothelial cells can take up to four weeks to successfully mature enough to seed onto samples. Thus, while the isolation procedure was performed, investigations utilizing these cells were not performed due to time constraints and cost.

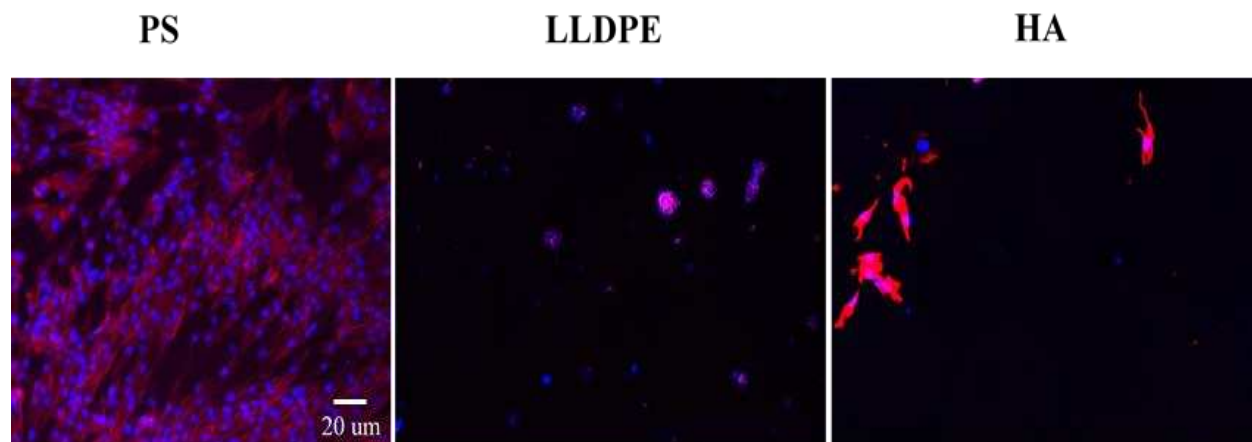


Figure 4.3.3. Representative images of porcine valvular endothelial cells cultured on PS, LLDPE, and HA-LLDPE at day 7. Findings demonstrate that while HA-LLDPE limits cellular adhesion it does not completely inhibit it under static conditions. Experiments were replicated with at least three different cell populations on at least three different samples ($n_{\min} = 9$).

4.3.4 SEM Results of HUVEC Adhesion to Different Surfaces

SEM imaging was employed to investigate the morphology of HUVECs on substrate surfaces after 24hrs and 7 days of cell growth. Analysis of cellular adhesion demonstrated that PS and LLDPE promoted greater cell density on substrate surfaces than HA-LLDPE as noted in previous studies (See **Fig. 4.3.4**). PS, used as a positive control, exhibited greater cell spreading on surfaces, with some flattening and dendritic extensions, especially at day 7. In agreement with the fluorescent data, LLDPE surfaces exhibited cell clustering and showed little to no spreading across the surfaces. However, LLDPE surfaces did support cellular growth and proliferation, giving support to previous evidence that LLDPE is non-toxic, and may be used as a good base material for biomaterial related modifications. HUVEC attachment was greatly mitigated on HA-LLDPE surfaces. After 7 days some flattening and cellular projections were identified. However, it is unknown whether this is due to cells attaching to portions of the material which exhibit less HA enhancement or if the cells are attaching to HA areas and are retaining the ability to spread to

some degree. Further investigation is required to determine the cause of this phenomena.

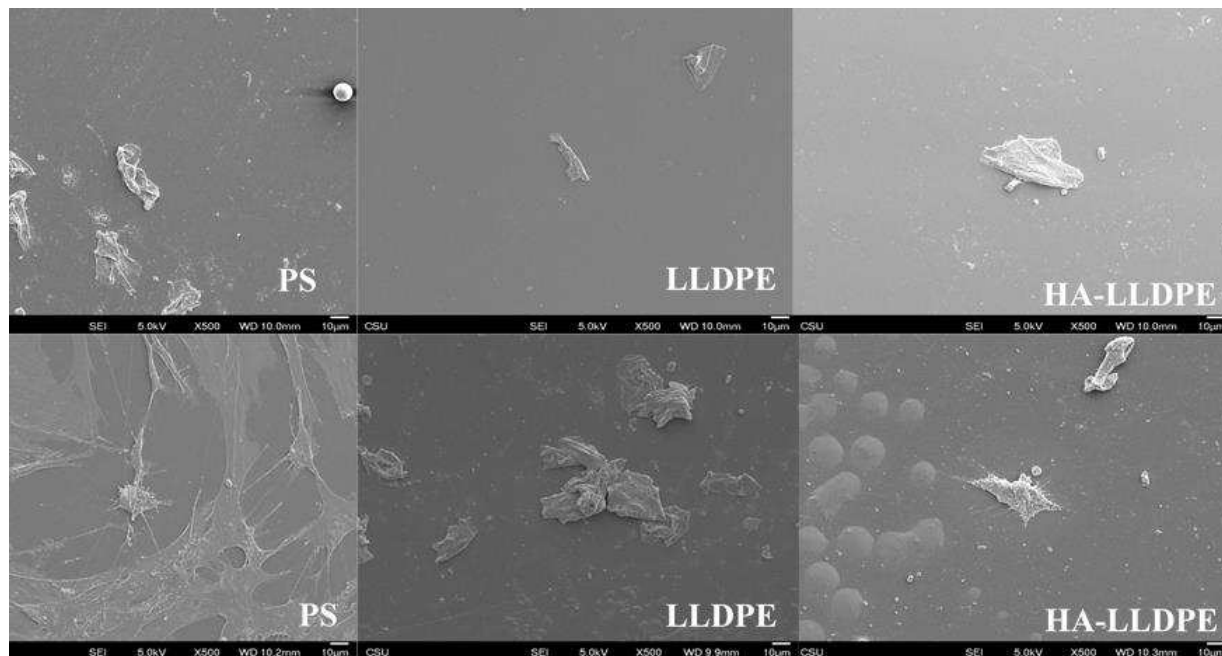


Figure 4.3.4: Representative SEM images of HUVEC attachment after 24hrs and 7 days of cell growth on substrate surfaces. Results support previous observations that HA-LLDPE surfaces mitigate cellular adhesion to surfaces under static conditions. Experiments were replicated with at least three different cell populations on at least three different samples ($n_{\min} = 9$).

4.3.5 Cell Viability Results on Different Surfaces

Cellular proliferation and metabolic activity are important indicators of cell viability. Non-viable cells attached to biomaterial surfaces can lead to unfavorable immune and inflammatory responses⁵⁶. To assist in determining the effects of investigative substrates on HUVECs, an alamarBlue assay was utilized. AlamarBlue quantifies cellular health by measuring the ability of cells to metabolize the non-toxic assay reagent resazurin to resorufin. The oxidation-reduction results in a colorimetric change and fluorescent by-product that can be quantified via spectrophotometry to determine the magnitude of cellular proliferation and resultant metabolic activity. Study outcomes indicate no significant differences between the PS and LLDPE groups,

however there was a marked reduction of resorufin in the HA-LLDPE group (See **Fig. 4.3.5**). PS is commonly used tissue culture substrate which supports cell viability. Therefore, it is evident that while LLDPE may modify the morphology of endothelial cells it does not seem to alter their viability. When considering these results in company with fluorescence and SEM imaging it is likely that the similar values for PS and LLDPE are due to comparable resultant cell densities on the substrate surfaces. Following this conclusion, it is likely that the reduction in resorufin in the HA-LLDPE group is due to a decrease in cellular adhesion to the substrate surfaces rather than an indication of substrate cytotoxicity resulting in cell death. Previous LDH assaying showed no signs that HA-LLDPE was toxic to blood cells or HUVECs³⁹. To confirm these results, cell counting on substrate surfaces was performed using a hemocytometer after gentle dissociation of cells from substrates immediately following alamarBlue assaying. Cell counting results noted an average reduction of 65% in cell attachment to the surface as compared to PS and a 68% reduction compared to LLDPE after 24 hours of cell expansion on substrate surfaces over three studies. After 7 days of cell expansion, an 82% reduction was noted on HA-LLDPE as compared to PS and a 74% reduction was noted as compared to LLDPE. All results were significant to ($p \leq .05$), data not shown. These results support previous findings of HUVEC DAPI counts which demonstrated that HA-LLDPE surfaces significantly limited cellular adhesion to the surfaces. Although there was a significant decrease in cellular adhesion, resazurin conversion was noted indicating that the cells which did attach to HA-LLDPE substrates were viable.

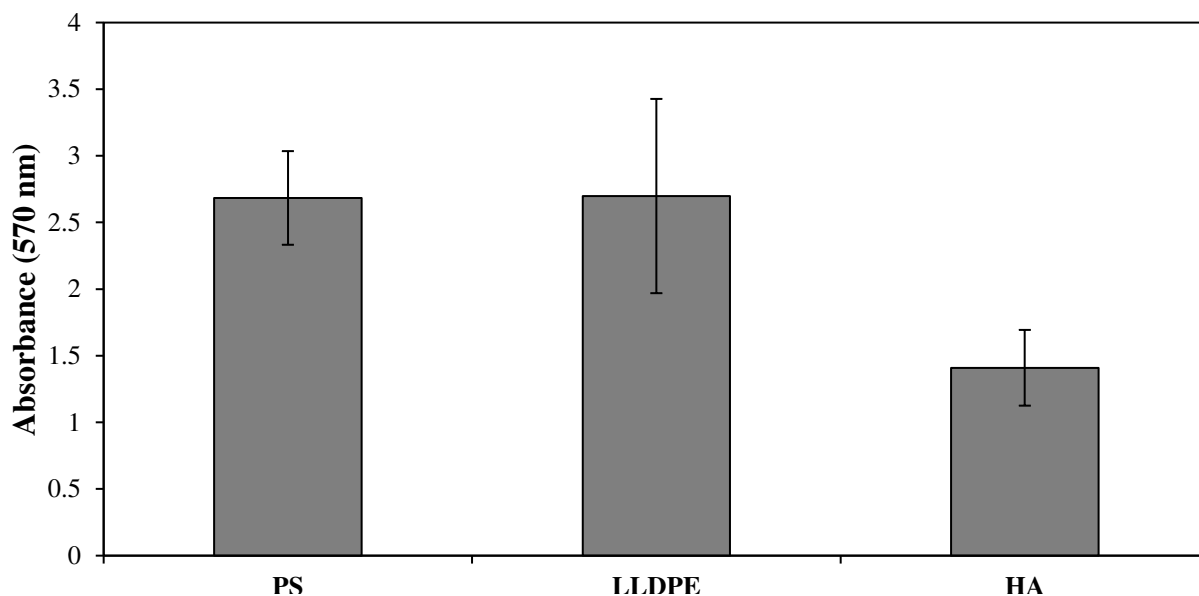


Figure 4.3.5: Representative alamarBlue results after 7 days of cell culture on sample substrate indicate HA-LLDPE surfaces resulted in less resorufin. This is likely due to less cellular adhesion on the surfaces on HA-LLDPE. Experiments were replicated with at least three different cell populations on at least five different samples ($n_{\min} = 15$). A one-way ANOVA was performed. Average values and standard deviations are as follows: PS(av=2.682; st.dev=.951); LLDPE(av=2.670;st.dev=.606); HA-LLDPE(av=2.215;st.dev=.128).

4.3.6 CD-31 Results on Different Surfaces

CD-31 also known as PECAM-1 is an important intercellular junction, vascular cell adhesion, and signaling molecule. It acts as an inhibitory receptor in platelets and leukocytes, plays roles in signal transduction, leukocyte trans-endothelial migration, endothelial cell vascular permeability, inflammation, and angiogenesis^{57,58}. In addition, CD31 is a pan-endothelial cell marker expressed in mature endothelium. CD-31 staining was used in this study to determine if cells which had adhered to the surface maintained the endothelial phenotype. Protein expression was not expected to be present after 24 hours of cell growth on substrates. Therefore after 24 hrs, only rhodamine and DAPI staining were performed to ensure cellular presence, with CD-31 and DAPI staining performed at 7 days only. At both time points, the proliferation of HUVECS was significantly higher on PS and LLDPE surfaces supporting previous fluorescent staining results

($p \leq .05$)^{13,15}. Day 1 images are not displayed here as they were comparable to the ones illustrated in **Fig. 4.3.2a**. After 24hrs HUVECs exhibited a rounded, cobblestone like morphology on PS surfaces. After 7 days, interconnected networks of cells formed monolayered sheets and exhibited the elongated spindle-like morphologies of mature HUVECs. CD31 expression was seen throughout, denoting mature, intracellular junctions. After 24hrs, LLDPE surfaces noted a rounded morphology and small, random clustering of HUVECs indicative of the effects hydrophobic surfaces⁵⁹. After 7 days, clustering was still apparent with CD31 expression observed, illustrating that the base material, LLDPE does not result in phenotypic change. As previously demonstrated in platelet studies, HUVECs exhibited a low level of attachment to HA-LLDPE surfaces. Again, CD31 expression was noted, leading to the conclusion that no phenotypic change of attached endothelial cells results even after 7 days of exposure to HA enhanced surfaces.

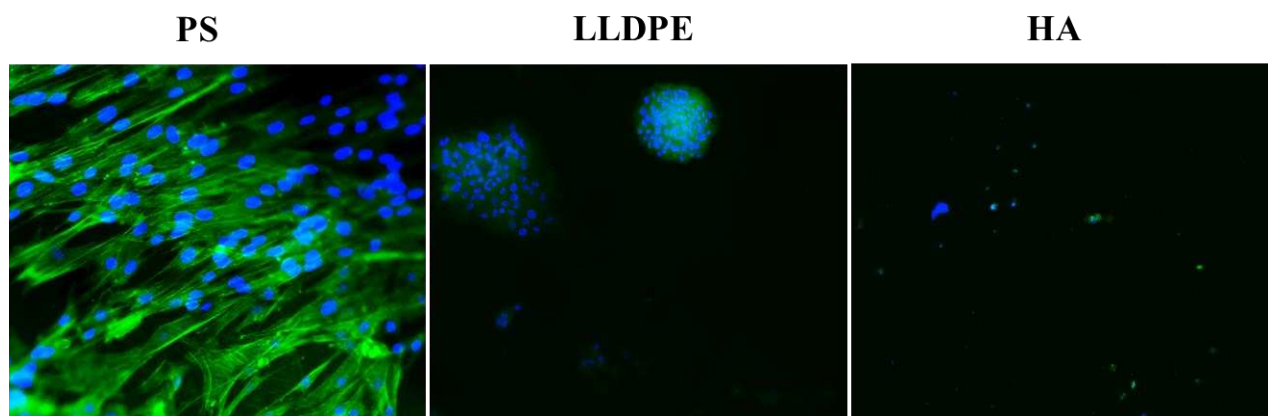


Figure 4.3.6: CD31 expression of HUVECs after 7 days of cell culture on PS, LLDPE, and HA-LLDPE. Results demonstrate that while LLDPE and HA enhanced surfaces modulate cell morphology, phenotype is preserved.

4.3.7 VEGF Results on Different Surfaces

VEGF is an important signaling protein and key regulator of normal vascular development. It is implicated in wound healing, hematopoiesis, and tissue remodeling at infarction sites, among other roles⁶⁰. It is especially important in angiogenesis, a requisite manifestation of vasculature

needed to shuttle blood to local regions^{61,62}. In addition, it assists in endothelial proliferation and migration, and plays roles in inflammation, and vascular permeability. In this study VEGF expression was examined to determine the ability of HUVECs to proliferate on substrate surfaces. Results indicate that both LLDPE and HA-LLDPE surfaces do not inhibit the expression of VEGF from HUVECs seeded onto substrates after 7 days. These results in conjunction with those of CD31 investigations indicate that neither LLDPE nor HA-LLDPE alter the fundamental functioning of HUVECs exposed to these material surfaces.

For biomaterials surfaces to endothelialize and offer an intrinsically non-thrombogenic surface, endothelial cells must remain in a mature, quiescent state³⁸. Phenotypic change and partial endothelialization can result in endothelial activation, unanticipated responses to blood constituents and hemodynamic forces, implant failure, and thrombosis^{38,63,64}. Ideally, a completely endothelialized biomaterial surface expressing a quiescent phenotype would be the most beneficial as a cardiovascular implant. In this instance, blood and its constituents would recognize the monolayers of cells as a native landscape resulting in optimal functionality. However, it may be possible to present a biomaterial surface that mitigates all cellular adhesion and yet is still compatible with the native environment. In these studies, it was revealed that HA-LLDPE limits the amount of cellular adhesion, but not completely under static conditions. In addition, HUVECs seem to maintain their phenotype and generally ability to function as endothelium. Thus, future work should first focus on performing studies which include flow conditions to ascertain whether endothelial cells will stay attached to HA-LLDPE under physiological shear stress. In addition, further exploration should also look more closely at why some endothelial attachment was observed on HA-LLDPE surfaces. It is possible that the fabrication process utilized to generate HA-LLDPE surfaces resulted in uneven distribution of HA across the surface, leaving some

regions absent HA. Although it is interesting to note that in general, cells which did attach to HA surfaces did exhibit some spread morphology rather than the condensed groupings and lack of extensions noted in the LLDPE groups. It is also reasonable to assume that these regions presented with a moderate hydrophilicity that supported attachment and spreading, however further investigation is required. Current development has sought to modify the fabrication process through vapor cross-linking to ensure a more even coverage of HA across the surface.

Due to the results which indicate that some endothelialization does occur on the HA-LLDPE surface it is possible to explore two paths (full endothelialization or total non-endothelialization). Full endothelialization may be possible by the manipulation of a few key factors. First, altering the molecular weight of HA used in the fabrication process may facilitate endothelialization. However, this also risks increasing the chances of blood protein and cell adhesion. However, if the surface was endothelialized prior to implantation and pre-treated under flow conditions to placate denuding, thrombosis due to platelet and macrophage adhesion may be mitigated. Another potential mechanism would be to investigate pre-treating HA-LLDPE surfaces with fibronectin before endothelial cell seeding onto samples as fibronectin has been shown to promote endothelialization and play a key role in regulating this event *in vivo*⁶⁵⁻⁶⁷. Total mitigation of cells on the surface may potentially be achieved by increasing the MW of the HA used during the cross-linking process. It must be kept in mind that these are the first studies to investigate endothelialization of these materials so future investigation on its improvement based on needs is imperative.

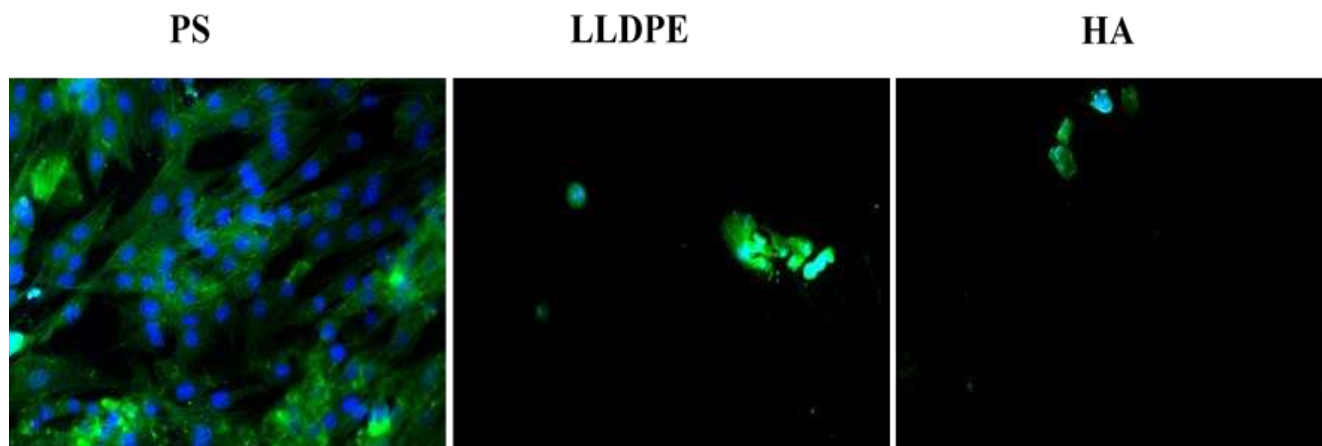


Figure 4.3.7: VEGF expression after 7 days of cell growth on substrates demonstrates that HUVECS cultured on HA-LLDPE maintains its phenotype and ability to proliferate.

4.3.8 Conclusions

In this study we sought to ascertain the ability of HA-LLDPE to mitigate HUVEC attachment to the surface and to determine if any phenotypic change was noted due to biomaterial exposure. Results demonstrated that similar to platelet adhesion studies, HA-LLDPE does limit cellular attachment. Changes in normal HUVEC morphology were also noted, however CD31 and VEGF investigations demonstrated that no phenotypic change was induced after 7 days of exposure to HA-LLDPE surfaces. As these are the first examinations of endothelial reaction to HA-LLDPE surfaces, future work will be needed to more closely examine why some cellular attachment was seen on HA-LLDPE surfaces. In addition, it will need to be determined whether full endothelialization or complete non-endothelialization is preferred. Mimicking the anti-coagulant properties of native vasculature is a key consideration in creating a non-thrombotic surface. Endothelialization of biomaterials is beneficial especially for long term implantation. Because HA is biocompatible and has shown to reduce blood protein and cell adhesion, it is hypothesized that even without an endothelialized surface it can offer the bio-modulating effects

required to reduce thrombosis and adverse inflammation. While these results may not be clinically relevant they do give insight into how HA-LLDPE interacts with endothelial cells.

REFERENCES:

1. Laurent TC, Fraser JR. Hyaluronan. *FASEB J.* 1992;6(7):2397-2404. doi:10.1016/S0140-6736(01)35637-4
2. Fraser JR, Laurent TC, Laurent UB. Hyaluronan: its nature, distribution, functions and turnover. *J Intern Med.* 1997;242:27-33. doi:10.1046/j.1365-2796.1997.00170.x
3. Allison DD, Grande-Allen KJ. Review. Hyaluronan: A Powerful Tissue Engineering Tool. *Tissue Eng.* 2006;0(0):060913044658042. doi:10.1089/ten.2006.12.ft-153
4. Hemshekhar M, Thushara RM, Chandranayaka S, Sherman LS, Kemparaju K, Girish KS. Emerging roles of hyaluronic acid bioscaffolds in tissue engineering and regenerative medicine. *Int J Biol Macromol.* 2016. doi:10.1016/j.ijbiomac.2016.02.032
5. Girish KS, Kemparaju K. The magic glue hyaluronan and its eraser hyaluronidase: A biological overview. *Life Sci.* 2007;80(21):1921-1943. doi:10.1016/j.lfs.2007.02.037
6. Laurent TC, Laurent UB, Fraser JR. The structure and function of hyaluronan: An overview. *Immunol Cell Biol.* 1996;74(2):A1-A7. doi:10.1038/icb.1996.32
7. Laurent TC, Fraser JR. Hyaluronan. *FASEB J.* 1992;6(7):2397-2404. doi:10.1016/S0740-8315(82)80016-8
8. Fronza M, Caetano GF, Leite MN, et al. Hyaluronidase modulates inflammatory response and accelerates the cutaneous wound healing. *PLoS One.* 2014;9(11). doi:10.1371/journal.pone.0112297
9. Albeiroti S, Ayasoufi K, Hill DR, Shen B, De La Motte CA. Platelet hyaluronidase-2: An enzyme that translocates to the surface upon activation to function in extracellular matrix degradation. *Blood.* 2015;125(9):1460-1469. doi:10.1182/blood-2014-07-590513

10. Amarnath LP, Srinivas A, Ramamurthi A. In vitro hemocompatibility testing of UV-modified hyaluronan hydrogels. *Biomaterials*. 2006;27(8):1416-1424. doi:10.1016/j.biomaterials.2005.08.008
11. Ruiz A, Flanagan CE, Masters KS. Differential support of cell adhesion and growth by copolymers of polyurethane with hyaluronic acid. *J Biomed Mater Res - Part A*. 2013;101(10):2870-2882. doi:10.1002/jbm.a.34597
12. Chuang TW, Masters KS. Regulation of polyurethane hemocompatibility and endothelialization by tethered hyaluronic acid oligosaccharides. *Biomaterials*. 2009;30(29):5341-5351. doi:10.1016/j.biomaterials.2009.06.029
13. Simon-Walker R, Cavicchia J, Prawel DA, Dasi LP, James SP, Popat KC. Hemocompatibility of hyaluronan enhanced linear low density polyethylene for blood contacting applications. *J Biomed Mater Res Part B Appl Biomater*. September 2017. doi:10.1002/jbm.b.34010
14. Li L, Wang N, Jin X, et al. Biodegradable and injectable in situ cross-linking chitosan-hyaluronic acid based hydrogels for postoperative adhesion prevention. *Biomaterials*. 2014;35(12):3903-3917. doi:10.1016/j.biomaterials.2014.01.050
15. Prawel DA, Dean H, Forleo M, et al. Hemocompatibility and Hemodynamics of Novel Hyaluronan-Polyethylene Materials for Flexible Heart Valve Leaflets. *Cardiovasc Eng Technol*. 2014;5(1):70-81. doi:10.1007/s13239-013-0171-5
16. Mani A, Pawar B, Pendyala G, Mustilwar R, Bhosale A, Bhadange S. Hyaluronic acid - A boon to periodontal therapy. *Pravara Med Rev*. 2016. doi:10.4103/1947-2714.112473
17. Wu X, Zhao Y, Tang C, et al. Re-Endothelialization Study on Endovascular Stents Seeded by Endothelial Cells through Up- or Downregulation of VEGF. *ACS Appl Mater Interfaces*. 2016.

doi:10.1021/acsami.6b00152

18. Liu T, Liu S, Zhang K, Chen J, Huang N. Endothelialization of implanted cardiovascular biomaterial surfaces: The development from in vitro to in vivo. *J Biomed Mater Res - Part A*. 2014. doi:10.1002/jbm.a.35025
19. Choi WS, Joung YK, Lee Y, et al. Enhanced Patency and Endothelialization of Small-Caliber Vascular Grafts Fabricated by Coimmobilization of Heparin and Cell-Adhesive Peptides. *ACS Appl Mater Interfaces*. 2016. doi:10.1021/acsami.5b12052
20. Zhang K, Chen J ying, Qin W, Li J an, Guan F xia, Huang N. Constructing bio-layer of heparin and type IV collagen on titanium surface for improving its endothelialization and blood compatibility. *J Mater Sci Mater Med*. 2016;27(4). doi:10.1007/s10856-016-5693-6
21. Bae IH, Jeong MH, Kim JH, et al. The control of drug release and vascular endothelialization after hyaluronic acid-coated paclitaxel multi-layer coating stent implantation in porcine coronary restenosis model. *Korean Circ J*. 2017. doi:10.4070/kcj.2016.0203
22. Yau JW, Teoh H, Verma S. Endothelial cell control of thrombosis. *BMC Cardiovasc Disord*. 2015. doi:10.1186/s12872-015-0124-z
23. Aird WC. Phenotypic heterogeneity of the endothelium: I. Structure, function, and mechanisms. *Circ Res*. 2007. doi:10.1161/01.RES.0000255691.76142.4a
24. Vlahakes GJ. Mechanical heart valves: The test of time... *Circulation*. 2007;116(16):1759-1760. doi:10.1161/CIRCULATIONAHA.107.729582
25. Hopkins RA. Tissue engineering of heart valves: Decellularized valve scaffolds. *Circulation*. 2005;111(21):2712-2714. doi:10.1161/CIRCULATIONAHA.104.527820
26. Schoen FJ, Levy RJ. Calcification of tissue heart valve substitutes: Progress toward understanding and prevention. *Ann Thorac Surg*. 2005;79(3):1072-1080.

doi:10.1016/j.athoracsur.2004.06.033

27. Bengtsson LA, Haegerstrand AN. Endothelialization of mechanical heart valves in vitro with cultured adult human cells. *J Heart Valve Dis.* 1993.
28. Jansson K, Bengtsson L, Swedenborg J, Haegerstrand A. In vitro endothelialization of bioprosthetic heart valves provides a cell monolayer with proliferative capacities and resistance to pulsatile flow. *J Thorac Cardiovasc Surg.* 2001. doi:10.1067/mtc.2001.110251
29. Kluin J, Talacua H, Smits AIPM, et al. In situ heart valve tissue engineering using a bioresorbable elastomeric implant – From material design to 12 months follow-up in sheep. *Biomaterials.* 2017. doi:10.1016/j.biomaterials.2017.02.007
30. Heath DE. Promoting Endothelialization of Polymeric Cardiovascular Biomaterials. *Macromol Chem Phys.* 2017;218(8). doi:10.1002/macp.201600574
31. Siedlecki CA. *Hemocompatibility of Biomaterials for Clinical Applications: Blood-Biomaterials Interactions.*; 2017.
32. Wang Z, Gao T, Cui L, Wang Y, Zhang P, Chen X. Improved cellular infiltration into 3D interconnected microchannel scaffolds formed by using melt-spun sacrificial microfibers. *RSC Adv.* 2016. doi:10.1039/c5ra25142g
33. Kim JJ, Hou L, Huang NF. Vascularization of three-dimensional engineered tissues for regenerative medicine applications. *Acta Biomater.* 2016. doi:10.1016/j.actbio.2016.06.001
34. Chiu LLY, Radisic M, Vunjak-Novakovic G. Bioactive Scaffolds for Engineering Vascularized Cardiac Tissues. *Macromol Biosci.* 2010. doi:10.1002/mabi.201000202
35. West J, Moon J. Vascularization of Engineered Tissues: Approaches to Promote Angiogenesis in Biomaterials. *Curr Top Med Chem.* 2008. doi:10.2174/156802608783790983
36. Jaganathan SK, Supriyanto E, Murugesan S, Balaji A, Asokan MK. Biomaterials in

cardiovascular research: Applications and clinical implications. *Biomed Res Int.* 2014;2014. doi:10.1155/2014/459465

37. Hauser S, Jung F, Pietzsch J. Human Endothelial Cell Models in Biomaterial Research. *Trends Biotechnol.* 2017. doi:10.1016/j.tibtech.2016.09.007

38. Khan OF, Sefton M V. Endothelialized biomaterials for tissue engineering applications in vivo. *Trends Biotechnol.* 2011. doi:10.1016/j.tibtech.2011.03.004

39. Simon-Walker R, Cavicchia J, Prawel DA, Dasi LP, James SP, Popat KC. Hemocompatibility of hyaluronan enhanced linear low density polyethylene for blood contacting applications. *J Biomed Mater Res - Part B Appl Biomater.* 2018;106(5). doi:10.1002/jbm.b.34010

40. Zhang J, Wang Y, Liu C, et al. Polyurethane/polyurethane nanoparticle-modified expanded poly(tetrafluoroethylene) vascular patches promote endothelialization. *J Biomed Mater Res - Part A.* 2018. doi:10.1002/jbm.a.36419

41. Ec L, Nad L. Lactate dehydrogenase Biochemistry and function of lactate dehydrogenase. *Biochemistry.* 1984. doi:10.1002/cbf.290020302

42. Chan FKM, Moriwaki K, De Rosa MJ. Detection of necrosis by release of lactate dehydrogenase activity. *Methods Mol Biol.* 2013;979:65-70. doi:10.1007/978-1-62703-290-2_7

43. Howell BF, McCune S, Schaffer R. Lactate-to-pyruvate or pyruvate-to-lactate assay for lactate dehydrogenase: A re-examination. *Clin Chem.* 1979;25(2):269-272. doi:10.1093/jac/dkr570

44. Azuma M, Shi M, Danenberg KD, et al. Serum lactate dehydrogenase levels and glycolysis significantly correlate with tumor VEGFA and VEGFR expression in metastatic CRC patients. *Pharmacogenomics.* 2007. doi:10.2217/14622416.8.12.1705

45. Taha M, E Silva FA, Quental M V., Ventura SPM, Freire MG, Coutinho JAP. Good's

buffers as a basis for developing self-buffering and biocompatible ionic liquids for biological research. *Green Chem.* 2014. doi:10.1039/c4gc00328d

46. Jaganjac M, Milković L, Cipak A, et al. Cell Adhesion On Hydrophobic Polymer Surfaces. *Mater Tehnol.* 2012.

47. Lee J, Khang G, Lee J, Lee H. Interaction of Different Types of Cells on Polymer Surfaces with Wettability Gradient. *J Colloid Interface Sci.* 1998;205(2):323-330. doi:10.1006/jcis.1998.5688

48. van Wachem PB, Beugeling T, Feijen J, Bantjes A, Detmers JP, van Aken WG. Interaction of cultured human endothelial cells with polymeric surfaces of different wettabilities. *Biomaterials.* 1985. doi:10.1016/0142-9612(85)90101-2

49. Tzoneva R, Faucheux N, Groth T. Wettability of substrata controls cell-substrate and cell-cell adhesions. *Biochim Biophys Acta - Gen Subj.* 2007. doi:10.1016/j.bbagen.2007.07.008

50. Campillo-Fernández AJ, Unger RE, Peters K, et al. Analysis of the Biological Response of Endothelial and Fibroblast Cells Cultured on Synthetic Scaffolds with Various Hydrophilic/Hydrophobic Ratios: Influence of Fibronectin Adsorption and Conformation. *Tissue Eng Part A.* 2009. doi:10.1089/ten.tea.2008.0146

51. Kaehler J, Zilla P, Fasol R, Deutsch M, Kadletz M. Precoating substrate and surface configuration determine adherence and spreading of seeded endothelial cells on polytetrafluoroethylene grafts. *J Vasc Surg.* 1989. doi:10.1016/0741-5214(89)90469-2

52. Anderson JS, Price TM, Hanson SR, Harker LA. In vitro endothelialization of small-caliber vascular grafts. *Surgery.* 1987. doi:0039-6060(87)90300-X [pii]

53. Vinard E, Lesèche G, Andreassian B, Costagliola D. In vitro endothelialization of PTFE vascular grafts: A comparison of various substrates, cell densities, and incubation times. *Ann Vasc*

Surg. 1999. doi:10.1007/s100169900232

54. Wang X, Cooper S. Adhesion of Endothelial Cells and Endothelial Progenitor Cells on Peptide-Linked Polymers in Shear Flow. *Tissue Eng Part A.* 2013. doi:10.1089/ten.tea.2011.0653

55. Dickinson RB, Cooper SL. Analysis of shear-dependent bacterial adhesion kinetics to biomaterial surfaces. *AIChE J.* 1995. doi:10.1002/aic.690410915

56. Rock KL, Lai J-J, Kono H. Innate and adaptive immune responses to cell death. *Immunol Rev.* 2011. doi:10.1111/j.1600-065X.2011.01040.x

57. Albelda SM, Muller WA, Buck CA, Newman PJ. Molecular and cellular properties of PECAM-1 (endoCAM/CD31): A novel vascular cell-cell adhesion molecule. *J Cell Biol.* 1991. doi:10.1083/jcb.114.5.1059

58. DeLisser HM, Christofidou-Solomidou M, Strieter RM, et al. Involvement of endothelial PECAM-1/CD31 in angiogenesis. *Am J Pathol.* 1997.

59. Shi B, Andrukhov O, Berner S, Schedle A, Rausch-Fan X. The angiogenic behaviors of human umbilical vein endothelial cells (HUVEC) in co-culture with osteoblast-like cells (MG-63) on different titanium surfaces. *Dent Mater.* 2014. doi:10.1016/j.dental.2014.05.005

60. Duffy AM, Bouchier-Hayes DJ, Harmey JH. Vascular Endothelial Growth Factor (VEGF) and Its Role in Non-Endothelial Cells: Autocrine Signalling by VEGF. In: *VEGF and Cancer.* ; 2004. doi:10.1007/978-1-4419-9148-5_13

61. Coultas L, Chawengsaksophak K, Rossant J. Endothelial cells and VEGF in vascular development. *Nature.* 2005. doi:10.1038/nature04479

62. Ferrara N. Vascular endothelial growth factor. *Arterioscler Thromb Vasc Biol.* 2009. doi:10.1161/ATVBAHA.108.179663

63. Ando J, Yamamoto K. Vascular Mechanobiology. *Circ J.* 2009. doi:10.1253/circj.CJ-09-

64. Li YSJ, Haga JH, Chien S. Molecular basis of the effects of shear stress on vascular endothelial cells. *J Biomech.* 2005. doi:10.1016/j.jbiomech.2004.09.030
65. Montaña V, Chevallier P, Mantovani D, Pauthe E. The effect of fibronectin/phosphorylcholine coatings on PTFE substrates on endothelial cells adhesion and hemocompatibility properties. *Eur Cells Mater.* 2013. doi:10.4161/21592535.2014.979679
66. Wang X, Liu T, Chen Y, et al. Extracellular matrix inspired surface functionalization with heparin, fibronectin and VEGF provides an anticoagulant and endothelialization supporting microenvironment. *Appl Surf Sci.* 2014. doi:10.1016/j.apsusc.2014.09.004
67. Li G, Yang P, Qin W, Maitz MF, Zhou S, Huang N. The effect of coimmobilizing heparin and fibronectin on titanium on hemocompatibility and endothelialization. *Biomaterials.* 2011. doi:10.1016/j.biomaterials.2011.03.025

CHAPTER 5

CONCLUSIONS AND FUTURE WORK

5.1. Conclusions

Heart valve replacement therapy has successfully helped to improve the quality of life and increase longevity of those suffering from valvular diseases compared to untreated conditions. Yet, they still suffer from draw-backs that can lead to serious health complications such as thrombosis, which can lead to stroke and death. It is vital for heart valve replacement technology to create a valve that will function as well, if not better, than native heart valves to limit complications and to ensure that patients can fully benefit from the advancements made. To this end, much research has been employed in the field of biomaterials to develop constructs which are hemocompatible, highly durable, and promote endothelialization. Polymer based heart valve leaflets may offer the answer needed to create exceptional heart-valves. Polymers present the ability to proffer a flexible leaflet design, extraordinary durability, and the capacity to be modified through various techniques to enhance compatibility with the physiology. Polymer technology combined with biological modifications such as hyaluronan enhancements have led to promising results in cardiovascular biomaterial technology and in heart valve development to maximize hemocompatibility. This work sought to ascertain the ability of a hyaluronan enhanced polymer, HA-LLDPE to mitigate pro-coagulant and immune responses and negate endothelial attachment to HA-LLDPE surfaces.

In this work, it was demonstrated that HA-LLDPE does an exceptional job of presenting a surface that is both minimally thrombotic and allays the immune response. HA-LLDPE reduces key blood protein and cell adhesion at the surface and was found to be nominally activating to platelets

compared to virgin LLDPE and pro-coagulant PS. Endothelialization studies noted some endothelialization to the surface of HA-LLDPE, which is a cause for concern as partial endothelialization of biomaterial surfaces can trigger adverse coagulant and immune responses. However, it should be noted that all studies were performed in a static environment. Flow conditions could drastically change the effects seen in these studies, especially for the development of heart valve leaflet applications. De-nuding of endothelial cells seeded onto biomaterial constructs is common under flow conditions. Due to this endothelialized biomaterials are normally pre-conditioned in a bio-reactor to ensure that endothelial cells can maintain adhesion to surfaces after implantation and achieve uniform endothelialization¹⁻⁵ pre-implantation.

5.2 Future Work

The foundational studies explored in this thesis sought to determine the feasibility for HA-LLDPE to be used as a material for heart valve leaflet applications. Future aims should first seek to determine if platelet, leukocyte, and endothelial adhesion would be found under flow conditions as hemocompatibility ultimately should be assessed for the individual application. In this instance a high velocity, high pressure flow environment will ultimately be needed. Various designs of physiological flow loops for testing exist and can offer more detailed information on what to expect *in vivo* due to the material only⁶⁻⁹ It should be noted that thrombosis due to flow profiles within the valve are dependent on design, placement, and regional flow characteristics which can be more readily assessed once the design of the valve and its fabrication are completed. Completion of the valve design can also help to assess how mechanical properties such as bending stiffness may affect blood-interface phenomena.

Secondly, endothelial studies noted that endothelialization of materials may be possible. Thus, it should be determined if pursuing potential endothelialization would be beneficial given the increased complexity, and cost. If full endothelialization of HA-LLDPE is possible and creates a surface whose hemocompatibility supersedes that of the regular HA-LLDPE material it would be a worth-while endeavor if it maintained cost effectiveness. Approaches to this could entail basic hemocompatibility (Ex. whole blood clotting, platelet and leukocyte adhesion/activation, contact activation assays) and endothelial assessments (seeding of endothelial cells to surfaces) after fabrication of HA-LLDPE materials with varying MW. If a MW HA-LLDPE film was found to present with both good hemocompatibility and endothelialization characteristics, bio-reactor conditioning and testing could follow. Consequently, if a particular MW of HA was found to completely limit endothelialization, future studies in a flow environment could proceed.

Lastly, while it was not explicitly discussed in this thesis, polymer valves have shown some proclivity to calcification as is found in the native valves and tissue valves¹⁰⁻¹⁴. Regions of the valves such as leaflets and commissures of the polymer valves are prone to calcification often associated with microthrombi at the surface¹⁵. Because HA-LLDPE has a polymer base it would be important for future investigations to assess the proclivity of HA-LLDPE towards calcification. Studies investigating the role of hyaluronan in calcification have noted a localization of hyaluronan around calcium nodules and a heterogenous distribution in calcified aortic valves^{16,17}. While the exact mechanism of what role HA may play in calcification is unknown it is critical to investigate whether the presence of HA could affect calcification of HA-LLDPE films especially under physiological flow conditions as calcification of polymer valves is thought to be dependent upon flow dynamics within the valve¹¹. Flow loops with calcium mixes have been developed to assess this phenomenon¹⁸. While this thesis work provided the foundational investigations to determine

the feasibility of the novel material HA-LLDPE for heart valve leaflet applications, future research should seek to determine hemocompatibility in physiologically simulated environments.

It has been ascertained that under static conditions coagulation and immune responses were mitigated. The logical next step would be to ascertain these responses under physiological flow like conditions to determine platelet, leukocyte, and endothelial adhesion. It will also be beneficial to determine if future work on HA-LLDPE fabrication could modulate endothelial cell adhesion on surfaces through the modification of MW. Lower HA MW are known to help in maintaining normal morphology of endothelial cells and promote adhesion and proliferation but may instigate immune reactions. It will be essential to determine if there an ideal MW that can offer both the benefits of promoting endothelial adhesion and proliferation but still limit adverse immune responses. Mimicking the anti-coagulant properties of native vasculature is a key consideration in creating a non-thrombotic surface and warrants future consideration, although it should be kept in mind that this route is more complex, and expensive than creating a surface that is hemocompatible and can completely limit endothelial adhesion to the surface. If an ideal molecular weight to promote endothelialization cannot be determined, is there an ideal MW that can completely negate all endothelial and blood cell attachment to the surface to completely mitigate the potential for adverse coagulant and immune responses? Endothelialization of biomaterials is beneficial especially for long term implantation. Because HA is biocompatible and has shown to reduce blood protein and cell adhesion, it is hypothesized that even without an endothelialized surface it can offer the bio-modulating effects required to reduce thrombosis and adverse inflammation.

Due to the results which indicate that some endothelialization does occur on the HA-LLDPE surface it is possible to explore two paths (full endothelialization or total non-endothelialization). Full endothelialization may be possible by the manipulation of a few key

factors. First, altering the molecular weight of HA used in the fabrication process may facilitate endothelialization. However, this also risks increasing the chances of blood protein and cell adhesion. However, if the surface was endothelialized prior to implantation and pre-treated under flow conditions to placate denuding, thrombosis due to platelet and macrophage adhesion may be mitigated. Another potential mechanism would be to investigate pre-treating HA-LLDPE surfaces with fibronectin before endothelial cell seeding onto samples as fibronectin has been shown to promote endothelialization and play a key role in regulating this event *in vivo*¹⁹⁻²¹. Total mitigation of cells on the surface may potentially be achieved by increasing the MW of the HA used during the cross-linking process. It must be kept in mind that these are the first studies to investigate endothelialization of these materials so future investigation on its improvement based on needs is imperative.

APPENDIX

EFFECT OF HYALURONAN ENHANCEMENTS OF LINEAR LOW-DENSITY POLYEHTYLENE ON PLATELET ADHESION AND ACTIVATION

Introduction

Hyaluronan (HA) is an ubiquitously produced glycosaminoglycan implicated in a wide range of cell functions¹⁻⁵. It exhibits superior anticoagulation properties leading to a prevailing interest in its use in cardiovascular biomaterial and tissue engineering applications⁶⁻¹⁴. Examples of HA enhanced biomaterials developed for use in cardiovascular medical devices include HA modified hydrogels for vascular tissue engineering applications⁶, immobilized HA on metallic surfaces¹³ HA-polydopamine conjugates on stainless steel substrates for use in vascular stents¹¹, HA micro-patterning on titanium substrates¹⁵, and cross-linked HA-LLDPE for use in flexible material cardiovascular applications such as prosthetic heart valve leaflets^{9,16}. HA enhanced biomaterial substrates have consistently demonstrated non-activating and non-adhesive interactions with blood proteins and platelets. These properties are essential in mitigating thrombotic events that can lead to embolism of heart valves and catheters, occlusion of stents, stroke, death, and bleeding risks associated with anticoagulant therapy¹⁷⁻¹⁹. Apart from its anticoagulant properties, HA is bacteriostatic, non-immunogenic, and non-toxic making it a superlative choice for use in modifying biomaterials⁶⁻⁸. In addition, previous research has demonstrated that HA can promote endothelial and smooth muscle cell adhesion, reduce calcification in bioprosthetic heart valves, regulate cell substrate receptors, increase the synthesis of collagen and elastin, and facilitate extracellular matrix remodeling; thereby increasing its

potential for use in multi-functional applications ^{2,7,20}. HA has the potential to be integrated with various materials to fine tune and enhance its mechanical properties, improve material patency, reduce degradation of macromolecules, and produce varying pore sizes that can be used to regulate cell and protein adhesion, as well as biomolecule transport ^{20,21}. Thus, continued investigation provides crucial insight into the means and methods by which HA enhancement can be applied.

The majority of investigative work into the physiological effects of HA enhanced biomaterials has focused on the modulation of substrate interactions through diverse immobilization techniques and varying HA molecular weight (MW) through chain length alteration. While some of anticoagulant properties of HA remain intact regardless of MW, low MW HA (below 200 kDa) can facilitate the adhesion and proliferation of endothelial cells and smooth muscles cells which have the potential to increase biocompatibility and hemocompatibility ^{7,8,22}. However, the MWs which promote endothelialization and angiogenesis are in contradiction to those which most effectively reduce platelet adhesion thereby leaving a gap in its applicability to support short and long term hemocompatibility if endothelialization is desired. Only a limited number of studies look at the effects of varying HA concentration on biomolecular regulation and blood cell adhesion at the HA-blood interface ^{9,10}. A prior study examining the effects of varying concentrations of 750 kDa HA-LLDPE on mechanical properties, platelet adhesion profile, and clotting resistance demonstrated that HA increased clotting resistance relative to plain LLDPE, but the effect appeared to be dependent upon the concentration of HA and whether an additional layer of HA was attached to the substrate ⁹. Furthermore, this study demonstrated that platelet adhesion decreased on the HA-LLDPE relative to plain LLDPE but did not study the effect of HA concentration in the HA-LLDPE, nor the effect of an additional layer of HA on the substrate [9]. Few studies to date have sought to thoroughly examine the effects of varying substrate HA

concentrations on biomaterial-blood compatibility. Due to the previous success of HA biomaterials on reducing blood protein adhesion, activation, and aggregation, increasing the breadth of knowledge of its applications is critical to producing successful materials for cardiovascular biomaterial implementation. In this study, we build on previous hemocompatibility investigations of HA-LLDPE^{9,16} by exploring the effects of LLDPE modified with varying concentrations of HA and differing HA concentrations combined with spin-coated HA.

The fabrication process of HA-modified LLDPE substrates has been previously described⁹. Prior work examined the effects of LLDPE enhanced with a 2% solution concentration of HA. These investigations concluded that it dramatically reduced blood protein and platelet adhesion and activation, contact activation, whole blood clotting, thrombin-anti thrombin response, and was found to be non-toxic to platelets¹⁶. In the current manuscript, we have investigated the effects of LLDPE enhanced with 2%, 2.5%, and 3% solution concentrations of HA (2% HA, 2.5% HA, and 3% HA); and these treatments combined with an additional HA spin coating (2% HA Spin, 2.5% HA Spin, and 3% HA Spin) on cytocompatibility, platelet adhesion, and activation. The goal of this study was to investigate the effects of differing HA concentrations with and without the addition of HA spin-coating to ascertain if this would provide additional benefits in enhancing anti-coagulant properties.

Materials and Methods

Fabrication of HA-LLDPE Substrates

LLDPE films were swollen for 60 mins in 2%, 2.5%, or 3% w/v of silylated hyaluronan cetyltrimethylammonium (SHACTA; 750 kDa HA) in a xylenes solution at 50°C contained in a dry N₂ filled glove-bag²³. Films were then dried for approximately 2-3 hrs in a vacuum oven at

50°C until no weight change was observed. Using a WS-650Mz-23NPPB spin coater (Laurell Technologies, North Wales, PA), a portion of the films were given an additional spin coat of their respective treatment solutions on each side with 2 ml of each solution dispensed at 400 rpm for 15 secs followed by a 1000 rpm step for 30 secs. SHACTA-impregnated LLDPE films (SHACTA-LLDPE) were then crosslinked in 2% v/v p(HMDI) xylenes solution for 60 mins at 50°C in a dry N₂ filled glove-bag. The crosslinked SHACTA-LLDPE (xSHACTA-LLDPE) was subsequently cured in a vacuum oven for 15 hrs at 50°C. Excess p(HMDI) was removed by soaking and agitating films in acetone for 1 min and subsequently drying in a vacuum oven for 5-10 mins at 50°C until no visible traces of acetone remained. A final step of hydrolysis to get rid of the trimethylsilyl and CTA groups was performed as described elsewhere⁹.

Characterization of HA-LLDPE Substrates

After drying in a vacuum oven overnight at 50°C, HA-LLDPE substrates were characterized using a Nicolet iS-50 FT-IR spectrometer with KBR beam splitter and diamond ATR crystal accessory at 4 cm⁻¹ resolution and 64 scans per spectrum from 400 to 4000 cm⁻¹. Spectra were processed with 2nd order polynomial baseline correction with correction for the linear offset using OMNIC software and normalized for the LLDPE hydrocarbon peak height at 2918 cm⁻¹. Peak areas of identically baseline corrected and normalized spectra can show relative quantitative differences of cross-linked HA in HA-LLDPE near the substrate due to the Beer-Lambert law. Peak areas were measured with Spectragryph software (F. Menges "Spectragryph-optical spectroscopy software", Version 1.2.7, 2017, <http://www.ffmpeg2.de/spectragryph>) between 3798.84 to 3096.92 corresponding to amide/hydroxyl peaks.

For contact angle measurements, HA-LLDPE substrates were hydrated in DI water overnight before being analyzed. The substrates were placed on a stage of a Rame-Hart Contact Angle goniometer. The dispensing needle was placed just above the substrate, and an initial drop was dispensed. For advancing angles, the volume of the drop was gradually increased; the tangent contact angle was measured as the contact line advanced outward, until a maximum angle stabilized as seen through plateauing of the angle value using DropImage Advanced software. The water was subsequently sucked back up slowly with the receding angle measured from the receding contact line until the angle stabilized or the angle was unmeasurable.

Platelet Rich Plasma Isolation and Incubation on HA-LLDPE Substrates

Ten ml of whole human blood was drawn via venous phlebotomy into tubes coated with EDTA (BD Vacutainer; Franklin Lakes, NJ). At least 3 healthy donors who had refrained from taking thromboxane inhibitors for a minimum of two weeks donated blood for the investigations. EDTA collection tubes were chosen in order to preserve platelet morphology during analysis as previously described. The protocol for blood isolation from healthy individuals was approved by Colorado State University Institutional Review Board. Platelet rich plasma (PRP) was isolated through centrifugation at 150g for 10 mins followed by a rest period of 10 mins to ensure that any partially activated platelets could return to their resting state. PRP from blood collection tubes was subsequently pooled together in a 50 ml conical tube and gently oscillated to ensure adequate mixing. One ml of PRP was then added to each substrate group: LLDPE; LLDPE enhanced with 2% HA, 2.5% HA, and 3% HA; 2% HA+Spin, 2.5% HA + Spin, and 3% HA + Spin. The substrates were allowed to incubate for 2 hrs in an incubator at 5% CO₂ and 37°C. The dimensions of each substrate were 8 mm x 1 mm retrieved from each fabricated HA “film” using a biopsy punch. Each

substrate was completely immersed in PRP, however only one side of each substrate was analyzed in each investigation to obtain data. All investigations were performed in a static environment with the exception of gentle shaking on a shaker plate during PRP incubation which was performed at 100 rpm/s.

Cytocompatibility of HA-LLDPE Substrates

A commercially available lactate dehydrogenase assay (LDH) was used to assess the cytocompatibility of different substrates in contact with platelets. The protocol provided by the manufacturer was used (Pierce Biotechnology: Rockford, IL). In brief, a reaction mix was prepared by combining a substrate mixture (lyophilizate and ultrapure water) with an assay buffer provided by the manufacturer. The substrates were incubated in PRP for 2 hrs, including a positive control group of lysis buffer added to PRP to ensure maximal lysing of blood cells. After incubation, 50 μ l of substrate incubated PRP was transferred to a 96 well plate. Fifty μ l of reaction mix was then added to the PRP and mixed gently by tapping. Substrates were then incubated for 30 mins in a dark hood. After 30 mins absorbance was read at 490nm and 680nm on a spectrophotometer.

Platelet adhesion on HA-LLDPE Substrates

Platelet adhesion on different substrates was determined through the use of fluorescent microscopy. After 2 hrs of incubation in PRP, the substrates were gently rinsed twice with PBS. One ml of 5 μ M solution of Calcein-AM (Thermo-Scientific) dissolved in PBS was added to the substrates and allowed to incubate at ambient temperature for 20 mins. Following incubation, the stain was carefully aspirated, and substrates were rinsed twice with PBS. All the substrates were immediately imaged with a Zeiss Axiovision fluorescent microscope using a 493/514 nm filter.

All fluorescence microscopy images were processed using Image J software.

Platelet Morphology on HA-LLDPE Substrates

Scanning electron microscopy (SEM) was used to visualize platelet morphology on different HA substrates. After 2 hrs incubation in PRP, the substrates were gently rinsed twice with PBS, fixed, and dehydrated. The fixation process included 45 mins of incubation in a primary fixative of 6% gluteraldehyde (Sigma), 0.1M sodium cacodylate (Polysciences), and 0.1M sucrose (Sigma) in DI water. Afterwards substrates were transferred to a buffer solution (primary fixative without gluteraldehyde) for 10 mins. This was followed by incubating the substrates to consecutive solutions of ethanol (35%, 50%, 70% and 100%) for 10 mins each to remove any excess water. Substrates were then stored in a desiccator until imaging. Prior to SEM visualization, the substrates were coated with a 10 nm layer of gold and imaged at 5 kV.

Platelet Activation on HA-LLDPE Substrates

Platelet activation on different HA substrate substrates was measured using a platelet factor 4 (PF4) enzyme linked immunoabsorbant assay kit (ELISA, RayBio). The protocol provided by the manufacturer was followed. After 2 hrs incubation in PRP, the substrate-exposed plasma was diluted (1:200) in the assay diluent, and incubated in the micro-assay well plate provided by the manufacture for 2.5 hrs. Afterwards, the wells were aspirated and washed 4 times in a wash buffer and subsequently incubated with biotinylated antibody for 1 hr. The antibody was aspirated and the wells were again washed to remove any unbound antibody. The wells were then incubated with a horseradish peroxidase (HRP)-streptavidin solution (1:25,000 in assay diluent) and incubated for another 45 mins. Finally, the HRP was aspirated, wells were washed, and a final incubation in a

tetramethyl benzidine buffer solution was performed. The reaction was stopped with a stop solution and the optical density was measured using a plate reader at 450 nm.

Statistics

A linear mixed model with a random intercept was fit to the data to compare treatment groups accounting for repeated measures of HA-LLDPE using the “lme4” package in the R open source statistical data software. Multiple comparisons of contact angles between treatments were analyzed using Tukey’s HSD post-hoc test using the “emmeans” package (<https://cran.rproject.org/web/packages/emmeans/vignettes/comparisons.html>). For the FTIR spectra, a log (x+1) transform of the peak area was used due to heavily skewed data and the presence of a zero for the virgin LLDPE. A linear mixed model and Tukey post-hoc test was also used for fitting. All models used Satterthwaite denominator degrees of freedom for significance testing.

Experiments with platelets were performed to evaluate the differences between PS, LLDPE, 2% HA, 2.5% HA, 3% HA, 2% Spin, 2.5% Spin, and 3% Spin on five substrates. Each experiment was repeated at least three times with three different whole blood PRP populations ($n_{\min} = 15$). Fluorescent imaging was performed using a Zeiss Axiovision fluorescent microscope at 10x magnification and analyzed using ImageJ software. Percent coverage of platelets were determined by the evaluation of 15 representative images taken per group over 3 studies ($n=45$) using Image J. Each image analyzed an area of $25 \mu\text{m}^2$. Qualitative SEM analysis was performed using the methods prescribed by Ko and Cooper ²⁴ on 15 representative images per group taken over 3 studies at 500x and 2500x ($n = 45$). Each image covered an area of $144 \mu\text{m}^2$. All results were

evaluated using a one-way analysis of variance (ANOVA) with Tukey's, Bonferonni, and Scheffe post-hoc analysis. Statistical significance was considered at $p < 0.05$.

Results and Discussion

In previously published work we sought to increase the hemocompatibility of virgin LLDPE for use in flexible cardiovascular biomaterials by incorporating HA into the molecular structure of LLDPE ^{9,16}. While previous research has primarily focused on HA modification of biomaterials for stent applications, the introduction of flexible HA enhanced biomaterials potentiates a wide range of uses including heart valve leaflets, vascular patches, and grafts. Previous studies indicated that the 2% HA substrates were cytocompatible to platelets, significantly reduced blood protein adsorption, platelet and leukocyte adhesion and activation, contact activation, and thrombin-antithrombin cleavage ¹⁶. The purpose of this study was to investigate the effects of varying concentrations of HA with and without the addition of HA spin-coating to determine if this would enhance hemocompatibility.

To confirm the presence of HA on different HA-LLDPE substrates, ATR-FTIR spectra were taken and compared to that of untreated LLDPE (**Figure 1**). The characteristic peaks for LLDPE are CH₃ and CH₂ asymmetric and symmetric stretching near 2914 and 2847cm⁻¹; CH₂ and CH₃ scissoring and stretching at 1472 and 1462cm⁻¹; and CH₂ rocking at 718cm⁻¹. All these peaks were present on untreated LLDPE spectra. The characteristic peaks for HA are OH and NH stretching near 3338cm⁻¹; carbonyl stretching of urethane linkages near 1765cm⁻¹; amide and carboxyl carbonyl stretching near 1685cm⁻¹; and CNH stretching characteristic of amides and urethanes due to HA and the HMDI cross-linker near 152cm⁻¹. All these peaks were present on different HA-LLDPE spectra long with characteristic peaks for LLDPE. ATR-FTIR determines

chemical composition up to 2 μm into the surface. The results show that the substrates were modified with HA.

Contact angle goniometry was used to characterize the wettability of HA-LLDPE substrates (**Figure 2**). The results indicate that due to high contact angle hysteresis (i.e. the difference between advancing and receding contact angles) of HA-LLDPE substrates, water droplets will not easily roll off and will spread on the surface, indicating that all the HA-LLDPE substrates are hydrophilic. In contrast, the contact angle hysteresis was lower for LLDPE substrates indicating the substrate is hydrophobic. Further, none of the advancing and receding contact angles for HA-LLDPE substrates were significantly different from each other, however, they were all significant different from LLDPE substrates ($p \leq 0.05$).

To ensure that the HA-LLDPE substrates did not facilitate +/- death, cytocompatibility investigations were performed. Cytocompatibility is based on a biomaterial's ability to discourage premature cell death when exposed to the native physiology. In order to determine the cytocompatibility of different HA substrates, a commercially available LDH assay was used. Different HA substrates were incubated in PRP and compared to a HEPES Buffer solution, virgin LLDPE, and platelets that were completely lysed with a Triton-X lysis buffer. As previously described, LLDPE and 2% HA was found to be non-toxic¹⁶. The present results confirmed the preceding outcomes and indicate that varying concentrations of HA do not significantly alter the cytocompatibility of the different HA substrates. No significant differences in cytotoxicity were noted between 2% HA, 2.5% HA, 3% HA, 2% HA Spin, 2.5% HA Spin, and 3% HA Spin substrates, LLDPE, or HEPES buffer solution (**Figure 3**). However, all substrates were significantly different from the total cell lysate. Upon exposure to a toxic material, LDH is released during necrosis and subsequent cell lysis. Thus, LDH assaying provides an indirect measurement

of a material's toxicity to the target cells. The results of this study demonstrate that varying HA concentration does not significantly induce cell death since it was similar to that of HEPES buffer solution. HEPES buffer is commonly used in cell culture to assist in maintaining enzyme structure and metabolic functions within cells and is considered non-toxic²⁵. Thus, the results indicate that none of the substrates resulted in any significant cytotoxic effects on PRP and can thus be safely used in the development of materials for blood-contacting applications.

Platelet adhesion to biomaterial substrates is an important indicator of hemocompatibility. Vastly reducing the amount of platelet adhesion to a biomaterial interface considerably reduces the potential for thrombotic incidence *in vivo*, thereby mitigating the potential for stroke, death, and implant rejection. Platelet adhesion analysis via fluorescence microscopy indicated that adhesion tended to increase with increasing concentration of HA (**Figure 4(a) and 4(b)**). Only the 2% HA was found to significantly reduce platelet adhesion as compared to the LLDPE. While trends indicate that 2% HA outperformed 2.5% and 3% HA treatment groups resulting in the least amount of platelet attachment on the substrates, no significant differences were seen. Further, no significant differences were found in the amount of platelet adhesion in the spin coated substrates, although 3% HA Spin always demonstrated the greatest number of platelets on the substrate. However, 2% HA markedly reduced platelet adhesion as compared to 2% HA Spin, 2.5% HA Spin, and 3 % HA Spin ($p \leq 0.05$). As illustrated in previous studies^{16,26,27} a marked reduction in bulk platelet adhesion has been shown to correspond to the anionic nature of HA enhanced substrates. Similar studies, investigating the hemocompatibility of cross-linked hydrogels have demonstrated that platelet entrapment may occur due to the irregularly shaped networks produced by cross-linking²⁸. HA is known to regulate the distribution and transport of plasma proteins and macromolecules dependent upon the space generated in the HA network^{1,2}. Under physiological

conditions these spaces can be naturally regulated to allow for the appropriate transport of biological products across the interface. HA naturally self-associates into tight helical configurations [29]. It has been well established that stabilizing HA via cross-linking generates varying pore sizes which can result from the intermolecular association of HA chains at the surface thus creating a mesh like surface ^{14,20}. However, the fabrication process of immersing LLDPE in HA solutions followed by cross-linking HA to itself creates a fixed network which may entrap proteins and platelets in the entangled matrix. This mesh like architecture can be seen in the “pools” of HA on the HA-LLDPE surface in SEM imaging (See Fig. X). The addition of HA by spin coating to HA-LLDPE cross-linked substrates may then exacerbate blood cell adhesion by increasing this effect. Thus, while lower concentrations of HA may result in pore sizes too large to catch proteins and platelets, higher concentrations of HA may facilitate immobility of platelets on the substrates and retain more plasma proteins. Future investigations are needed to confirm these phenomena. Furthermore, platelets are known to preferentially bind to hydrophobic substrates ²⁷. Thus, it could then be hypothesized that excessive platelet adhesion to HA-LLDPE substrates could occur via three mechanisms; (a) the incorporation of inadequate amounts of HA in the LLDPE network allowing platelets to be exposed to the hydrophobic LLDPE phase; (b) the addition of too much HA resulting in the trapping of positively charged proteins, which facilitate platelet adhesion; or (c) the entrapment of platelets themselves due to the varying pore sizes which generate a physical matrix that subsequently ensnare platelets.

SEM imaging appears to confirm the third phenomena specifically for spin-coated substrates. Different HA-LLDPE substrates illustrate “pooling” and “clustering” of HA across the surface, which indicate potential areas of increased concentration and entanglement. These areas are highlighted in (**Figure 5**). While hydrated, it is assumed that HA is spread more uniformly

throughout the substrate. However, it is likely that HA is prone to accumulate, even in its hydrated state, as its hydrophilic nature is incompatible with the hydrophobic phase of the native LLDPE network.

Qualitative assessment reveals that HA prominent regions seem to increase with increasing concentration of HA, however further investigation is needed. In addition, protuberances located in the HA pools indicate some platelet entrapment within the accumulated regions. Thus, it could be assumed that when hydrated, HA regions spread out but may retain some areas of high concentration that could trap platelets within the HA-LLDPE matrix. While not all platelets attached at the substrate correspond to “pools” visualized with SEM, the entanglement of the HA within LLDPE network during fabrication may still result in pore sizes that capture both protein and platelets. Previous studies have shown using cross-linked HA can produce various pore sizes and degradation profiles ²⁰. Due to the difficulties in properly assessing platelet activation in the accumulated HA regions, PF4 assaying was used to determine platelet activation.

Platelet activation was determined by quantifying the release of PF4, a protein liberated through the process of alpha degranulation during increasing levels of platelet activation. PF4 is generally recognized as a pro-thrombotic agent and an antagonist of heparin-like molecules ³⁰. PF4 concentration was normalized to the percent coverage of overall platelets which had adhered to the substrate in corresponding Calcein-AM images (**Figure 6**). LLDPE substrates liberated approximately 10ng/ml. While PF4 concentration induced by LLDPE fell within the acceptable range for human plasma ⁶, it was still significantly higher than the observed levels produced by different HA-LLDPE substrates with the exception of 3% HA Spin (PF4 \approx 9ng/ml). 2% HA (PF4 \approx 5ng/ml) was not found to significantly increase platelet activation as compared to 2.5% HA (PF4 \approx 5ng/ml) but was found to significantly reduce PF4 release compared to 3% HA (PF4

≈ 7ng/ml) ($p \leq 0.05$). 2% HA Spin (PF4 ≈ 6ng/ml), 2.5% HA Spin (PF4 ≈ 7.7 ng/ml) and 3% HA Spin were found to be the most activating of all HA-LLDPE substrates and demonstrated significant increase in PF4 release between different groups ($p \leq 0.01$) although they still fell within the acceptable range for blood contacting materials. PF4 and fluorescence microscopy images results express a correlation between increasing concentration levels of HA and platelet adhesion and activation. Thus, in future work it would be prudent to monitor higher concentrations of HA on biomaterial substrates to ensure adverse platelet adhesion and activation does not occur. Increased platelet adhesion to the substrate is detrimental as it increases the potential for platelets to activate overtime. Thus, as compared to the other test substrates, it could be concluded that 2% HA substrates would be the best candidate for use in biomaterial applications seeking to mitigate platelet activation on the substrate.

Conclusions

HA enhanced LLDPE has the potential to be used in a vast array of biomedical applications. The current study revealed that HA-LLDPE retains anticoagulant properties such as reduced platelet adhesion and activation, even when increasing concentrations during the cross-linking process. However, the results imply that higher concentration levels may affect the levels of platelet adhesion and activation at the substrate surface. Because HA-LLDPE is produced by cross-linking HA after solubilization in xylenes, HA prone accumulation cannot be regulated. Thus, varying pore sizes resulting from the manufacturing process leads to matrix formation which traps whole platelets and aggregates within in its network, as seen in similar investigations of HA-enhanced biomaterials. While the addition of spin-coating rendered negative effects on hemocompatibility, gaining insight into the nature of HA modifications are essential to furthering

biomaterial investigations into HA-enhanced biomaterial technologies. Future work will aim to assess endothelialization of HA-LLDPE substrates to further increase hemocompatibility at the HA-blood interface. In addition, investigations into altering the molecular weight HA used to enhance the HA-LLDPE materials may prove useful to fine tuning the hemocompatibility of these flexible materials for use in cardiovascular applications.

REFERENCES:

1. Nagy N, Kuipers HF, Frymoyer AR, et al. 4-Methylumbelliferone treatment and hyaluronan inhibition as a therapeutic strategy in inflammation, autoimmunity, and cancer. *Front Immunol.* 2015;6(MAR). doi:10.3389/fimmu.2015.00123
2. Laurent TC, Fraser JR. Hyaluronan. *FASEB J.* 1992;6(7):2397-2404. doi:10.1016/S0740-8315(82)80016-8
3. Tamer TM. Hyaluronan and synovial joint: function, distribution and healing. *Interdiscip Toxicol.* 2013;6(3). doi:10.2478/intox-2013-0019
4. Fraser JR, Laurent TC, Laurent UB. Hyaluronan: its nature, distribution, functions and turnover. *J Intern Med.* 1997;242:27-33. doi:10.1046/j.1365-2796.1997.00170.x
5. Toole BP. Hyaluronan: from extracellular glue to pericellular cue. *Nat Rev Cancer.* 2004;4(7):528-539. doi:10.1038/nrc1391
6. Amarnath LP, Srinivas A, Ramamurthi A. In vitro hemocompatibility testing of UV-modified hyaluronan hydrogels. *Biomaterials.* 2006;27(8):1416-1424. doi:10.1016/j.biomaterials.2005.08.008
7. Ruiz A, Flanagan CE, Masters KS. Differential support of cell adhesion and growth by copolymers of polyurethane with hyaluronic acid. *J Biomed Mater Res - Part A.* 2013;101(10):2870-2882. doi:10.1002/jbm.a.34597
8. Chuang TW, Masters KS. Regulation of polyurethane hemocompatibility and endothelialization by tethered hyaluronic acid oligosaccharides. *Biomaterials.* 2009;30(29):5341-5351. doi:10.1016/j.biomaterials.2009.06.029

9. Prawel DA, Dean H, Forleo M, et al. Hemocompatibility and Hemodynamics of Novel Hyaluronan-Polyethylene Materials for Flexible Heart Valve Leaflets. *Cardiovasc Eng Technol.* 2014;5(1):70-81. doi:10.1007/s13239-013-0171-5
10. Barbucci R, Lamponi S, Magnani A, et al. Influence of sulfation on platelet aggregation and activation with differentially sulfated hyaluronic acids. *J Thromb Thrombolysis.* 1998;6(2):109-115. doi:10.1023/A:1008841303634
11. Wu F, Li J, Zhang K, et al. Multifunctional Coating Based on Hyaluronic Acid and Dopamine Conjugate for Potential Application on Surface Modification of Cardiovascular Implanted Devices. *ACS Appl Mater Interfaces.* 2016;8(1):109-121. doi:10.1021/acsami.5b07427
12. Zhang K, Li JA, Deng K, Liu T, Chen JY, Huang N. The endothelialization and hemocompatibility of the functional multilayer on titanium surface constructed with type IV collagen and heparin. *Colloids Surfaces B Biointerfaces.* 2013;108:295-304. doi:10.1016/j.colsurfb.2012.12.053
13. Pitt WG, Morris RN, Mason ML, Hall MW, Luo Y, Prestwich GD. Attachment of hyaluronan to metallic surfaces. *J Biomed Mater Res A.* 2004;68(1):95-106. doi:10.1002/jbm.a.10170
14. Thierry B, Winnik FM, Merhi Y, Griesser HJ, Tabrizian M. Biomimetic hemocompatible coatings through immobilization of hyaluronan derivatives on metal surfaces. *Langmuir.* 2008;24(20):11834-11841. doi:10.1021/la801359w
15. Li J, Zhang K, Yang P, et al. Research of smooth muscle cells response to fluid flow shear stress by hyaluronic acid micro-pattern on a titanium surface. *Exp Cell Res.*

2013;319(17):2663-2672. doi:10.1016/j.yexcr.2013.05.027

16. Simon-Walker R, Cavicchia J, Prawel DA, Dasi LP, James SP, Popat KC.

Hemocompatibility of hyaluronan enhanced linear low density polyethylene for blood contacting applications. *J Biomed Mater Res Part B Appl Biomater*. September 2017.

doi:10.1002/jbm.b.34010

17. Bick RL. Hemostasis defects associated with cardiac surgery, prosthetic devices, and other extracorporeal circuits. *Semin Thromb Hemost*. 1985;11(3):249-280. doi:10.1055/s-2007-1004381

18. Bittl JA. Coronary stent occlusion: Thrombus horribilis. *J Am Coll Cardiol*. 1996;28(2):368-370. doi:10.1016/S0735-1097(96)00183-0

19. Gorbet MB, Sefton M V. Biomaterial-associated thrombosis: Roles of coagulation factors, complement, platelets and leukocytes. In: *The Biomaterials: Silver Jubilee Compendium*. ; 2006:219-241. doi:10.1016/B978-008045154-1.50025-3

20. Allison DD, Grande-Allen KJ. Review. Hyaluronan: A Powerful Tissue Engineering Tool. *Tissue Eng*. 2006;0(0):060913044658042. doi:10.1089/ten.2006.12.ft-153

21. Li J, Zhang K, Ma W, et al. Investigation of enhanced hemocompatibility and tissue compatibility associated with multi-functional coating based on hyaluronic acid and Type IV collagen. *Regen Biomaterials*. 2016:149-157. doi:doi: 10.1093/rb/rbv03

22. Zhang K, Chen J ying, Qin W, Li J an, Guan F xia, Huang N. Constructing bio-layer of heparin and type IV collagen on titanium surface for improving its endothelialization and blood compatibility. *J Mater Sci Mater Med*. 2016;27(4). doi:10.1007/s10856-016-5693-6

23. Zhang M, James SP. Silylation of hyaluronan to improve hydrophobicity and reactivity

for improved processing and derivatization. *Polymer (Guildf)*. 2005;46(11):3639-3648.
doi:10.1016/j.polymer.2005.03.022

24. Ko TM, Cooper SL. SURFACE-PROPERTIES AND PLATELET-ADHESION CHARACTERISTICS OF ACRYLIC-ACID AND ALLYLAMINE PLASMA-TREATED POLYETHYLENE. *J Appl Polym Sci*. 1993;47(9):1601-1619. doi:10.1002/app.1993.070470908

25. Lepe-Zuniga JL, Zigler JS, Gery I. Toxicity of light-exposed Hepes media. *J Immunol Methods*. 1987;103(1):145. doi:10.1016/0022-1759(87)90253-5

26. Okano T, Nishiyama S, Shinohara I, et al. Effect of hydrophilic and hydrophobic microdomains on mode of interaction between block polymer and blood platelets. *J Biomed Mater Res*. 1981;15(3):393-402. doi:10.1002/jbm.820150310

27. Lee J, Khang G, Lee J, Lee H. Interaction of Different Types of Cells on Polymer Surfaces with Wettability Gradient. *J Colloid Interface Sci*. 1998;205(2):323-330.
doi:10.1006/jcis.1998.5688

28. Kulik E, Ikada Y. In vitro platelet adhesion to nonionic and ionic hydrogels with different water contents. *J Biomed Mater Res*. 1996;30(3):295-304. doi:10.1002/(SICI)1097-4636(199603)30:3<295::AID-JBM4>3.0.CO;2-L

29. Cowman MK, Spagnoli C, Kudasheva D, et al. Extended, relaxed, and condensed conformations of hyaluronan observed by atomic force microscopy. *Biophys J*. 2005;88(1):590-602. doi:10.1529/biophysj.104.049361

30. De Mel A, Chaloupka K, Malam Y, Darbyshire A, Cousins B, Seifalian AM. A silver nanocomposite biomaterial for blood-contacting implants. *J Biomed Mater Res - Part A*. 2012;100 A(9):2348-2357. doi:10.1002/jbm.a.34177

31. Kulik E, Ikada Y. In vitro platelet adhesion to nonionic and ionic hydrogels with different water contents. *J Biomed Mater Res*. 1996;30(3):295-304. doi:10.1002/(SICI)1097-4636(199603)30:3<295::AID-JBM4>3.0.CO;2-L